Dissertation zur Erlangung des Doktorgrades

der Fakultät für Chemie und Pharmazie

der Ludwig-Maximilians-Universität München

Sequence defined oligomers as a carrier platform for therapeutic pDNA and mRNA delivery

Ana Krhač Levačić

aus Novo mesto, Slowenien

2018

Erklärung

Diese Dissertation wurde im Sinne von § 7 der Promotionsordnung vom 28. November 2011 von Herrn Prof. Dr. Ernst Wagner betreut.

Eidesstattliche Versicherung

Diese Dissertation wurde eigenständig und ohne unerlaubte Hilfe erarbeitet.

München, 23.04.2018

.....

Ana Krhač Levačić

Dissertation eingereicht am: 14.05.2018

1. Gutachter: Prof. Dr. Ernst Wagner

2. Gutachter: PD Dr. Carsten Rudolph

Mündliche Prüfung am: 21.06.2018

Meiner Familie

Rebeka Elin

Table of Contents

1 Introduction

The introduction provides a review of sequence defined oligomers used as a carrier platform technology for therapeutic nucleic acid delivery, with a focus on pDNA and mRNA, followed by a brief summary about optimization of DNA vectors for enhanced gene transfer.

Sections 1.1, 1.2, 1.3 have been adapted from:
A. Krhac Levacic, S. Morys and E. Wagner. Solid-phase supported design of carriers for therapeutic nucleic acid delivery. Bioscience Reports 37 (2017) doi 10.1042/BSR20160617

Section 1.4 has been adapted from:
A. Krhac Levacic, S. Morys, S. Kempter, U. Lächelt and E. Wagner. Minicircle versus plasmid DNA delivery by receptor-targeted polyplexes. Human Gene Therapy 28(10) (2017) 862-874

1.1 Non-viral gene therapy

Administration of nucleic acids with therapeutic potential offers a promising approach for the treatment of several human diseases that reached already medical use [1-5]. Availability of efficient and safe delivery systems is of primary importance for wider spread of successful gene-based therapies. Due to large size, biodegradability and the negative charge of exogenous nucleic acids (NA) such as plasmid DNA (pDNA), mRNA, small interfering RNA (siRNA), microRNA (miRNA), or antisense oligonucleotides, transfer of therapeutic NAs to target cells requires help of viral and non-viral gene delivery systems. Although in current therapeutic clinical trials viral vectors dominate due to their higher efficiency, synthetic carriers show their advantages in the type of nucleic acid cargo (including also artificial chemically modified forms) [6, 7], manner of production, formulation property, and storage [8-10]. Research on lipidic, peptide or polymer-based carriers that complex therapeutic nucleic acid by electrostatic interaction, is of particular interest for non-viral delivery. These vehicles should complex nucleic acids by formation of stabile polyplexes or

lipoplexes [11] and protect against degradation in the bloodstream and reach target cells. The next requirement is an efficient intracellular delivery by entering via endocytosis into the intracellular space [9, 12, 13]. Endocytosis via invagination of nanoparticles by the lipid cell membrane into endosomal vesicles requests later escape from endosome instead of endolysosomal degradation [14-16]. In case of pDNA, either the whole polyplexes or the released nucleic acid must subsequently enter the nucleus via passive, active, or cell-cycle dependent mechanisms [17-21] and be transcribed [22]. Nucleic acids such as siRNA, miRNA, or mRNA need to reach the cytoplasm for bioactivity. Compared to pDNA gene delivery, mRNA has several advantages including its direct activity in the cytoplasm, thus avoiding the requirement for nuclear import, improved effectivity in non-dividing cells (as liver hepatocytes [23]) as well as in hard-to-transfect cells (dendritic cells and macrophages), and absence of risk of insertional mutagenesis. High immunogenicity and limited stability of unmodified RNA present a major challenge for successful application, but chemical modifications of mRNA were shown to improve efficacy of mRNA gene therapy [24-27].

Although on the one side, stability of complexes is important in the time of extracellular delivery steps, on the other side, the carrier should release the NA in the intracellular space and should not influence its functionality. Thus, for a successful nucleic acid delivery, synthetic nucleic acid shuttles have to be responsive to a changing bioenvironment just like natural viruses. Chemistry, size, and topology (linear, branched, comb, hyperbranched, and dendritic) of the shuttle, as well as size and physicochemical characteristics of formed nanostructures can play a decisive role for the biological activity [28-38]. For carrier optimization under such complex situations, a careful structure–activity relationship of carriers and their nucleic acid delivery characteristics is mandatory. This also requests synthetic methods to produce carriers in chemical precise form. One option outlined in this thesis presents the application of solid-phase assisted synthesis (SPS). Synthesis of peptides by SPS was introduced by Merrifield in 1963 [39] and has been refined to a very potent technology, which has been even applicable for the assembly of whole proteins such erythropoietin [40]. Analogous progress has been made in the area of SPS of oligonucleotides, applying phosphoramidite chemistry as initially developed by Caruthers [41]. Synthesis of oligonucleotides nowadays is routine; even the synthesis

and subsequent recombinant assembly of oligonucleotides into a whole bacterial DNA genome was possible [42]. By nature of chemistry, nucleic acid analogs with favorable characteristics over their natural counterparts were generated [6, 7, 43].

Although mRNA delivery possesses broad application prospects, as a new application area it still requires more improvement compared to DNA delivery [26, 44]. Numerous studies have attempted to increase efficiency of mRNA delivery inspired by pDNA or siRNA delivery, but due to difference between those nucleic acids, effective cationic polymers for delivery of large pDNA or small siRNA might not necessarily be successful for mRNA delivery [24, 25]. Therefore, for a broader overview the sections 1.1, 1.2 and 1.3 present also sequence defined oligomers used as a carrier system for siRNA delivery. Protamine was used as the first generation of mRNA delivery systems [26, 44], but nowadays various delivery carriers are the subject of research [45-49]. Liposomal systems [50-58] present the greatest interest in the case of mRNA delivery, contrary to pDNA delivery, where polymers are the most broadly investigated [25, 26]. At the moment, immunotherapeutic application is the only field with already available clinical experience [59].

1.2 Carrier requirements

The multiple requirements for carriers to successfully deliver nucleic acids are described in **Figure 1** in schematic form.

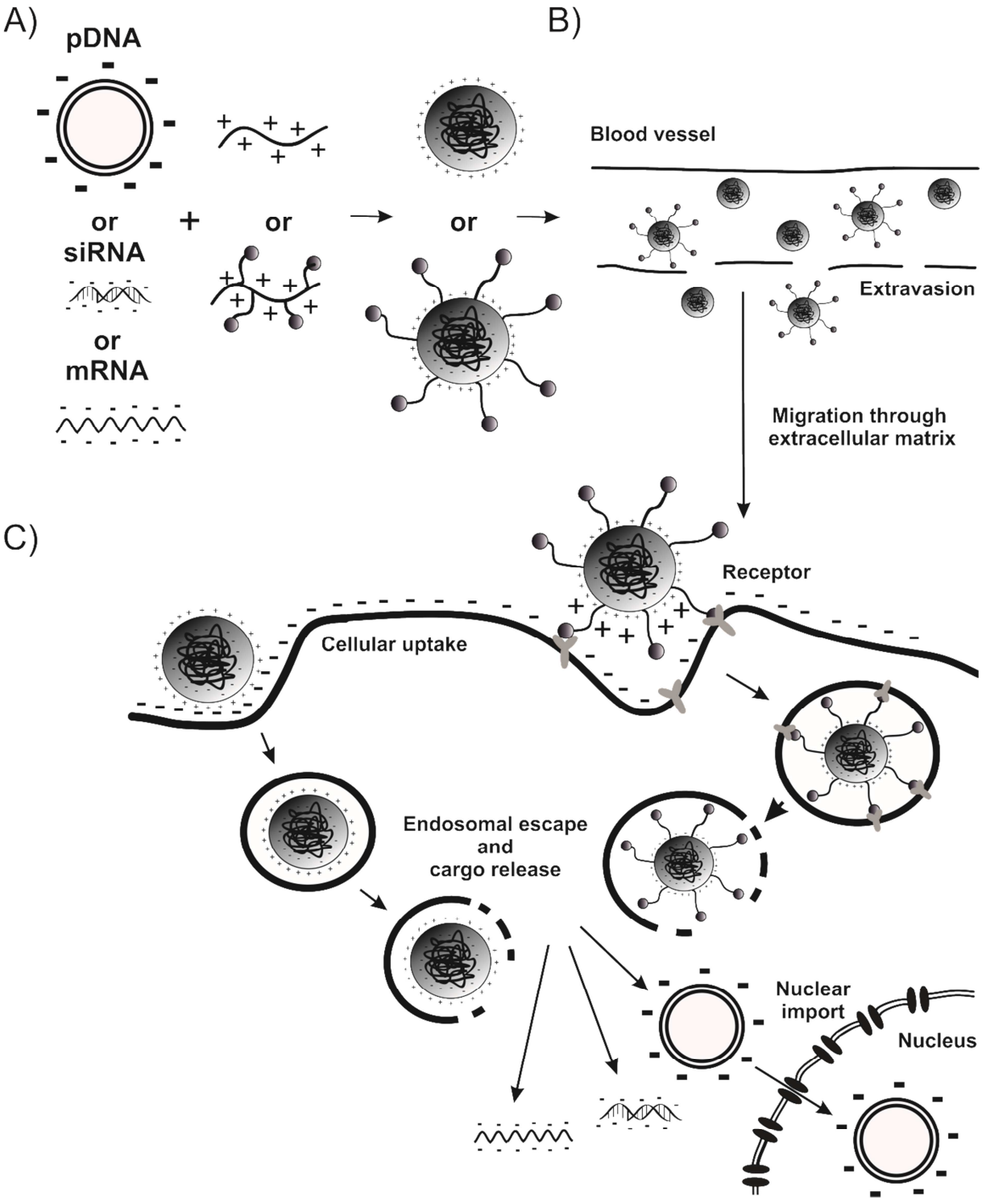

Figure 1 Barriers for the nucleic acid delivery via polyplexes. **(A)** Formation of stable polyplexes. **(B)** Protection against rapid clearance and unspecific interactions with blood components, and **(C)** overcoming cellular barriers.

1.2.1 Nucleic acid binding

Non-viral carriers tailored by solid-phase synthesis can be composed either solely of natural amino acids, solely of artificial building blocks, or of a combination of both (**Figure 2**). Especially homopolymers of the basic amino acid residues lysine (**Figure 2A**), ornithine, and arginine had shown ability to bind and condensate nucleic acid [60-63]. Later on, instead of polymerized amino acids, defined oligopeptides were developed via SPS [64-68]. Linear [64] as well as branched [68] oligolysine peptides were evaluated regarding nucleic acid binding and compaction as well as gene transfer. A minimum of six to eight cationic amino acids are required to compact pDNA into polyplexes active in gene delivery. The DNA binding and compaction ranked from arginine > lysine ~ ornithine residues. Nucleic acid binding represents only one crucial step for successful gene delivery; not surprisingly, despite good nucleic acid binding oligolysine peptides could mediate gene transfer only to a limited extent, because of insufficient endosomal escape. In several cases, combination with lysosomatropic chloroquine or lipidic helper molecules was necessary to mediate successful nucleic acid delivery [69-72].

Branched peptides containing α,ε-modified lysines as branching points, and lysines and protonatable histidine as nucleic acid binding arms were found as very effective in either pDNA or siRNA transfer [73-77]. It had been observed that the type of nucleic acid cargo strongly influences the carrier performance [69, 78, 79]. Interestingly, combinatorial work pointed out that little changes in topology can decide on whether the carriers is effective for pDNA or siRNA delivery [76, 77]. These peptides with incorporated histidines had significantly decreased cytotoxicity as compared with classical transfection polymers [80].

Introduction of cysteines into oligolysine peptides offered a biodegradable and cross-linking motif that allowed polymerization of Cys-Lys_{10}-Cys corresponding to polylysine Lys_{205} [81, 82]. Analogously, increased pDNA binding was obtained by introduction of cysteines via SPS into Trp-Lys_{18} peptides, which led to enhanced polyplex stability against salt induced stress [83]. Shorter peptides consisting of only six lysines mediated sufficient stability and notable gene transfer after cysteine dependent cross-linking [84]. With the help of convergent solid-phase synthesis,

defined bioreducible polylysine derivatives comprising up to 74 lysines could be synthesized [85], revealing the possibilities of solid-phase synthesis.

In another approach, Rice and colleagues introduced acridine onto the ε-amine of a lysine suitable for SPS [86]. These acridinylated oligolysines complexed pDNA by charge dependent ionic interaction and also by polyintercalation (**Figure 2B**) [86-89]. Further, formulation of polyplexes using the same PEGylated polyacridine peptide to bind mRNA through ionic interaction and overcoming mRNA instability was also demonstrated [23]. In general, strong complexation presents a key for pDNA vectors, but might be a big disadvantage in the case of mRNA delivery due to ineffective mRNA release. Based on theoretical considerations, binding of far more flexible single stranded mRNA to cationic polymers is stronger comparing to binding to double-stranded nucleic acids such as pDNA [90].

Analogous to classical peptide synthesis, artificial building blocks such as triethylene tetramine or fatty acids were incorporated together with natural amino acids [91-93]. Wang et al. [92] designed a novel lipopeptide system (EHCO) based on (1-aminoethyl)iminobis [N-(oleoylcysteinylhistinyl-1-aminoethyl) propionamide] (**Figure 2C**) containing cysteines and oleic acids for siRNA nanoparticle stabilization, histidines for endosomal protonation, and (promoted by the fatty acids) endosomal membrane destabilization. The use of completely unnatural building blocks in SPS nucleic acid carriers was first introduced by Hartmann, Börner, and colleagues [94-100]. By alternating coupling of diamines (3,3'-diamino-N-methyl-dipropylamine or a bis-tBoc-protected spermine) and a diacid (succinic acid anhydride), the first sequence-defined oligo(amidoamines) were yielded. Optionally, disulfide linkage or a terminal PEG chain was introduced, and the sequence-defined oligomers were used for pDNA polyplex formation. Schaffert et al. [101] optimized the use of artificial amino acids for sequence-defined oligomer synthesis (**Figure 2D**). The design of the building blocks was based on the proton sponge diaminoethane motif of PEI. Triethylentetramine, tetraethylenpentamine, or pentaethylenhexamine were used with tBoc protection groups at the secondary amines and converted into artificial amino acids by introducing succinic acid onto one of the terminal primary amines, and Fmoc on the other primary amine [101, 102]. With these novel artificial amino acids, oligomers were generated benefiting from the nucleic acid binding abilities as well as

exhibiting a proton sponge effect, well known from PEI [28, 103]. In combination with commercially available Fmoc α-amino acids, fatty acids, and also other artificial blocks introducing bioreducible breaking points [104], more than 1000 oligomers with different topologies for pDNA as well as siRNA delivery were synthesized. These topologies include linear [33, 105], two-arm [105], three-arm [105-108], four-arm [102, 105, 109], comb architectures [34] as well as compounds with two cationic arms attached to a third arm of polyethylene glycol (PEG) of defined length and a targeting ligand (**Figure 2E**) [107-113].

With the precision of chemical design, in contrast with classical polymers like PEI or polylysine, oligomers could be generated to address simple questions on structure–activity relationships. For example, linear sequences of the building block Stp (succinyl tetraethylene pentamine, exhibiting three protonatable nitrogens per repetition) were prepared and the effect of increasing molecular weight of PEI-like oligomers on formed pDNA polyplexes could be investigated [33]. Very clearly, oligomers containing 20 Stp units (i.e. 100 nitrogen backbone) demonstrated good pDNA compaction, high marker gene transfer (6-fold higher than with gold standard LPEI 22kDa) in cell culture transfections, and an oligomer length-dependent 10-fold lower cytotoxicity than LPEI (containing in average an approximately 500 nitrogen backbone).

For further polyplex stabilization, terminal cysteines [105, 106] or twin cysteines [114, 115] served the formation of bioreducible disulfides. Optionally, further nanoparticle stabilization by incorporation of hydrophobic domains consisting of saturated as well as unsaturated fatty acids [104-106, 116, 117], or tyrosine trimers [104, 116] at peripheral or central positions lead to T-shaped, i-shaped, or U-shaped oligomers with favorable properties for siRNA delivery *in vitro* as well as *in vivo*. Also the influence of different lengths of shielding agents in PEGylated two-arm structures on pDNA compaction and polyplex stability was examined [108]. An increased length of PEG (from 12 to 24 ethylene oxide units), resulting in a decreased polycation to PEG ratio, led to less compacted pDNA polyplexes as compared with unshielded polyplexes.

Remy and colleagues [118-120] took a completely different approach, designing a covalent incorporation of cationic carrier elements into nucleic acids. They adapted oligonucleotide SPS for synthesizing oligospermine–siRNA conjugates, which mediated efficient gene silencing in the absence of any other carrier. In course of their work, also lipidic elements were incorporated for improved efficacy [121].

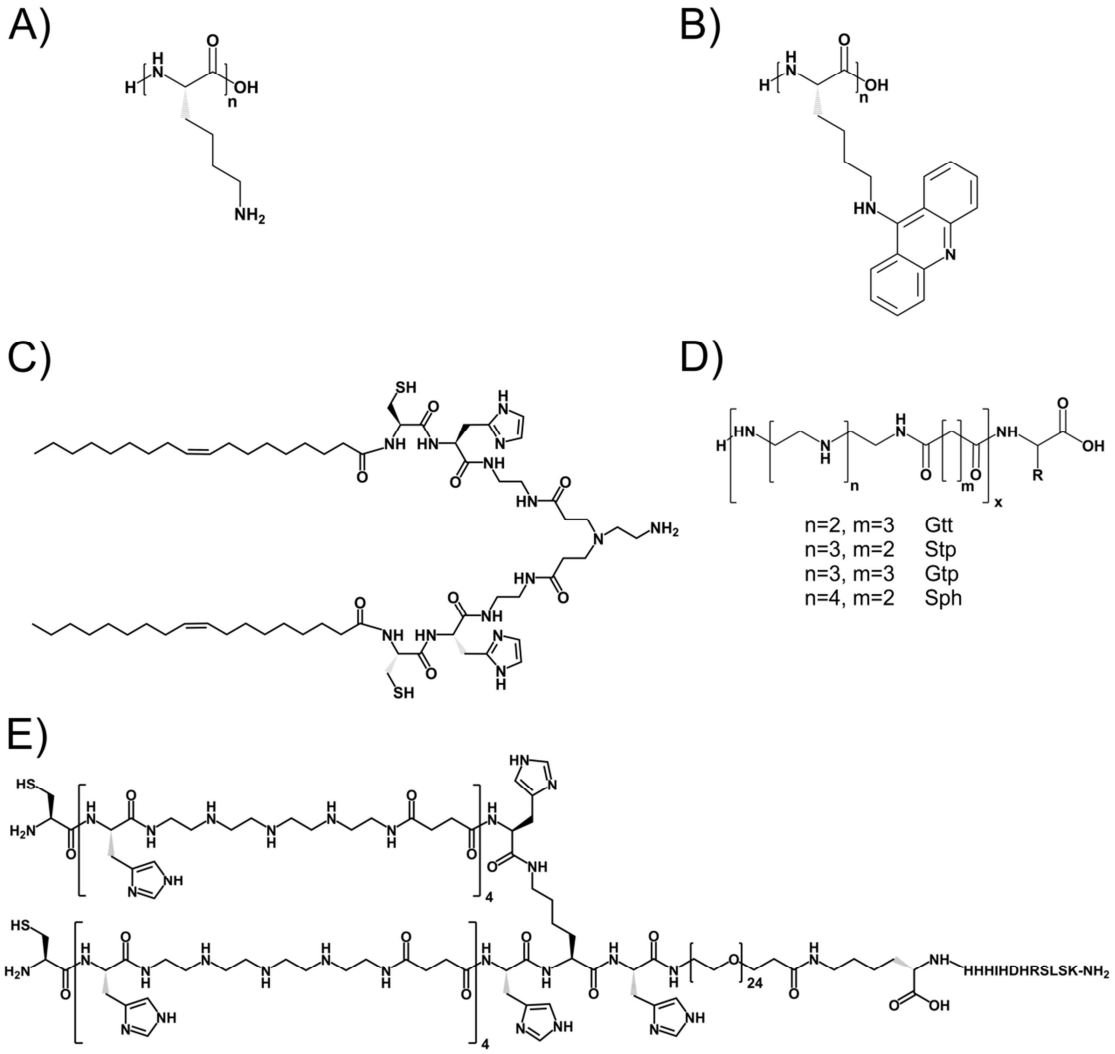

Figure 2 Oligopeptides and oligomers with nucleic acid binding motifs generated by SPS. Nucleic acid binding motifs of **(A)** oligolysine and **(B)** acridine-modified oligolysine. **(C)** EHCO, a lipopeptide containing oleic acid, histidine, cysteine, and artificial aminoethyl blocks for nucleic acid binding. **(D)** Artificial amino acids derived from PEI repeat unit that are assembled by SPS to retrieve a nucleic acid binding domain within sequence-defined oligomers. **(E)** Example of HGFR/c-Met targeted PEG-2-arm oligomer.

1.2.2 Polyplex shielding

Nucleic acid complexation usually requires an excess of cationic charged carrier and thereby usually results in formation of nanoparticles with positive surface potential. This positive charge often displays an advantage for gene transfer efficacy *in vitro* due to unspecific binding to negatively charged cell surfaces [122, 123] or by facilitating endosomal escape [124-126]. In the extracellular space, however, positively charged polyplexes depending on the applied cationic carrier may mediate undesired interactions with the complement system, blood cells, or other blood components [127-130]. Introduction of a hydrophilic surface shielding domain into artificial carriers has shown to reduce these interactions. PEG represents the most prominent and well-established shielding agent and has been successfully used for shielding of polyplexes in numerous instances, including SPS-designed nucleic acid carriers [12, 88, 127, 131-135]. But also poly(N-(2-hydroxypropyl)methacrylamide) (pHPMA) [136, 137], hydroxyethyl starch (HES) [138], polysarcosine [139], or repeats of Pro-Ala-Ser (PAS) [108] have been investigated as alternative hydrophilic shielding agents (**Figure 3**).

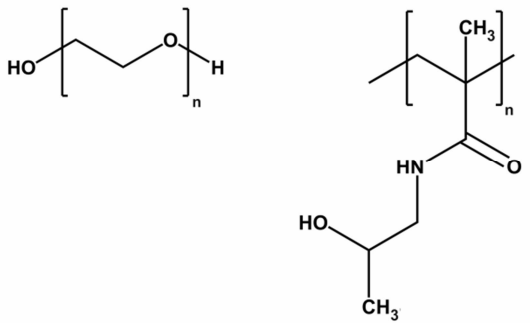

Figure 3 Chemical structures of the most prominent agents used for shielding. Left: polyethylene glycol (PEG), right: poly(N-(2-hydroxypropyl)methacrylamide) (HPMA).

For example, Fmoc-PEG*x*-COOH was directly integrated into sequence-defined carriers during SPS [107, 111, 112, 140, 141]. Using folate or methotrexate (MTX) as folate receptor (FR) targeting ligands, small unimolecular siRNA nanoplexes were generated, which demonstrated FR-dependent *in vivo* gene silencing, and in case of MTX also therapeutic antitumor activity [140, 141].

Although PEGylation may greatly improve pharmacokinetics and biodistribution to tumor target tissue, it may also negatively affect nucleic acid compaction and intracellular performance [108, 142, 143]. The length of the PEG chain, and consequently the ratio of hydrophilic to cationic polymer within the polyplex, controls characteristics like nucleic acid compaction, polyplex size, and stability [108]. In a recent report by Kos et al. [107], systemic c-Met targeted gene transfer of pDNA polyplexes was successful, but only if combination polyplexes of a ligand-PEG carrier with a non-PEGylated compaction carrier were applied. Alternatively, to avoid difficulties with nucleic acid compaction, PEG was also introduced after pDNA [137, 144] or siRNA [145-147] polyplex formation ("post-PEGylation"). For siRNA delivery, this approach led to increased tumor-specificity of RNA delivery *in vivo*, but only if tumor-specific ligands (EGFR binding peptide [145], transferrin protein [146], or folate [147]) were applied. Contrary to difficulties with nucleic acid compaction in the case of pDNA or siRNA, when PEG was directly integrated into carriers during SPS, PEGylation improved mRNA binding as well as transfection efficiency [126].

Reduced intracellular efficacy is the second problem of the so-called "PEG-Dilemma". As previously shown for other carriers, this problem can be overcome by introducing a pH-labile shield [134, 148-150]. Removal of the shield at endosomal pH in the endolysosomal compartment was found to recover transfection activity *in vitro* and *in vivo*, also for pDNA polyplexes of sequence-defined oligomers [137].

1.2.3 Ligands for cellular targeting

After formulation, carriers loaded with nucleic acid have to be able to reach target cells. Physical concentration via adsorption, electrostatic interactions, and ligand–receptor interaction are possibilities for successful intracellular entry of vehicles. Nanoparticles, comprise nucleic acid and cationic core exhibiting target specific ligands, may facilitate specific binding to receptors expressed on the surface of target cells. Afterward, carriers can be taken up by the cell via receptor-mediated endocytosis [14]. When polyplexes are positively charged, unspecific ionic interactions can still reduce the value of targeting ligands. Hence, targeting ligands are introduced in combination with shielding agents described above. As mentioned, targeting ligands plus shielding agents can be included directly during the SPS,

conjugated after the synthesis, or introduced after polyplex formation. Many different targeting ligands such as antibodies and their fragments, glycoproteins, peptides, and small molecules that can bind to receptors overexpressed in cancer or other target cells, have been investigated [13, 151-153]. Up to now, several different receptor-targeted carriers based on SPS already showed favorable characteristics for enhanced nucleic acid delivery.

The group of Rice [154] designed an asialoglycoprotein receptor (ASGP-R) targeted carrier with triantennary galactose-terminated oligosaccharide as a ligand, which combined with the endosomalytical reagent chloroquine, enhanced DNA delivery on the HepG2 cell line. The same group showed receptor specific uptake of pDNA/polyacridine glycopeptides (**Figure 2B**). They introduced high-mannose N-glycane as a targeting ligand attached to modified forms of polyacridine peptides [155, 156].

The ligand RGD (arginine–glycine–aspartic acid) is one of the most commonly used peptides for nucleic acid nanoparticle targeting cell–surface integrins [70, 71, 107, 111, 157, 158]. RGD–oligolysine peptide in combination with lysosomatropic chloroquine or lipidic helper molecules mediated targeted nucleic acid delivery [69-72, 75]. Leng et al. [74] developed a library of effective vehicles for siRNA delivery, branched peptides composed of histidines, and lysines (HK) with optionally attached RGD ligand. A promising integrin targeted siRNA delivery system, which showed efficient gene silencing in U87 glioma cells, was introduced by Wang et al. [158]. This system was based on (1-aminoethyl)iminobis [N-(oleoylcysteinylhistinyl-1-aminoethyl) propionamide] (EHCO) (**Figure 2C**). RGD was attached to siRNA nanoparticles via a PEG spacer. Analogously, bombesin was applied as another receptor ligand, which binds specifically to the gastrin-releasing peptide receptor, neuromedin B receptor, and the orphan receptor bombesin receptor subtype 3 that are overexpressed in various cancers. Systemic administration of the targeted nanoparticles loaded with anti-HIF-1α siRNA showed significant tumor growth inhibition *in vivo* [158].

Martin et al. [111] demonstrated ligand-dependent pDNA delivery by designing cyclic RGD-PEG-Stp 2-arm oligoaminoamides (**Figure 2E**); the same strategy was successfully developed for the targeting peptide B6, which was initially assumed to

enhance uptake via the transferrin receptor (TfR) but later on was discovered as an TfR independent tumor cell uptake facilitator [159, 160]. These initial conjugates were devoid of endosomal buffering histidines, therefore the presence of the endosomolytic reagent chloroquine was necessary for high level transfection. Subsequent work demonstrated a greatly improved transfection activity of PEGylated 2-arm structures upon incorporation of alternating histidines into the Stp carrier backbone [109]. This kind of oligomer, containing the peptide ligand cMBP2 binding to hepatocyte growth factor receptor/c-Met, showed enhanced gene delivery efficacy and target-specificity *in vitro* in Huh7 hepatoma and DU145 prostate carcinoma. Upon intravenous application *in vivo* in a hepatocellular carcinoma xenograft mouse model, specific and ligand-dependent gene transfer was detected, but only if combination polyplexes of a ligand-PEG carrier with a non-PEGylated compaction carrier were applied. Using a plasmid encoding the theranostic gene sodium iodide symporter (NIS), radioiodide-mediated tumor detection, and antitumoral activity were demonstrated [107, 161].

In order to achieve improved selectivity and transfection activity, a dual-targeting concept, which simultaneously targets two different overexpressed receptors in tumors, was also investigated. Cyclic RGD peptide, B6 peptide, and the epidermal growth factor receptor targeting peptide GE11 were evaluated. In the investigated DU145 prostate cancer cell culture, which expresses all involved receptors, the most successful pDNA delivery was obtained by the combination of GE11 and B6 ligands [162]. EGFR targeting via peptide GE11 was also used for siRNA lipopolyplexes, which were surface-PEGylated with maleimide–PEG–GE11. These formulations showed potential for EGFR-specific siRNA and miRNA-200c delivery [145].

Transferrin (Tf) as an iron transport protein is targeting the transferrin receptor (TfR) overexpressed in many different malignant cells. Therefore, it was applied as ligand in pLys/pDNA polyplexes [163, 164]. Previously, a Tf–pLys system was used for the preparation of IL-2 gene modified cancer vaccines in the first polyplex *ex vivo* human clinical gene therapy trial [165]. Tf–PEI conjugates were also shown to enhance gene transfection efficiency up to 1000-fold in TfR overexpressing cell lines [132, 166-168]. A Tf–PEG-coated cationic cyclodextrin carrier was very effective in siRNA delivery, which was the basis for the first TfR-targeted *in vivo* siRNA human clinical trial [169].

Zhang et al. [170] combined sequence-defined, histidinylated 4-arm oligomers with Tf–PEI conjugates for efficient TfR-targeted pDNA delivery. An alternative TfR-targeted system was introduced by Prades et al. [171] with applying the retroenantio approach to a peptide that targets TfR; this was found capable to overcome the blood–brain barrier. Based on T-shaped lipo-oligomers, TfR-targeted siRNA polyplexes were generated by post-introduction of INF7 and PEG–Tf or PEG–TfR antibody (TfRab) onto the polyplex surface. These carriers mediated effective target-dependent gene silencing and potent tumor cell killing *in vitro*, as well as a tumor-target specific biodistribution *in vivo,* but limited *in vivo* stability [146].

Folic acid (FA), the vitamin with high-binding affinity to the FA receptor in many tumor types [172], was also effectively incorporated into 2-arm and 4-arm oligomers [109, 110, 112, 173, 174] or lipo-oligomers [147] for pDNA or siRNA delivery. FA–PEG–Stp 2-arms can formulate single influenza peptide INF7 conjugated-siRNA into very small nanoplexes [110]. The INF7 peptide was strictly required for endosomal escape. The analogous siRNA nanoplexes using MTX as targeting and cytotoxic ligand were able to cure mice from KB tumors after intratumoral application [140]. Combination of FA targeted PEGylated 2-arm oligomer with untargeted, 3-arm oligomer by directed disulfide exchange reaction resulted in generation of larger ~100 nm TCP polyplexes, which enabled FA specific gene silencing *in vivo* also upon intravenous administration [174]. Optimization of FA–PEG containing carriers was extended in a library approach, evaluating 2-arms versus 4-arms, different building blocks, presence/absence of buffering histidines or polyplex-stabilizing tyrosine trimers. A two-arm folate-targeted oligomer containing histidines and tyrosine trimers was recognized as the most promising FA-containing carrier for the delivery of both pDNA and siRNA [112]. Folate receptor targeting by PEGylating siRNA lipopolyplexes was developed by Müller et al. [147]. Tetra-γ-glutamyl FA had to be used as targeting ligand; PEGylation with standard FA–PEG (but not FA-free PEG) resulted in nanoparticle aggregation.

For targeting brain tumors, the blood–brain barrier (BBB) or at least the blood–tumor barrier presents a significant bottleneck. A combinatorial approach for effective glioma-targeted siRNA delivery was introduced by An and colleagues [175]. For siRNA lipopolyplex formation, a T-shaped oligoaminoamide was combined with an

angiopep 2 (LRP-targeting peptide) attached via PEG to a sequence-defined 2-arm oligomer (compare **Figure 2E**). After intravenous delivery, receptor-enhanced accumulation in a brain tumor and enhanced gene silencing of a target gene were observed. Similarly, another glioma targeting ligand, I6P7, an interleukin-6 receptor binding peptide derived from IL-6, was included into a similar sequence defined carrier construct for glioma-targeted delivery of pDNA [113]. In this case, a histidinylated carrier version was applied and combined with a histidinylated compaction carrier analogously as described above for c-Met targeting [107]. *In vitro* and *in vivo* results demonstrated transfer across BBB as well as therapeutic antitumoral effects against the brain tumor when pING4 gene transfer was performed [113].

1.2.4 Endosomal escape

Effective endosomal escape to release the entrapped polyplexes into the cytosol is an important event for successful nucleic acid delivery. Otherwise, nucleic acid will be digested during the conversion of endosomes toward lysosomes or recycled to the cell surface and removed out of the cell. Endosomes are intracellular vesicles and mostly serve for sorting, trafficking, and recycling of endocytosed material. Active transport of protons from the cytosol into the vesicle generated by the action of the proton pump ATPase is a reason for acidification of a series of vesicles. Based on the proton sponge hypothesis (**Figure 4A**), Jean-Paul Behr and colleagues [103] screened a series of “proton-sponge” polymers which exhibit weakly basic functionalities with p*K*a values between physiological and endosomal pH. Thus during endocytic trafficking, such polymers would experience increase in protonation. Increased cationization and counterion concentration might be a reason for osmotic swelling and rupture of the endosomes membrane, causing the escape of polyplexes into the cytosol. Such considerations were the basis for the development of polyethylenimine (PEI) as transfection agent [28], or subsequent SPS-based oligoaminoamides [102, 105] utilizing the aminoethylene motif of PEI. Uchida et al. [176] and later on Lächelt et al. [109] showed that oligoaminoethylene building blocks with even numbered amine groups (two or four protonatable nitrogens) have the highest buffer capacity around pH 5–6. Data accumulating during the last two decades rule out a purely osmotic effect for endosomal escape [124, 130, 148, 177-

180]. Direct interaction of protonated, cationized polymer domains with the endosomal phospholipid domain appear as essential for vesicle destabilization. In addition, free polycations (not bound to polyplexes) were found to critically contribute to gene delivery [181-184], and instead of complete lysis, only partial vesicle disruption was observed [180]. Contrary to aforementioned observation regarding pDNA polyplexes [176], in the case of mRNA, polyplexes with odd number aminoethylene motif showed enhanced mRNA transfection efficacy compared to building blocks with even number of repeats [185]. It was concluded that high endosomal escape capability of even numbered amino groups resulted in less effective system due to its low cytoplasmic stability. Therefore the balance between endosomal escape and stability of mRNA in the cytoplasm should be established. The same group improved endosomal escape with polyplex nanomicelles prepared by self-assembly of PEGylated poly(amino acid) block copolymer for *in vivo* mRNA transfection into the central nervous system [186, 187]. Another proof of importance of the balance between good buffering capacity and sufficient stability of mRNA complexes was shown by Dohmen et al. who observed favorable endosomal release of (2-3-2) tetramine *in vitro* and *in vivo* [188].

A)

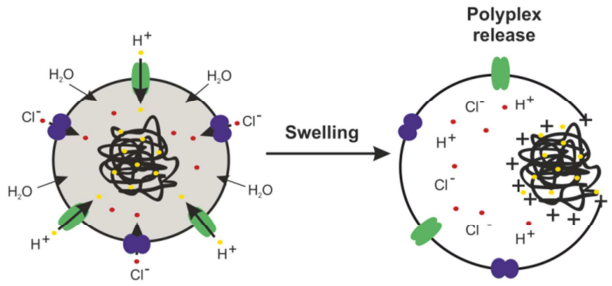

B)

INF7	GLFE AIEG FIEN GWEG MIDG WYGC
H5WYG	GLFH AIAH FIHG GWHG LIHG WYG
JTS-1	GLFE ALLE LLES LWEL LLEA
KALA	WEAK LAKA LAKA LAKH LAKA LAKA LKAC EA
LAH4	KKAL LALA LHHL AHLA LHLA LALK KA
Melittin	GIGA VLKV LTTG LPAL ISWI KRKR QQ

Figure 4 Strategies for endosomal escape. **(A)** Schematic presentation of endosomal release by the proton sponge effect. Note that beyond osmotic swelling, direct destabilization of the phospholipid domain by the cationized polymer domains contributes to endosomal escape. **(B)** Membrane destabilization by amphiphilic lytic peptides.

Nonprotonatable polymers such as polylysine can be converted into proton sponges. It is known that histidinylation of polylysine or PEI offers higher endosomal buffer capacity based on a p*K*a around 6 of the imidazole groups; therefore, protonatable histidines were introduced into sequence-defined oligolysine-based carriers [73-77, 84, 107, 109, 112, 189-194]. Consequently, total buffer capacities as well as nucleic acid transfer increased both *in vitro* and *in vivo*. Several groups reported about positive effect of histidines in the structures. Incorporation of histidines into a peptide of Cys-His-$(Lys)_6$-His-Cys improved *in vitro* gene expression also in the absence of chloroquine as described by McKenzie et al [84]. Read and colleagues reported efficient intracellular delivery of siRNA and mRNA with histidine-rich reducible polycations [82]. The lab of Mixson developed a series of branched (HK) peptides containing lysines for nucleic acid binding and histidines for endosomal-buffering [73]. They further modified HK peptides of different length by adding histidine-rich tails. Thus, increased buffer capacity further improved transfection efficiency [76]. Gonçalves et al. also reported about efficiency of acid-protonable groups in histidine-rich polymer and improved pDNA as well as mRNA transfection [194].

The proton sponge effect is not the only solution to overcome the endolysosomal entrapment. In fact, previous studies with (non-proton sponge) polylysine carriers already had shown that integration of fusogenic peptides (**Figure 4B**) such as influenza-derived INF1-7, JTS-1, or H5WYG into polylysine/pDNA polyplexes improved gene transfer significantly. The latter mentioned peptides mimic the functions of viral proteins and enable permeabilization of the endosomal membrane triggered by acidification of endosomes [195-197]. As reported by Dohmen et al. [110], the endosomolytic peptide INF7, originally designed as the glutamic acid-enriched analog of the influenza hemagglutinin membrane protein HA2 N-terminus, was coupled to the 5'-end of the siRNA sense strand, which maintains its silencing efficiency with increased endosomal escape when formulated into nanoplexes INF7 also greatly improved TfR-targeted siRNA lipoplexes when incorporated by post-modification of lipoplex surface [146]. Artificial amphipathic cationic peptides such as KALA and LAH4, or derivatives of the bee venom melittin facilitated significantly improved gene transfer [198-200]. The latter peptides own two important properties for efficient gene transfer - possibility of DNA binding and destabilization of membranes. The positive charge of KALA allows electrostatic interactions with the

negatively charged pDNA. However, the positive charged amphiphile KALA can also interact with the endosomal membrane and consequently can cause membrane leakage [198]. Next, partially mimicking the proton sponge activity of PEI and presence of histidine residues are responsible for improved endosomal escape in the case of LAH4 [199]. Boeckle et al. [200] showed that melittin–PEI conjugates can enhance gene transfer, but also cause high toxicity due to lysis of the plasma membrane. Therefore, modifications with acidic residues (glutamic acid or histidine) should allow high lytic activity at acidic pH to induce membrane destabilization in endosomes. Polyacridine peptides modified with melittin (by either a maleimide-Cys or a thiopyridine-Cys linkage) were used in pDNA transfection with efficacies as high as for PEI [86]. And Bettinger et al. [90] demonstrated high efficiency of the PEI 2 kDa–melittin conjugate in mRNA delivery in post-mitotic primary cells. Also others peptides called cell-penetrating peptides (CPPs) promote endosomal escape, for example, PepFect6 [91] and PepFect14 [201].

In case of cationic lipoplexes, endosomal escape may occur through local, transient perturbations of the endosomal membrane by lipid mixing; cationic lipids possess the ability to form nonbilayer structures and charge neutral ion pairs with the negatively charged phospholipids (shift to the inner part of endosome caused by lipoplexes) [202]. Analogously, incorporation of fatty acids into polycation structures presents another option for generating amphiphilic characteristics that facilitate endosomal escape. The group of Lu generated lipo-oligomer carriers for pDNA and siRNA delivery, with two oleic acid residues triggering a pH-dependent disruption of lipid membranes [92]. Also Schaffert, Fröhlich, and colleagues generated lipo-oligomer carriers based on oligoaminoamides, which were modified with pairs of fatty acids incorporated at terminal lysine amines in i-, T-, or U-shaped topologies [105, 106, 117]. The type of incorporated fatty acid had more influence on the performance than the topology. Oligomers modified with the unsaturated (C18) fatty acids oleic acid and linoleic acids demonstrated best transfection efficiency due to endosomal pH-specific lytic activity. Furthermore, myristic acids (C14) caused high, but pH-independent lytic activity but also cytotoxic effects. Recently, Klein et al. [104] designed T-shaped oligomers containing a bioreducible disulfide bond between the cationic and lipid building block. Thus, the carriers would dissociate via GSH-mediated cleavage in the cytosol into nontoxic fragments leading to enhanced

intracellular nucleic acid release while improving polyplex stability in the extracellular space. Using this strategy, bis-myristyl and bis-cholanic acid based lipo-oligomers should enable high lytic activity, high siRNA delivery and silencing activity in the absence of cytotoxicity.

1.2.5 Cargo release and nuclear delivery

Polyplex stability is a critical issue for extracellular delivery, where high stability is of highest importance; it also is a critical parameter in intracellular delivery and subsequent cargo release at the target site, where nucleic acid release or at least exposure in bioactive form is important. To mediate gene silencing, siRNA and miRNA need only to reach the cytoplasm for incorporation into the RISC complex. For pDNA, further transport through the cytoplasm toward the nucleus (before or after endosomal escape, with or without complexation with cationic carrier), entry across the nuclear envelope, and accessibility for transcription are required.

Events following endosomal escape (fate of the polymer, nucleic acid, and different sortings of endosome) are still poorly understood. In fact, cargo release and productive delivery very much depend on the specific cargo size, the carrier, cell type, and different intracellular routes [203, 204]; it is impossible to provide a general statement on the fates. First of all, even with effective nanoparticle systems, endosomal release is a rare event and bottleneck in the delivery process, therefore subsequent steps are difficult to track [180, 205, 206]. Even with potent siRNA LNPs, only 1–3% of internalized siRNA molecules were delivered into the cytosol [207, 208]. For these LNPs, a narrow window of siRNA release from maturating endosomes approximately 5–15 min after internalization was observed. Releasing endosomes were recognized by cytosolic galectin-8/-9, which target them for autophagy [208]. Moreover, exocytosis of recycling siRNA nanoparticle-loaded vesicles was identified as a limitation [209]. In a different study, gene silencing potency correlated with intracellular siRNA lipopolyplex stabilization instead of early endosomal exit [210].

Only few studies have been performed comparing lipoplexes (e.g. lipofectamine) and polyplexes (with PEI), but significant differences were observed in the intracellular delivery steps [180, 202, 211, 212]. Endosomal escape of lipoplexes by mixing of

cationic lipids with the negatively charged phospholipids of endosomal membranes should release nucleic acids in lipid-free form [202, 213]. For some lipoplex-mediated transfection using oligocationic lipids, however, despite effective nuclear delivery of pDNA, an insufficient release and availability for transcription were reported as possible limitation for gene transfer [214]. For polyplexes, the site of release from polycations such as PEI is even less clear, although delivery of small polyplexes was been reported. Interestingly, free PEI was found to not only enhance endosomal escape, but also assist in transfer of pDNA into the nucleus (by ~5-fold), enhance the pDNA-to-mRNA transcription efficiency (by ~4-fold), and facilitate the nucleus-to-cytosol translocation of mRNA (by 7–8-fold) [184].

Nuclear import is a crucial size-dependent process, and presents the next important barrier for delivery of larger nucleic acids such as pDNA [12]. The nuclear pore complex (NPC) only allows the passage of small molecules such as oligonucleotides [180, 215, 216] whereas polyplexes greater than ~50 nm do not have this capacity. In that case, nuclear entry relies on nuclear membrane breakdown during cell division process [217]. The importance of the nuclear import step has been demonstrated in cell cycle studies. Transfection efficiency of branched PEI polyplexes was strongly enhanced in the G2/M phase, when the nuclear envelope breaks down. In contrast, linear PEI polyplexes showed lower cell cycle dependence. Conjugation of short cationic nuclear localization signals (NLS) peptide for an active, targeted transport through the NPC has been evaluated as a possible solution for cell-cycle independent gene transfer [12, 18-20, 218]. The exact conditions to successfully utilize the properties of NLS peptides are still unclear and therefore only a small number of carriers which could reach the nucleus have been described [157, 219-224]. Further optimizations of nuclear import are required for improved pDNA delivery into non-dividing cells.

1.3 Challenges of *in vivo* delivery

In vivo delivery faces several additional hurdles. As mentioned in previous chapter, polyplex shielding and receptor-targeting are possible measures to avoid undesired reactions such as innate immune responses and to provide some specificity upon systemic administration, for example, in passive or active tumor targeting [127, 128]. For this purpose, numerous targeting ligands for various cell surface receptors have been evaluated *in vivo* [9, 69, 107, 113, 132, 160, 161, 169, 175, 210, 225-232]. The polyplex size may be at least as crucial for *in vivo* performance as the ligand selection; for example, free siRNA or nanoparticles exhibiting a size of approximately 6 nm are quickly cleared by the kidney [110, 233]. Passive targeting of blood-circulating nanoparticles by the EPR effect (enhanced permeability and retention of tumor tissue) offers polyplexes of a size of 20 nm up to 400 nm distribution into solid tumors via leaky vasculature [234, 235]; the EPR effect, however, can be tumor type- and patient-specific and also heterogeneous within tumors. Polyplex delivery may be ineffective in less vascularized tumors [236]. For tumors such as stroma-rich pancreatic cancer, only smaller nanoparticles were effective [237]. Despite the many efforts, the efficiency of tumor targeting is still low; Chan and colleagues reviewed published work and concluded that on average only 0.7% of the dose is accumulating at the target tumor site [238]. Apart from targeting, shielding, and nanoparticle size, the stability of polyplexes is an additional challenge for *in vivo* performance; thus, additional measures such as bioreversible internal covalent cross-linkage of polyplexes or incorporation of bioresponsive domains into carriers for noncovalent stabilization have to be investigated [129, 144, 239-242].

Another critical aspect for *in vivo* gene delivery is the reduction of polyplex- and carrier-triggered toxicity. The transfection efficiency of frequently used high molecular weight PEI goes hand in hand with an N/P dependent cytotoxicity; mechanistic details are reviewed in Hall et al. [130]. Nevertheless, linear PEI has already been developed for clinical application with encouraging results [243]. The therapeutic window in systemic administration and wider therapeutic use still would strongly benefit from reduced carrier cytotoxicity. In that view, degradable PEI analogs are highly desirable [244]. In this regard, SPS offers excellent opportunities to design structurally precise carriers with cysteine residues for cleavable linkages. During

polyplex formation, the cysteines form bioreducible disulfides and thus enhance stability in the extracellular part of the gene delivery process. When having reached the bioreductive environment of the cytosol, bioreducibility of the polyplexes enhances cargo release and also cause fragmentation of the carriers into smaller less toxic pieces [65, 81, 82, 84, 85, 105, 114].

1.4 Optimization of DNA vectors for enhanced gene transfer

Apart from enhancing the gene transfer process by improving carrier molecules, DNA vectors can also be optimized [245-248]. Standard plasmids contain a eukaryotic expression cassette (the gene of interest and regulatory sequences) and a backbone, including bacterial sequences. Antibiotic resistance-encoding genes and the origin of replication are necessary to maintain and amplify pDNA vectors in the bacterial hosts. However, bacterial sequences, including CpG dinucleotide motifs, reduce the efficacy, biocompatibility, and safety of pDNA vectors. Regulatory agencies recommend avoidance of antibiotic resistance-encoding genes in production of plasmids for therapeutic use [249]. Minicircle (MC) DNA contains only the therapeutic gene of interest and regulatory sequences. Bacterial backbone sequence and antibiotic-resistant genes are excluded. This may result in reduced risk of spreading antibiotic-resistant genes, enhanced immunocompatibility, improved transfer efficiency, and prolonged transgene expression compared to those of standard plasmids [250-255]. In fact, MC DNA has already displayed greatly improved transgene expression in several *in vitro* [22, 256, 257] and *in vivo* studies [252-255, 258-270].

1.5 Aim of the thesis

Although non-viral vectors have reached clinical evaluation and encouraging therapeutic effects [271-273], the safety and efficiency of non-viral systems still need to be improved for broader application in gene therapy. DNA plasmid vectors are easy to produce, formulate, and store [8-10]. In theory, pDNA vectors ultimately need to enter the cell nucleus for expressing the encoded genes, but in practice, numerous additional extracellular and intracellular barriers also have to be overcome [8, 9, 12, 13, 274, 275]. Gene transfer can be facilitated by physical and biochemical DNA delivery techniques. For example, nanosized polyplexes are formed by complexation of negatively charged nucleic acid with positively charged cationic oligomers [8, 9, 12]. Recently, precise analogs of linear polyethylenimine (linPEI), a frequently used transfection carrier, [29, 243, 276] were generated by solid-phase supported syntheses [101, 105]. By this sequence-defined assembly process, libraries of oligoaminoamides can be generated presenting different functional modifications (nucleic acid compaction and nanoparticle stabilization, surface shielding, receptor binding, endosomal escape) in defined topologies, which might be most suitable for the specific cargo and application [107, 109, 112, 115-117]. Besides improving carrier molecules, optimization of DNA vectors is also possible [245-248]. Reduced efficacy, biocompatibility, and safety of pDNA vectors is the consequence of antibiotic resistance-encoding genes and the origin of replication in the pDNA which are necessary to maintain and amplify pDNA vectors in the bacterial hosts. Therefore, the use of minicircle (MC) DNA without bacterial backbone sequence and antibiotic-resistant genes offers several advantages [250-255].

The first aim of the thesis was the evaluation of the efficiency and comparison of physicochemical and transfection characteristics of polyplexes formed with sequence-defined oligoaminoamides and either pDNA (pCMV-luc) or MC DNA (MC07.CMV-luc). Properties like size, stability, compaction and gene transfer should be analyzed. Untargeted as well as receptor-targeted DNA complexes had to be used in this study. The well-known transfection polymer linPEI was to be included as transfection standard.

The second aim of the thesis was to explore the requirements of efficient carriers for mRNA delivery. For this purpose, different sequence-defined oligoaminoamides, previously synthesized for the purpose of pDNA or siRNA delivery, should be screened. The main focus was to be put on oligomers containing tyrosine tripeptides or/and fatty acids in the structure. Biophysical characterization and transfection characteristics of those oligomers should be examined and compared. This study aimed at the investigation of oligomer structure – transfection activity relationships.

2 Materials and Methods

2.1 Chemicals and reagents

Cell culture media and antibiotics were purchased from Invitrogen (Karlsruhe, Germany), fetal bovine serum (FBS) from Life Technologies (Carlsbad, USA), Trypsin/EDTA and collagen from Biochrom (Berlin, Germany), HEPES from Biomol GmbH (Hamburg, Germany), glucose from Merck (Darmstadt, Germany) and WFI from B. Braun (Melsungen, Germany). Luciferase cell culture lysis buffer and D-luciferin sodium salt were obtained from Promega (Mannheim, Germany), CellTiter-Glo® from Promega (Wisconsin, USA), thymidine, DAPI (4′,6-diamidino-2-phenylindole), MTT (3-(4,5-dimethylthiazol-2-yl)-2,5-diphenyltetrazolium bromide), dimethyl sulfoxide (DMSO) and ethidium bromide (EtBr) from Sigma-Aldrich (Munich, Germany) and GelRed™ was obtained from Biotum (Hayward, USA). All flasks and multi-well plates were manufactured by TPP (Trasadingen, Switzerland). LinPEI was synthesized by Wolfgang Rödl, LMU Pharmaceutical Biotechnology as described in [277] and succPEI was resynthesized by Dr. Ulrich Lächelt as described in [278]. Sequence-defined oligomers were synthesized by Dr. Stephan Morys, Dr. Ulrich Lächelt, Dr. Philipp Klein, Sören Reinhard, Dr. Dongsheng He and Dr. Christina Troiber, all from LMU Pharmaceutical Biotechnology.

2.2 Vectors

pCMV-luc encoding firefly luciferase under control of the CMV promoter (PF461) and MC07.CMV-luc as applied in work described in section 3.1 were produced and purified by PlasmidFactory GmbH (Bielefeld, Germany). Note that pCMV-luc is different from pCMVL frequently used in other work of our laboratory.

mRNA-luc encoding firefly luciferase and mRNA-EGFP encoding enhanced green fluorescent protein as applied in work described in section 3.2 were produced, purified and provided by ethris GmbH.

2.3 Biophysical characterization

2.3.1 Polyplex formation

2.3.1.1 pDNA polyplex formation

Indicated amounts of pCMV-luc or MC07.CMV-luc and the calculated amounts of oligomer or oligomers combination at indicated N/P (nitrogen/ phosphate) ratios were diluted in separate tubes of equal volumes of HBG (20 mM of HEPES, 5% glucose, pH 7.4) each. Only protonatable nitrogens of the Stp units and N-terminal amines of cysteine residues were considered in the N/P calculations. In the case of oligomers combination, cmb-targeted oligomer was mixed with three-arm oligomer at an optimized 70:30 cationic ratio to reach the total N/P ratio of 6 or 12 prior to polyplex formation with the DNA. The oligomer solution was added to the nucleic acid solution, mixed by pipetting, and incubated for 30 min at room temperature under exposure to air oxidation in a closed Eppendorf reaction tube.

2.3.1.2 mRNA polyplex and lipopolyplex formation

Indicated amounts of mRNA-luc or mRNA-EGFP and the calculated amounts of oligomer at indicated N/P (nitrogen/ phosphate) ratios were diluted in separate tubes of equal volumes of WFI (water for injection), HBS (20 mM of HEPES, pH 7.4) or HBG (20 mM of HEPES, 5% glucose, pH 7.4) each. The nucleic acid solution was added to the oligomer solution, mixed by pipetting, and incubated for 30 min at room temperature under exposure to air oxidation in a closed Eppendorf reaction tube.

2.3.2 Particle size and zeta potential measurement

Particle size and zeta potential of formulations were measured in a folded capillary cell (DTS 1070) by dynamic laser-light scattering using a Zetasizer Nano ZS with backscatter detection (Malvern Instruments, Malvern, United Kingdom). For the measurement of pCMV-luc or MC07.CMV-luc particles (section 3.1), experiments were performed with 2 µg of nucleic acid and oligomer or oligomers combination at N/P ratio 12 in a total volume of 200 µL of HBG. For the measurement of mRNA-luc particles (section 3.2), particles were prepared with 2.5 µg of nucleic acid and oligomer at N/P ratio 12 in a total volume of 200 µL of HBS or HBG. For size

measurements, the equilibration time was 0 min, the temperature was 25°C, and an automatic attenuator was used. The refractive index of the solvent was 1.330, and the viscosity was 0.8872 mPa s; the refractive index of polystyrene latex (1.590) was fixed. Results were plotted as Z-Average and standard deviation (SD) out of three runs, with 12 sub-runs each. For zeta potential measurements, the samples were diluted to 800 µL in 20 mM of HEPES buffer (pH 7.4). Zeta potentials were calculated by the Smoluchowski equation and are displayed as an average (mV) of three runs with up to 15 sub-runs each.

2.3.3 Agarose gel-shift assay for mRNA binding

For mRNA gel-shift assay, a 1% agarose gel was prepared by dissolving agarose in TBE buffer (trizma base 10.8 g, boric acid 5.5 g, disodium EDTA 0.75 g, in 1 L of water) and boiling it up to 100 °C. Afterwards, GelRed for the detection of the nucleic acid was added and the agarose solution was casted in the electrophoresis unit and left to form a gel. Polyplexes and lipopolyplexes were prepared as described above containing 250 ng of mRNA-luc in 20 µL HBG. Then, 4 µL of loading buffer (prepared from 6 mL of glycerol, 1.2 mL of 0.5 M EDTA, 2.8 mL of H_2O, 0.02 g of bromophenol blue) were added to each sample before they were placed into the sample pockets. Electrophoresis was performed at 120 V for 80 min.

2.3.4 Ethidium bromide compaction assay and polyanionic stress test

Polyplexes containing 2 µg of pCMV-luc or MC07.CMV-luc were formed at N/P ratio 12 in a total volume of 200 µL of HBG. In parallel to these polyplexes, the following were prepared: HBG buffer (blank value), linPEI polyplexes, and 2 µg of pCMV-luc or MC07.CMV-luc in 200 µL of HBG buffer, which was considered as maximum ethidium bromide (EtBr) fluorescence intensity (100% value) (section 3.1). For the compaction study of mRNA particles (section 3.2), particles were prepared as described above with 2 µg of mRNA-luc at N/P ratio 12. HBG buffer, succPEI polyplexes, and 2 µg of mRNA-luc in 200 µL of HBG buffer were also prepared at the same time. After a 30 min incubation time, 700 µL of EtBr solution (c = 0.5 µg/mL) was added to each sample. The fluorescence intensity of EtBr was measured after an additional 3 min incubation at the excitation wavelength ex = 510 nm and

emission wavelength em = 590 nm using a Cary Eclipse spectrophotometer (Varian, Germany). The fluorescence intensity of EtBr was calculated in relation to the 100% value. To investigate polyplex stability against polyanionic stress, 250 IU of heparin-sodium-25000 (Ratiopharm, Ulm, Germany) was added to the each sample after EtBr addition, and the fluorescence intensity of EtBr was measured again.

2.3.5 mRNA lipopolyplexes under reducing conditions

Lipopolyplexes containing 2 µg of mRNA-luc were formed at N/P ratio 12 in a total volume of 200 µL of HBG. In parallel to these lipopolyplexes, the following were prepared: HBG buffer (blank value), succPEI polyplexes, and 2 µg of mRNA-luc in 200 µL of HBG buffer, which was considered as maximum ethidium bromide (EtBr) fluorescence intensity (100% value). After lipopolyplex incubation, 50 µL of a GSH solution (50 mM, pH 7.4) was added to the lipopolyplex solution. Consequently, the resulting solutions had the final concentrations 10 mM. The solutions were incubated at 37°C for 90 min. A 700 µL of EtBr solution (c = 0.5 µg/mL) was added to each sample and an ethidium bromide compaction assay (see section 2.3.4) was performed.

2.3.6 Transmission electron microscopy

For transmission electron microscopy (TEM), samples were prepared with 200 ng of pCMV-luc or MC07.CMV-luc and oligomer or oligomers combination at N/P ratio 12 in Millipore water. The formvar/carbon-coated 300 mesh copper grids (Ted Pella, Inc., Redding, CA) were activated by mild plasma cleaning. Then, the copper grids were incubated with 20 µL of the polyplex solution for 2.5 min. Excess liquid was blotted off using filter paper. Prior to staining, the copper grids were washed with 5 µL of staining solution for 5 s. Afterwards, the copper grids were incubated with 5 µL of a 2% aqueous uranylformate solution for 20 s. Excess liquid was again blotted off using filter paper, followed by air-drying for 30 min. Samples were then characterized using a JEM-1011 (Jeol, Freising, Germany) operating at 80 kV.

2.4 Biological characterization *in vitro*

2.4.1 Cell culture

Human prostate cancer cell line (DU145) was cultured in RPMI-1640 medium, mouse neuroblastoma cells (N2a), hepatocellular carcinoma cells (Huh7) and breast adenocarcinoma (MDA-MB-231) were grown in Dulbecco's modified Eagle's medium (DMEM) and cervix carcinoma (KB) cells were grown in folate free RPMI-1640 medium. All cell culture media were supplemented with 10% fetal bovine serum (FBS), 4 mM of stable glutamine, 100 IU/mL of penicillin, and 100 lg/mL of streptomycin. All cell lines were cultured at 37°C and 5% CO_2 in an incubator with a relative humidity of 95%.

2.4.2 Determination of HGFR/c-Met expression on DU145 cell line

A total of $1x10^6$ cells in 100 µL of FACS buffer (10% FBS in PBS) were incubated with the monoclonal mouse anti-human HGFR/c-Met antibody (1:200 dilution) or IgG control for mouse primary antibodies (1:100 dilution) for 1 h on ice. Afterwards, the cells were washed twice with FACS buffer. The cells were then stained with Alexa 488-labeled goat anti-mouse secondary antibody (1:400 dilution) for 1 h on ice, washed, counterstained with DAPI (1 µg/mL), and analyzed on a Cyan ADP Flow Cytometer (Dako, Hamburg, Germany) using Summit acquisition software (Summit, Jamesville, NY). DAPI fluorescence was excited at 405 nm and detected with a 450/50 bandpass filter; Alexa-488 fluorescence was excited at 488 nm and detected with a 530/40 nm bandpass filter. The percentage of HGFR/c-Met positive cells was determined as compared to control IgG stained cells.

2.4.3 Luciferase assay

2.4.3.1 Luciferase gene transfer of DNA polyplexes

DU145 cells (10000 cells/100 µL) were seeded 24 h prior to nucleic acid delivery in 96-well plates. Transfection efficiency of oligomers was evaluated using 200 ng of pCMV-luc or MC07.CMV-luc per well. Additionally, 320 ng of pCMV-luc per well were used in the case of equimolar experiment. Polyplexes were formed at different N/P ratios in a total volume of 20 µL of HBG. linPEI (N/P 9) was used as a positive control, and HBG buffer was used as a negative control. Before treatment, the cell culture medium was exchanged with 80 µL of fresh medium containing 10% FBS. Polyplex solution was added to each well and incubated on cells at 37°C for a determined period of time (0.75 or 24 h). In the case of 0.75 h incubation time, medium was replaced 0.75 h after transfection by fresh medium, and cells were further incubated for 23 h. In the case of 24 h incubation time, cells were incubated with polyplex solution for 24 h after initial transfection. All experiments were performed in quintuplicate. For all experiments 24 h after initial transfection, cells were treated with 100 µL of luciferase cell culture 5x lysis buffer. Luciferase activity in the cell lysate was measured by using a Centro LB 960 plate reader luminometer (Berthold Technologies, Bad Wildbad, Germany) and LAR buffer supplemented with 1 mM of luciferin solution. Transfection efficiency was evaluated as relative light units (RLU) per well (10000 cells).

2.4.3.2 Luciferase transfer of mRNA polyplexes and lipopolyplexes

One day prior to nucleic acid delivery 10000 DU145, N2a, Huh7, MDA-MB-231 and 8000 KB (on collagen coated plates) cells/well in 96-well plates were seeded. Transfection efficiency of oligomers was evaluated using 250 ng of mRNA-luc per well. Polyplexes were formed at N/P ratio 12 in a total volume of 20 µL of WFI, HBS or HBG. WFI, HBS and HBG buffers were used as negative controls. LinPEI (N/P 9), brPEI (N/P 10) and succPEI 10% (w/w 4) were used as positive controls. Before treatment, the cell culture medium was exchanged with 80 µL of fresh medium containing 10% FBS. Nanoparticle solution was added to each well and incubated on cells at 37°C for 24 h. All experiments were performed in triplicates. For all experiments 24 h after initial transfection, cells were treated with 100 µL of luciferase cell culture 5x lysis buffer. Luciferase activity in the cell lysate was assayed by

luminometer as described above. Transfection efficiency was evaluated as relative light units (RLU) per well.

2.4.4 Cell synchronization and cell cycle status analysis

Double-thymidine block was used to induce cells to be arrested at different phases of a cell cycle. DU145 cells were seeded 24 h prior to treatment with thymidine into 12-well plates with a density of $7.5x10^4$ cells in 1000 µL of growth media. For double-thymidine block treatment, cells were treated with 2.5 mM of thymidine (Sigma–Aldrich) in growth media for 16 h (first block). Afterwards, cells were washed twice with PBS, and then fresh growth media without thymidine was added to the cells for another 10 h (first release). Then, the thymidine-free growth media was replaced with fresh medium with 2.5 mM for another 16 h (second block). At the end of second block, the cells were washed twice with PBS and released in thymidine free growth medium (second release). Cells were collected at different time points of second release and centrifuged and incubated on ice for 3 h in 100 µL of propidium iodide staining solution (0.1% sodium citrate, 0.1% Triton X-100, and 50 µg/mL of propidium iodide). Thereafter, cells were washed, taken up in PBS, and the cell cycle was analyzed by flow cytometry at an excitation wavelength of 488 nm and detection of emission with a 613/20 bandpass filter. Cells were gated by forward/sideward scatter and pulse width for exclusion of doublets. For each time point, 20000 cells were analyzed. Data were recorded by Cyan ADP flow cytometer (Dako) using Summit acquisition software (Summit) and analyzed by FlowJo 7.6.5 flow cytometric analysis software.

2.4.5 Cell cycle dependent transfections

DU145 cells were seeded 24 h prior to treatment with thymidine into 96-well plates with a density of $7.5x10^3$ cells in 100 µL of growth media. A double-thymidine block was applied, as described above, to synchronize cells in specific phases of cell cycle. At the end of the second block, the cells were washed twice with phosphate-buffered saline (PBS) and released in 80 µL of thymidine free growth medium (second release). Polyplexes were prepared as described containing 200 ng of pCMV-luc or

MC07.CMV-luc in 20 µL of HBG. Polyplex solutions were added to each well at different time points (0, 6, 8, or 12 h) after second release. Transfection medium was replaced after 45 min at 37°C, and cells were further incubated at 37°C for 24 h. All experiments were performed in quintuplicate. Afterwards, luciferase activity in the cell lysate was determined as described above, and metabolic activity of transfected cells as described below.

2.4.6 Metabolic activity of transfected cells

2.4.6.1 MTT assay

The cells were transfected as described in section 2.4.3.1. At 24 h after initial transfection, 10 µL of MTT (3-(4,5-dimethylthiazol-2-yl)-2,5-diphenyltetrazolium bromide) was added to each well, reaching a final concentration of 0.5 mg/mL. Medium with unreacted dye was removed after an incubation time of 2 h at 37°C. The 96-well plates were stored at -80°C for at least 1 h, and afterwards the purple formazan product was dissolved in 100 µL dimethyl sulfoxide per well. The absorbance was determined by using a microplate reader (Tecan Spectrafluor Plus, Tecan, Switzerland) at 530 nm with background correction at 630 nm. The relative cell viability (%) related to the buffer-treated control cells was calculated as ([A] test / [A] control)x100%.

2.4.6.2 CellTiter-Glo® assay

The cells were transfected as described in section 2.4.3.2. At 24 h after initial transfection, the medium in the well was replaced by 50 µL of fresh medium and 50 µL of CellTiter-Glo® Reagent (Promega, USA). The relative metabolic activity was determined as the ratio of measured luminescent signal proportional to the amount of ATP present over the signal of untreated cells. For this purpose Centro LB 960 plate reader luminometer (Berthold Technologies, Bad Wildbad, Germany) was used.

2.4.7 EGFP expression

DU145 cells were seeded in 24-well plates at the density 50000 cells/well. On the following day, cells were transfected with lipopolyplexes formed with 1.5 µg of mRNA-EGFP at N/P ratio 12 in a total volume of 100 µL of HBS or HBG. 24 h after transfection, cells were washed with 500 µL PBS, detached with trypsin/EDTA and resuspended in PBS with 10% FCS. Samples were analyzed for EGFP expression using flow cytometry (Cyan™ ADP flow Cytometer - Dako, Hamburg, Germany) and Summit acquisition software - Summit, Jamesville, NY, USA) and analyzed by FlowJo 7.6.5 flow cytometric analysis software.

2.4.8 Fluorescence microscopy

DU145 cells were seeded in 8-well chamber slides at a density 30000 cells/well. The next day, culture medium was replaced with 240 µL fresh growth medium. mRNA polyplexes at N/P ratio 12 in 60 µL HBS or HBG, containing 750 ng mRNA-EGFP were added to each well and incubated at 37°C for 24 h. After 24h, cells were washed twice with 500 µl PBS and fixed with 4 % PFA solution for 30 min at room temperature. Pictures were obtained using Zeiss Axiovert 200 fluorescence microscope (Carl Zeiss AG, Germany).

2.4.9 Statistical analysis

Results are presented as arithmetic mean ±SD and the number of replicates. Statistical significances were analyzed using Student's two-tailed t-test. Significance levels were indicated with the following symbols: ns, $p > 0.05$; * $p \leq 0.05$; ** $p \leq 0.01$; *** $p \leq 0.001$; and **** $p \leq 0.0001$.

3 Results

3.1 Minicircle versus plasmid DNA delivery by receptor-targeted polyplexes

This chapter has been adapted from:
A. Krhac Levacic, S. Morys, S. Kempter, U. Lächelt and E. Wagner. Minicircle versus plasmid DNA delivery by receptor-targeted polyplexes. Human Gene Therapy 28(10) (2017) 862-874

Minicircle (MC) DNA presents a promising alternative to plasmid DNA (pDNA) for non-viral gene delivery in terms of biosafety and improved gene transfer. Here, luciferase pDNA (pCMV-luc) and analogous MC DNA (MC07.CMV-luc) were formulated into polyplexes with c-Met targeted, PEG-shielded sequence-defined oligoaminoamides, or linear PEI (linPEI) as standard transfection agent. Distinct physicochemical and biological characteristics were observed for polyplexes formed with either pDNA or MC DNA as vectors.

3.1.1 Vector constructs and polyplex design

pCMV-luc or MC07.CMV-luc were used for polyplex formation (see **Figure 5A**). pCMV-luc is a double-stranded plasmid DNA of 6233 bp encoding the firefly luciferase reporter gene under control of the cytomegalovirus promoter, while MC07.CMVluc is smaller MC DNA (3881 bp) encoding the same gene under the same promoter. For formulation of DNA, linPEI was used as established and effective standard polymeric carrier [29, 243, 276]. Four sequence-defined cationic oligoaminoamides were generated (**Figure 5B** and **Table 1**) by solid-phase assisted synthesis using Fmoc-based peptide synthesis technology. Repeats of the artificial amino acid succinoyl-tetraethylenepentamine (Stp) alternating with natural histidines served as the central cores for nucleic acid complexation and endosomal buffering function. Terminal cysteines provide disulfide-mediated stabilization of DNA polyplexes. Lysine residues were integrated as branching units, providing non-

targeted carriers with three-arm topology (3-arm, 3-arm-Y; see **Figure 5B**, left). Alternatively, one cationic arm was replaced by polyethylene glycol PEG24 and the c-Met targeting peptide cmb [159, 279, 280] (cmb-PEG, cmb-PEG-Y; see **Figure 5B**, right). PEG24 (containing a precise chain length of 24 oxyethylene units) was chosen to shield polyplexes against unspecific interactions [107, 108], and the cmb-ligand to trigger receptor-mediated endocytosis, as recently demonstrated [107, 159, 161]. Oligomers three-arm (***689***) and cmb-PEG (***442***) were previously described [107]. The additional incorporation of tyrosine trimers (Y_3) had been found advantageous for aromatic and hydrophobic polyplex stabilization [112, 116]. Therefore, in the current study, the Y_3-containing analogous carriers, three-arm-Y (***849***) and cmb-PEG-Y (***852***), were also synthesized. Efficient DNA compaction (**Figure 5C**) is an important requirement for gene transfer. Recent work from our lab revealed suboptimal pDNA packaging by cmb-PEG; apparently, the PEG shielding domain interfered with DNA condensation (**Figure 5C**, top) [107, 108]. The PEG-free three arm oligomer and also the cmb-PEG/three-arm (7:3 mol/mol) carrier combination (**Figure 5C**, bottom) effectively compacted DNA, resulting in effective pDNA gene transfer *in vitro* and *in vivo* [107]. For this reason, combination polyplexes were also analyzed in the current comparison of pDNA and MC DNA polyplexes.

Table 1 List of oligomers included in this study.

Structure (from C- to N-terminus)	ID	Abbreviation
K-α[cMBP2]- ε[PEG_{24}-H-K-α,ε -[(H-Stp)$_4$-H-C]$_2$]	***442***	cmb-PEG
K-α[cMBP2]- ε[PEG_{24}-H-K-α,ε -[(H-Stp)$_4$-H-Y_3-C]$_2$]	***852***	cmb-PEG-Y
C-H-(Stp-H)$_3$-K-α,ε[(H-Stp)$_3$-H-C]$_2$	***689***	3-arm
C-Y_3-H-(Stp-H)$_3$-K-α,ε[(H-Stp)$_3$-H-Y_3-C]$_2$	***849***	3-arm-Y

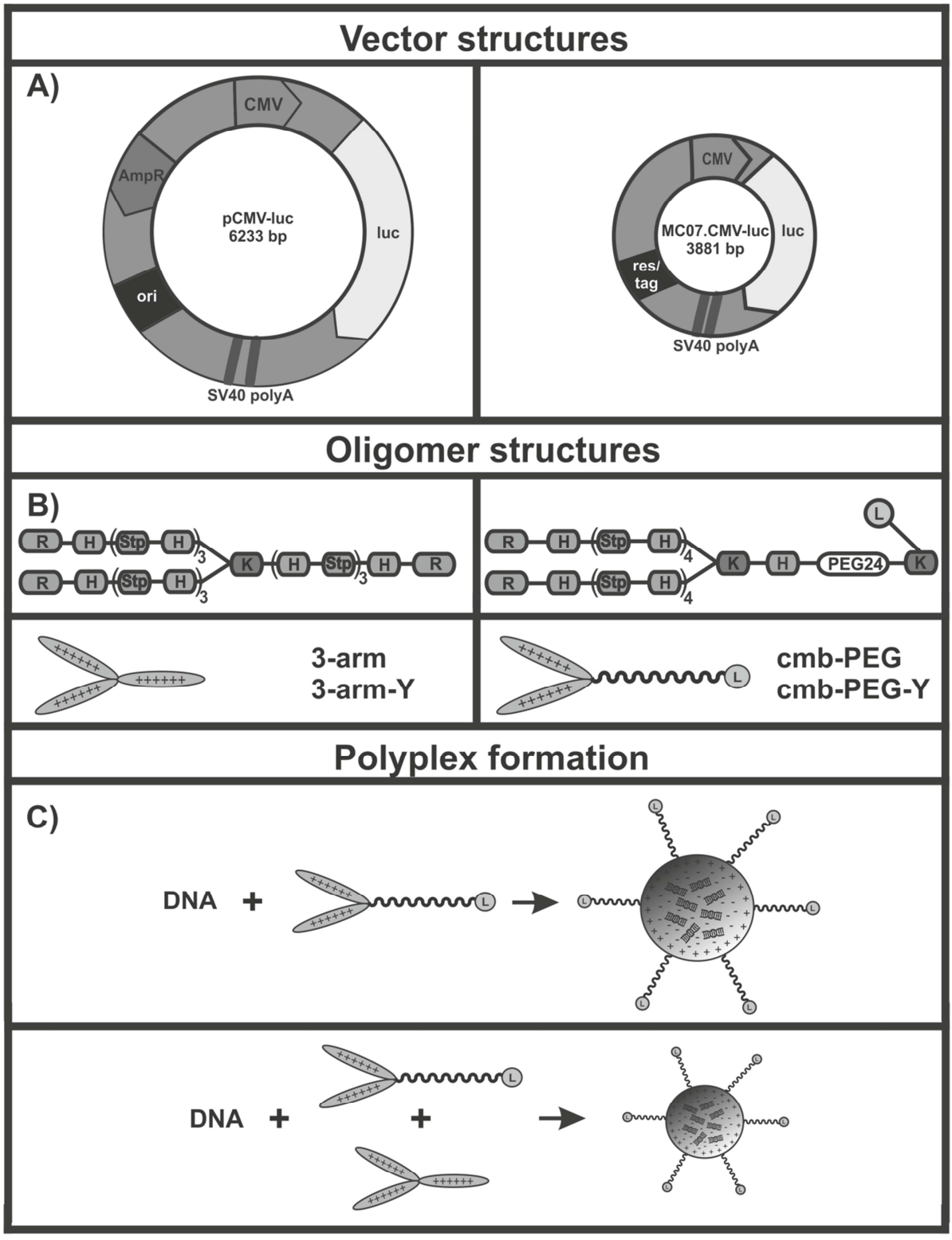

Figure 5 Schematic structures of **(A)** plasmid pCMV-luc and minicircle (MC) MC07.CMV-luc. **(B)** Sequence-defined nonshielded three-arm (left) and cmb-PEG (right) oligoaminoamide carriers. R represents terminal cysteines in three-arm and cmb-PEG oligomers while in the case of tyrosine trimer containing three-arm-Y and cmb-PEG-Y oligomers represents C-Y_3 on the N-terminus or Y_3-C on the C-terminus. **(C)** Standard (top) polyplex formulations and combination formulations of cmb-targeted oligomer and three-arm oligomer (bottom) used in this study.

3.1.2 Physicochemical characterization of polyplexes

Nucleic acid compaction with synthetic gene carriers into nanosized particles is an important requirement for successful gene delivery. This study compared pCMV-luc and MC07.CMV-luc polyplex formation using a series of different characterizations. Particle sizes and zeta potential of polyplexes formed at N/P ratio 12 were determined by dynamic light scattering (**Table 2**). The majority of carriers formed nanoparticles of <200 nm, within the size limit for cellular uptake via receptor-mediated endocytosis [14]. Zeta potential measurements display the expected positive surface charges of +~20mV for the nonshielded linPEI and Y_3 oligomer, and surface charges of +~14mV for cmb-PEG decorated polyplexes, consistent with published work [107]. Comparing complexation with pDNA or MC, well-compacting cationic polymers such as linPEI or Y_3 oligomers formed polyplexes with similar diameters, irrespective of the different size of the cargos; linPEI polyplexes had a hydrodynamic diameter of ~90 nm. This is not surprising and is in agreement with previous work testing various nucleic acid cargos [9]. For plain polycations, the different cargo DNA size is compensated by aggregating different cargo copy numbers into one polyplex. The situation is different for carriers that avoid nano-aggregation and form monomolecular DNA polyplexes [133, 281]. In the current work, in contrast to linPEI, the tyrosine-free oligoaminoamides form polyplexes where sizes significantly differ for pDNA and MC. Especially for cmb-PEG with lower compaction activity, hydrodynamic diameters of MC polyplexes were only ~55% of the pDNA polyplexes. These findings are consistent with a previously established decorated rod model [133, 143]. Mixing of cmb-PEG with PEG-free three-arm results in combination polyplexes with far less difference between pDNA and MC (170 nm vs. 140 nm diameter).

Table 2 Particle size (Z-average) and zeta potential of pCMV-luc and MC07.CMV-luc polyplexes formed in HBG buffer determined with DLS. Variations refer to the standard deviation of three measurements of the same sample. Combination polyplexes refer to 70 mol% of cmb-targeted oligomer and 30 mol% of 3-arm oligomer. PDI: Polydispersity index.

		pCMV-luc			MC07.CMV-luc		
Polyplex	**N/P**	**Z-average [nm]**	**Mean PDI**	**Mean zeta potential [mV]**	**Z-average [nm]**	**Mean PDI**	**Mean zeta potential [mV]**
linPEI	9	93,7 ± 8,2	0,30 ± 0,07	21,0 ± 0,4	92,2 ± 1,2	0,2 ± 0,01	20,1 ± 1,4
cmb-PEG-Y	12	143,1 ± 1,5	0,04 ± 0,01	11,4 + 0,7	136,1 ± 3,9	0,09 ± 0,01	13,0 ± 1,1
3-arm-Y	12	131,1 ± 0,9	0,13 ± 0,01	20,6 ± 0,7	136,9 ± 2,5	0,15 ± 0,02	20,4 ± 0,7
combination	12	134,3 ± 2,8	0,05 ± 0,01	13,7 ± 0,3	104,7 ± 5,1	0,24 ± 0,02	14,8 ± 0,6
cmb-PEG	12	189,5 ± 0,4	0,04 ± 0,01	12,0 ± 0,7	103,2 ± 3,7	0,30 ± 0,04	14,3 ± 0,8
3-arm	12	206,3 ± 2,6	0,12 ± 0,03	14,8 ± 0,9	144,3 ± 2,4	0,15 ± 0,01	15,2 ± 0,6
combination	12	169,0 ± 3,1	0,06 ± 0,02	13,1 ± 1,1	139,9 ± 4,0	0,31 ± 0,03	14,3 ± 1,0

Differences in size and morphologies of the more stable polyplexes (with linPEI and tyrosine oligomers) were analyzed in more detail by transmission electron microscopy (**Figure 6**). Considering the methodological differences, TEM data are well consistent with DLS. In general, nominal sizes of hydrodynamic diameters by DLS (~90-140 nm) are larger than TEM diameters (~30-100 nm) due to the emphasis of DLS on larger particle fractions (light scatter intensity ~r6) on the one hand, and the dehydrated stage of TEM samples on the other hand. TEM confirmed stabile particles formation for all carriers, with nanoparticle shapes differing between the carriers but not the DNA used in polyplex formation. In contrast to DLS, TEM provided evidence for the presence of smaller ultrastructures for MC than for pDNA polyplexes. For example, linPEI formed spherical structures with both DNA vectors, with sizes of 50-90 nm for pDNA and smaller 25-70 nm for MC. The addition of a three-arm structure to the cmb-targeted structure led to a smaller and more compact particle in the case of polyplex formation with both plasmids. In accordance with a recent observations [107], the PEGfree three-arm-Y structure formed compact spherical structures of around 30-50 nm. In contrast, oligomer cmb-PEG-Y formed less compact rods (80-100 nm for pDNA / 50-60 nm for MC) or toroids (40-50 nm for pDNA / 30 nm for MC) demonstrating a DNA cargo size-dependence. As expected, the oligomer combination resulted in better compacted rod structures, with a clear

size difference between pDNA and MC formed polyplexes (65-100 nm vs. 35-40 nm). Notably, the majority of nanoparticles were <50nm (at least in one dimension), which would be compatible with the <50nm nuclear envelope pore limit to enable transport of polyplexes into the nucleus [21].

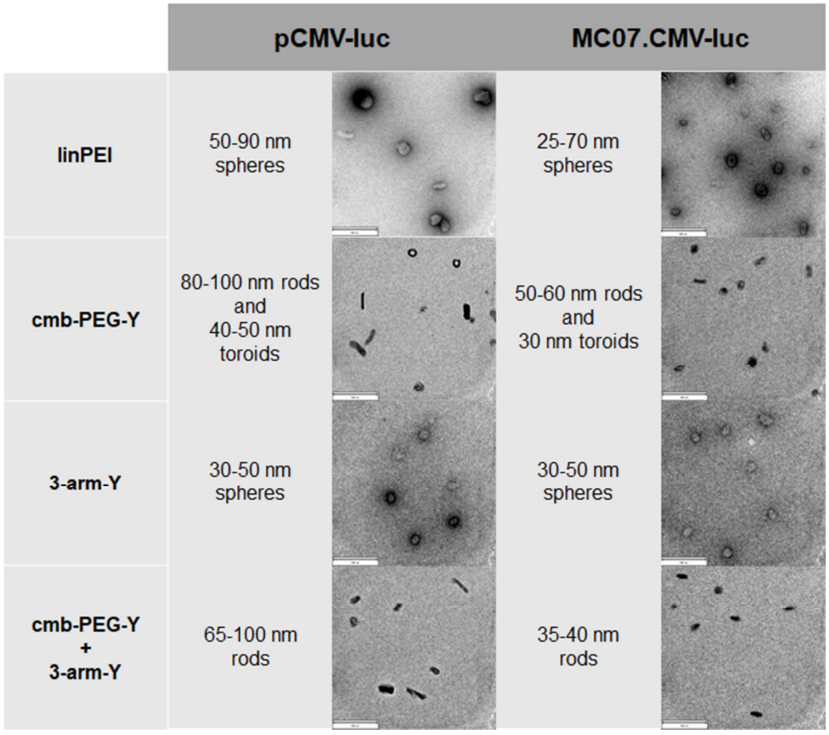

Figure 6 Transmission electron microscopy (TEM) images of pCMV-luc and MC07.CMV-luc polyplexes formed at N/P 12 in deionized water and stained with uranylformate. Combination polyplexes refer to 70 mol% of cmb-PEG-Y and 30% of three-arm-Y. Scale bar: 200 nm.

The EtBr exclusion assay (**Figure 7**) provides an alternative mode for evaluation of DNA binding ability of carriers. The decreased fluorescence correlates with an increased compaction of polyplexes (**Figure 7A**). Compaction was best for linPEI polyplexes, irrespective of the type of DNA (<5% EtBr fluorescence). Interestingly, polyplexes formed with oligoaminoamides displayed better compaction for MC compared to pDNA. Consistent with the other presented work, MC DNA combination polyplexes showed even better compaction (only 6-8% EtBr fluorescence). **Figure 7B** presents the EtBr fluorescence after the addition of 250IU of heparin sulfate to mimic physiological anionic dissociative stress, resulting in partial release of DNA from polyplexes [129]. Under these conditions, both pDNA and MC polyplexes of linPEI are dissociated (>90% EtBr fluorescence). Oligoaminoamide polyplexes, which

are stabilized by bioreversible disulfide crosslinks, are more resistant to the applied heparin stress. Again, polyplexes formed with MC DNA display higher stability than pDNA polyplexes, and MC combination polyplexes the highest stability (~25% EtBr fluorescence).

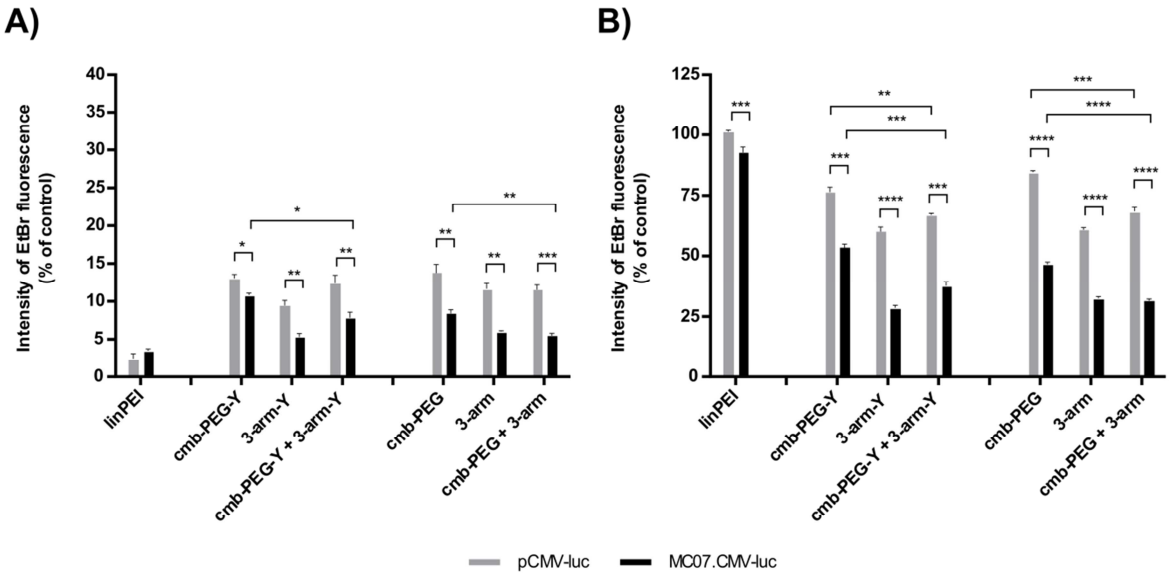

Figure 7 Ethidium bromide exclusion assay to determine the ability of DNA compaction of the oligomers, inversely correlating with the remaining fluorescence of DNA intercalating ethidium bromide (EtBr). Results are presented in % against free pCMV-luc or MC07.CMV-luc. Polyplexes at N/P 12 without **(A)** or with **(B)** treatment by 250 IU of heparin. Statistical analysis (Student's t-test): * $p < 0.05$; ** $p < 0.01$; *** $p < 0.001$; **** $p < 0.0001$.

3.1.3 Transfection efficiency of polyplexes formed with pCMV-luc or MC07.CMV-luc

To compare transfection efficiency of polyplexes formed with either pCMV-luc or MC07.CMV-luc, luciferase gene transfer in the prostate carcinoma cell line DU145 was performed. This cancer cell line expresses the cell surface receptor HGFR/c-Met (**Figure 8**).

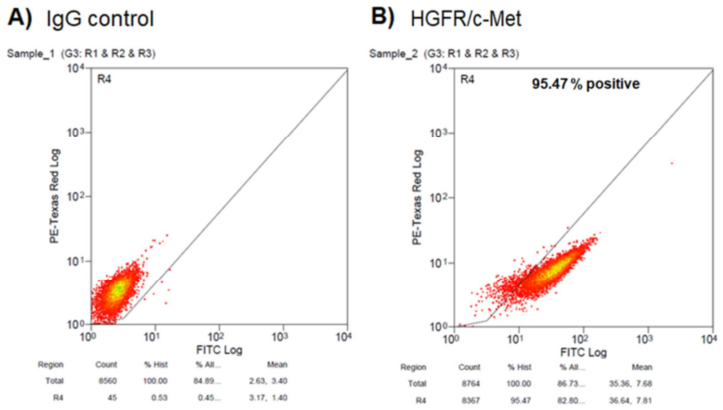

Figure 8 HGFR/c-Met expression on DU145 cell line. The results were obtained with the IgG control **(A)** and monoclonal mouse anti-human HGFR/c-Met antibody **(B)**. For the detection of receptor level expression by flow cytometry, Alexa 488-labeled goat anti-mouse secondary antibody was used.

First, cells were incubated with polyplexes for a defined period in complete serum-supplemented medium, and luciferase gene expression (**Figures 9** and **10A**) as well as metabolic activity of cells (**Figures 10B** and **11**) was recorded after 24 h. Metabolic activity assays confirmed that the transfection were performed under nontoxic conditions. As shown in **Figure 9A**, polyplexes formed with MC07.CMV-luc and linPEI mediated better transfection than polyplexes formed with pCMV-luc. The advantage was particularly pronounced (5-fold higher transfection) in short-term (0.75 h) incubations with polyplexes, but still visible (2.3-fold higher transfection) in 24 h long-term incubations. For pCMV-luc polyplexes, this prolonged incubation was necessary to reach the same transgene expression levels as obtained with MC07.CMV-luc polyplexes after short incubation. Also, for three-arm-Y polyplexes, upon 24 h of incubation, an advantageous gene transfer by MC compared to pDNA was observed (**Figure 9B**). For receptor-mediated transfections, cells were incubated with cmb-PEG or cmb-PEG-Y polyplexes for only 0.75h. Previous work demonstrated enhanced, HGF receptor-specific uptake at these short incubation times [107]. Additionally, the corresponding combination polyplexes (targeted oligomers plus three-arm oligomers) were applied (**Figure 9C**). Also, in these settings, polyplexes formed with MC07.CMV-luc showed 6- to 13-fold higher transfection efficiency than polyplexes formed with pCMV-luc. An advantageous effect of the novel c-Met targeted oligomers with integrated tyrosine trimers analogously was also noted, as previously observed for folate receptor targeted pDNA polyplexes [112, 116].

Altogether, the beneficial effect of tyrosine trimer integration, formation of combination polyplexes, and use of MC added up to a ~200-fold enhanced gene expression. In the presented transfections, polyplexes with equal mass quantities of DNA were used. To rule out that the higher copy number of MC07.CMV-luc than the corresponding pCMV-luc vector is responsible for the enhanced transfection, additional polyplex transfections were performed with equimolar quantities of vectors. Under these conditions, linPEI and combination polyplexes formed with MC also showed around 3.5- and 3-fold higher transfection efficiency, respectively, in comparison to equimolar quantities of pDNA polyplexes (**Figure 9D** and **E**).

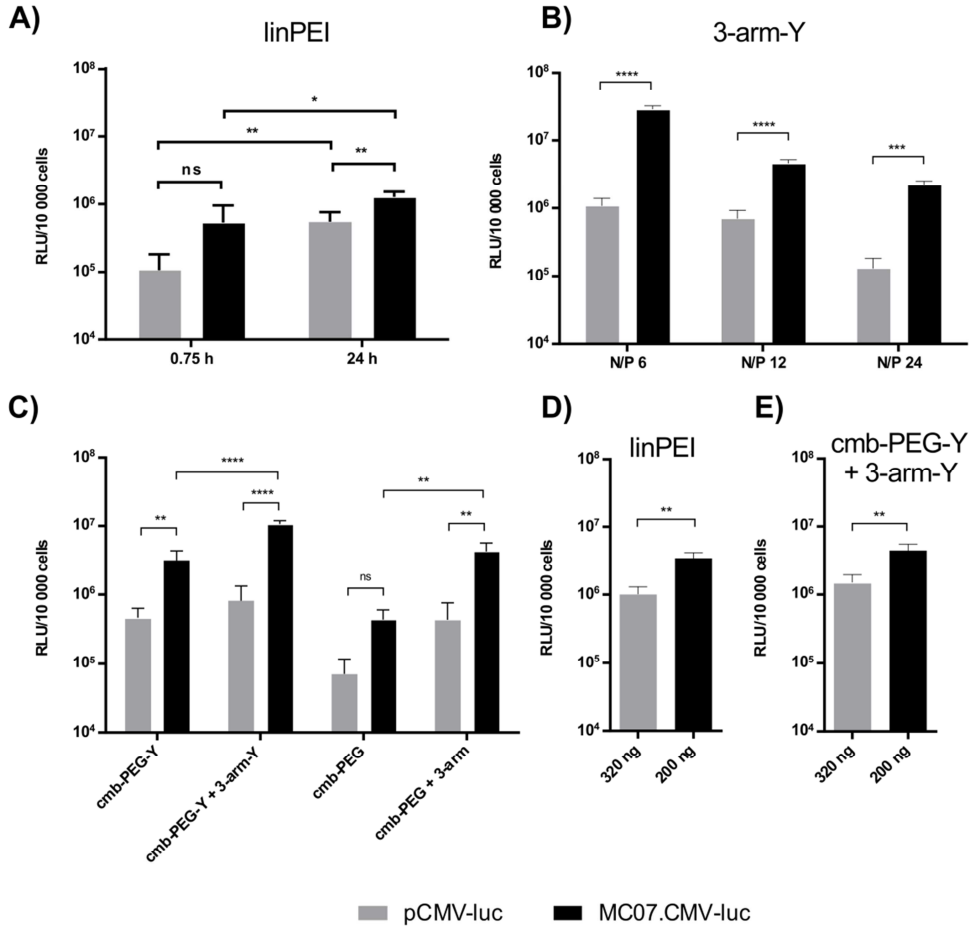

Figure 9 Luciferase reporter gene expression in the DU145 prostate carcinoma cell line at 24 h after transfection with pCMV-luc (gray) or MC07.CMV-luc (black) polyplexes. **(A)** Transfections after 0.75 and 24 h of incubation with linPEI at N/P 9. **(B)** Transfections after 24 h of incubation with three-arm-Y at indicated N/P ratios. **(C)** Transfections after 0.75 h of incubation with cmb-PEG-Y, cmb-PEG, and corresponding combination polyplexes at N/P 12. **(D)** Transfection after 24 h incubation with linPEI polyplexes at equimolar vector ratio. **(E)** Transfection after 0.75 h incubation with cmb-PEG-Y/three-arm-Y combination polyplexes (N/P 6) at equimolar vector ratio. Combination polyplexes: 70 mol% of cmb-PEG(-Y) and 30 mol% of three-arm(-Y).

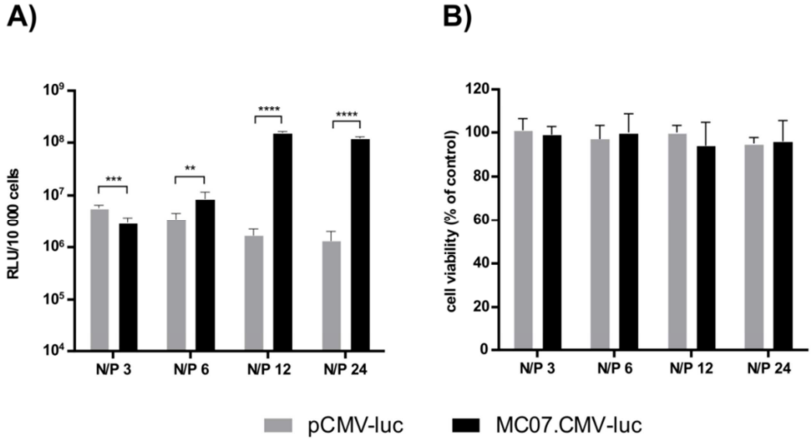

Figure 10 Luciferase reporter gene expression of pCMV-luc or MC07.CMV-luc in DU145 cell line of polyplexes formed with cmb-PEG-Y. Transfections were performed at four different ratios: N/P 3, 6, 12 and 24. **(A)** Polyplexes formed with cmb-PEG-Y; transfection time of only 0.75 h because of the faster receptor-enhanced cell uptake. Statistical analysis (Student's t-test): ns $p > 0.05$, * $p < 0.05$; ** $p < 0.01$; *** $p < 0.001$ **** $p < 0.0001$. **(B)** Corresponding cell viability assays of DU145 cells after transfections. Cell viability was calculated as percentage to cells treated with HBG.

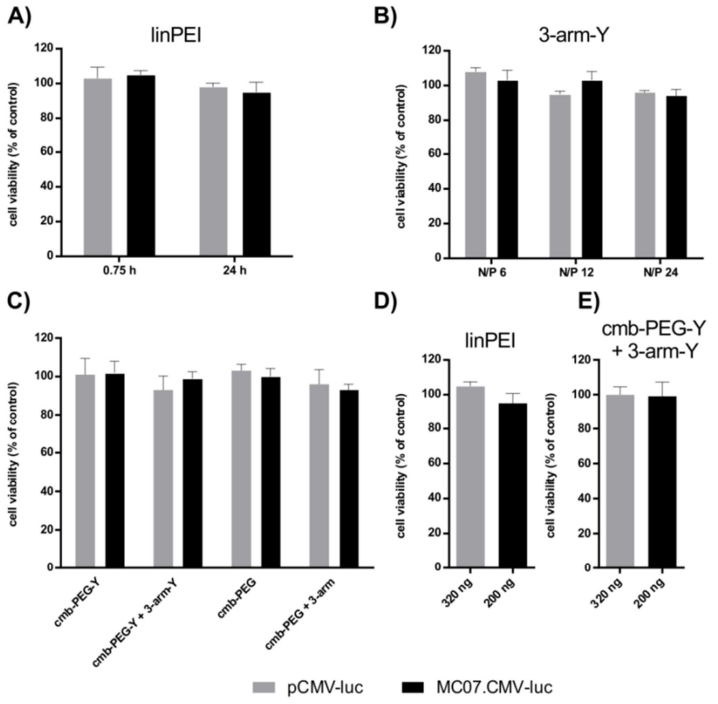

Figure 11 Corresponding cell viability assays of DU145 cells after transfections as presented in Figure 9. Cell viability was calculated as percentage to cells treated with HBG. **(A)** Transfections after 0.75 h and 24 h incubation with linPEI at N/P 9. **(B)** Transfections after 24 h incubation with 3-arm-Y at indicated N/P ratios. **(C)** Transfections after 0.75 h incubation with cmb-PEG-Y, cmb-PEG, and corresponding combination polyplexes at N/P 12. **(D)** Transfection after 24 h incubation with linPEI polyplexes at equimolar vector ratio. **(E)** Transfection after 0.75 h incubation with cmb-PEG-Y /3-arm-Y combination polyplexes (N/P 6) at equimolar vector ratio.

3.1.4 Overcoming intracellular barriers

To explain the advantage of MC DNA in polyplex transfection, transfections using DU145 cells were performed in different stages of cell cycle (**Figure 13**). For synchronization, a double-thymidine block was used [282, 283]. The cell cycle stage was monitored by flow cytometry (**Figure 12**). Upon second release (0 h), 88% of cells were in G1 phase, at 6 h after release 45% of cells peaking in S phase, and at 8 h 60% of cells in G2/M phase.

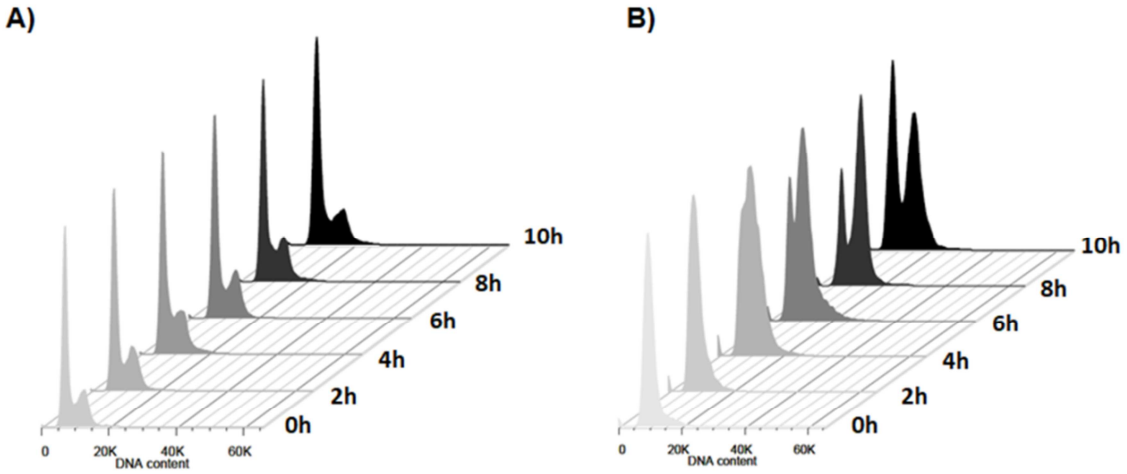

time points	G1	S	G2	RMS
0h	55,91	26,34	14,7	4,18
2h	57,2	23,34	13,89	4,68
4h	46,36	31,23	16,63	4,74
6h	54,93	25,49	16,1	4,03
8h	50,54	26,67	17,52	4,04
10h	58,67	23,3	13,52	3,31

time points	G1	S	G2	RMS
thymidine + 0h	87,78	7,86	3,7	4,55
thymidine + 2h	78,95	16,01	3,83	5,22
thymidine + 4h	74,1	21,88	3,14	5,78
thymidine + 6h	21,17	44,73	20,12	8,58
thymidine + 8h	19,31	9,27	60,32	6,82
thymidine + 10h	34,92	19,3	33,49	6,99

Figure 12 Cell cycle analysis of synchronous DU145 cells treated with double-thymidine block. Cells were analyzed with flow cytometer every 2h after second release. **(A)** Non treated control cells. **(B)** Cells treated with thymidine.

Cells were transfected at time points 0 h (G1), 6 h (largely S), 8 h (G2/M), and 12 h (after M). Three different formulations, the well-compacting carriers linPEI and the cmb-PEG-Y plus three-arm-Y combination, and the less compacted cmb-PEG-Y, were selected for packaging pDNA or MC DNA. Irrespective of cell cycle stage, the MC formulations mediated up to a 10-fold higher gene expression (**Figure 13**). The transfections confirmed the lack of significant cell cycle dependence for linPEI/pDNA polyplexes, which correlates with previous studies [18]. An absence of cell cycle

dependence was also observed for linPEI/MC polyplexes. An analogous lack of cell cycle dependence was found for both types (pDNA and MC) of well-compacted cmb-PEG-Y/three-arm-Y combination polyplexes. Interestingly, for the less compacting carrier cmb-PEG-Y, the pDNA- but not the MC-mediated transfection shows cell cycle dependence at 12 h (after mitosis), which is about 10-fold lower than for transfection before mitosis (0 or 6 h), and also about 10-fold lower than the better compacted pDNA polyplex (**Figure 13,** top left). Importantly, MC DNA polyplexes (**Figure 13,** top right) display lack of cell cycle dependence for all formulations, suggesting an advantage from their inherent smaller size.

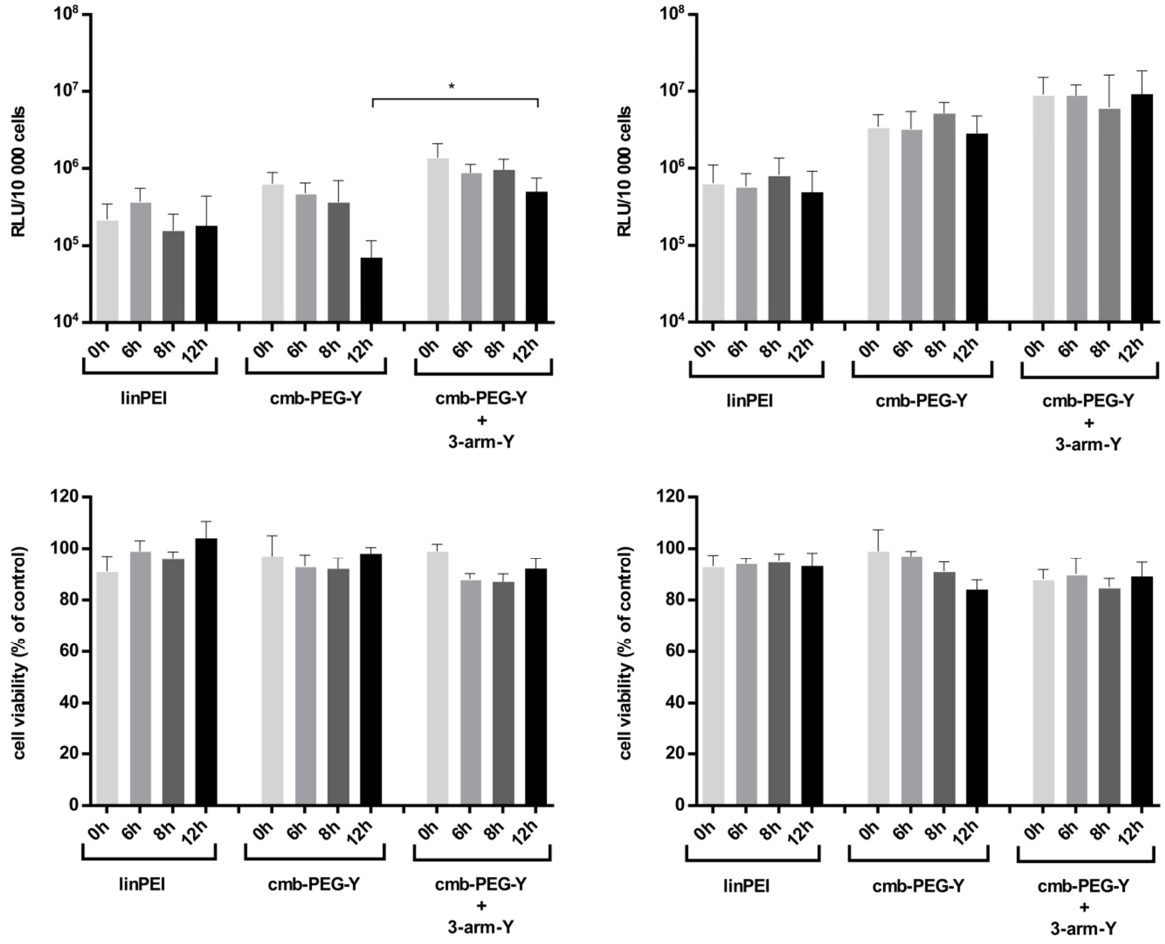

Figure 13 Cell cycle dependence of gene transfer. DU145 cells were transfected in specific phases of cell cycle after release from double thymidine block; primarily G1 phase (0 h), S phase (6 h), G2 phase (8 h), and G1 phase of the second cycle (12 h). Luciferase reporter gene expression (top) and corresponding cell viability by MTT assay (bottom) at 24 h after 0.75 h of incubation with pCMV-luc (left) or MC07.CMV-luc polyplexes (right) at N/P ratio 12.

3.2 Sequence defined oligomers as carriers for mRNA delivery

In the gene delivery process, successful interaction between the gene delivery vector, extracellular surrounding and the cell are required for efficient delivery of a gene to a target cell. Insufficient nuclear transport of plasmid DNA (pDNA) is highly responsible for their lower transfection efficiency compared to viral vectors. Therefore, therapeutic gene delivery using messenger RNA (mRNA) has become an interesting alternative to pDNA gene therapy. Compared to pDNA gene delivery, mRNA has following advantages. First of all, mRNA exerts its function in the cytoplasm, where transgene expression starts prompt, therefore gene silencing mechanisms operating in the nucleus are irrelevant and the risk of insertional mutagenesis can be excluded. Due to the transfection procedures without destruction of nuclear envelope, cell viability is well maintained. Besides, mRNA is also effective in non-dividing cells as well as hard-to-transfect cells, thus mRNA delivery possesses broad application prospects. Nevertheless, mRNA delivery possesses also some disadvantages such as strong immunogenicity and limited stability of conventional mRNA [23-27]. Delightedly, these disadvantages have recently been greatly improved by various chemical modifications [284]. Despite that, effective delivery carrier for cellular entry and cytosolic release is also required. Complexation of negatively charged nucleic acid with positively charged cationic polymers and lipids for delivery via endocytic pathways has become an interesting method not only for pDNA, but also for mRNA [188].

In the current study, we focused on the development of an appropriate system for mRNA delivery. Firstly, we evaluated different sequence-defined oligoaminoamides synthesized previously in purpose of pDNA or siRNA delivery (the library was established in our group) for single stranded mRNA transfection. Secondly, starting from first successful mRNA carrier candidates, we explored the structure-activity relationship (SAR) requirements of refined carriers for successful mRNA delivery.

3.2.1 Evaluation of mRNA-luc transfection efficiency using polyethylenimine or different sequence-defined oligoaminoamides

Chemically modified stabilized non-immunogenic messenger RNA encoding firefly luciferase (mRNA-luc) was produced, purified and provided by ethris GmbH. Our first transfections were based on the use of gene delivery "gold standard" polyethylenimine (PEI) in 22 kDa linear and 25 kDa branched form as very potent pDNA transfection agents [28, 29] and succinylated PEI 25 kDa branched (succPEI) as an excellent siRNA transfection agent [278]. Different linear and branched PEI with various molecular weights had been previously tested to enable regulation of polyplex stability, transfection efficacy and toxicity [285-288]. To compare transfection efficiency of the selected different PEI types (**Figure 14A**), polyplexes were formed with mRNA-luc in different solutions (WFI: water for injection, HBS: HEPES buffered saline, HBG: HEPES buffered glucose) and luciferase mRNA transfer and expression was evaluated in various cancer cell lines (DU145: prostate carcinoma, N2a: mouse neuroblastoma, Huh7: hepato cellular carcinoma, MDA-MB-231: breast adenocarcinoma, KB: cervix carcinoma). Cells were incubated with polyplexes for 24h in 10% serum-supplemented medium, and afterwards luciferase gene expression as well as cell viability assay (**Figure 14B and C**) were recorded. As shown in **Figure 14B** (top), polyplexes formed in different solutions showed similar transfection profile in different cell lines. The lowest transfection was observed in the case of linPEI (polyplexes formed at optimal N/P ratio 9) in almost all cell lines (except DU145) and all three solutions. BrPEI polyplexes (formed at optimal N/P ratio 10) mediated better transfection than linPEI polyplexes (except in Huh7 and KB cells in the case of HBS solution polyplex formation), whereas the highest transfection efficiency was observed with succPEI (10% succinylation [278], w/w ratio 4) polyplexes in HBS and HBG polyplexes formation and in the case of WFI polyplex formation only for DU145 cell line.

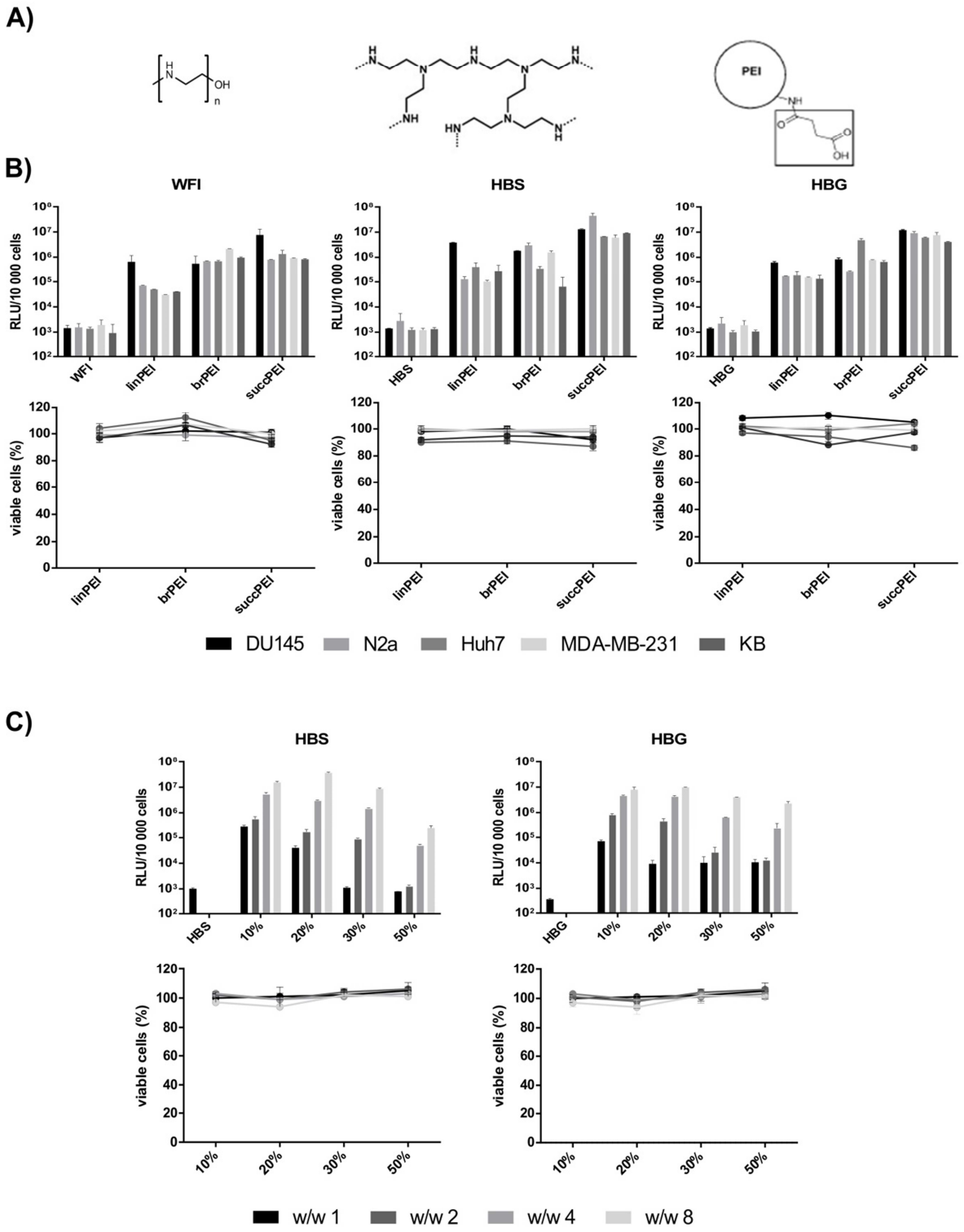

Figure 14 (A) Chemical structures of linPEI 22 kDa, brPEI 25 kDa and succPEI 25 kDa. **(B)** Luciferase reporter gene expression and corresponding cell viability assay in the different cell lines at 24 h after transfection with mRNA polyplexes. Polyplexes were formed in different solutions (WFI, HBS or HBG). LinPEI polyplexes at N/P ratio 9, brPEI at N/P ratio 10 and succPEI at w/w ratio 4 were formed. **(C)** Transfections and corresponding cell viability assay (DU145 cell line) after 24 h of incubation with succPEI polyplexes with different succinylation percentage of PEI. Cell viability was assessed by Cell Titer Glo® Assay (Promega) and calculated as percentage to cells treated with HBS or HBG.

The succPEI 10%, 20%, 30% and 50% had been synthesized analogously as described in [278] using stoichiometric amounts of succinic anhydride for 10%, 20%, 30% or 50% modification. In case of succPEI 10% indeed 10% succinylation (determined by NMR) was achieved. However, with increasing succinic anhydride amount, the reaction is less effective and based on NMR evaluation, the degree of modification is 10%, 15%, 16% and 18% respectively. SuccPEI polyplexes were formed with equal mass quantities of mRNA-luc, and four different w/w ratios have been tested (**Figure 14C**). SuccPEI with modification degree higher than 10% was not advantageous for transfection efficiency in any of the tested w/w ratio, therefore for the further experiments succPEI with 10% succinylation and w/w ratio 4 was used as a positive control. It was confirmed that the transfections were taking place under nontoxic conditions (**Figures 14B** and **C** bottom) through measuring metabolic cell activities via CellTiter-Glo assay.

In order to find appropriate carriers and also identify critical bottlenecks for mRNA delivery, we performed a screening of our established transfection oligomer library of sequence defined oligomers produced by solid-phase-assisted synthesis. Therefore, more than 60 oligomers with various sequences and topological structures were tested: linear, branched 2-arm, 3-arm, 4-arm, 8-arm, T-shape, U-shape, comb-like oligomers. Results showed that oligomers containing tyrosine tripeptides (Y_3) or/and fatty acids in their structures mediated higher transfection efficiency. The advantage of tyrosine tripeptides (Y_3) within the structure was particularly pronounced in the case of 3-arm oligomers used in both HBS and HBG polyplex formations (**Figure 15**). The addition of tyrosine tripeptides (Y_3) lead to higher transfection, 3-arm-Y showed significant enhanced efficiency (7.6-fold higher) over succPEI, however only when HBS buffer was used for polyplex formation (**Figure 15B** left).

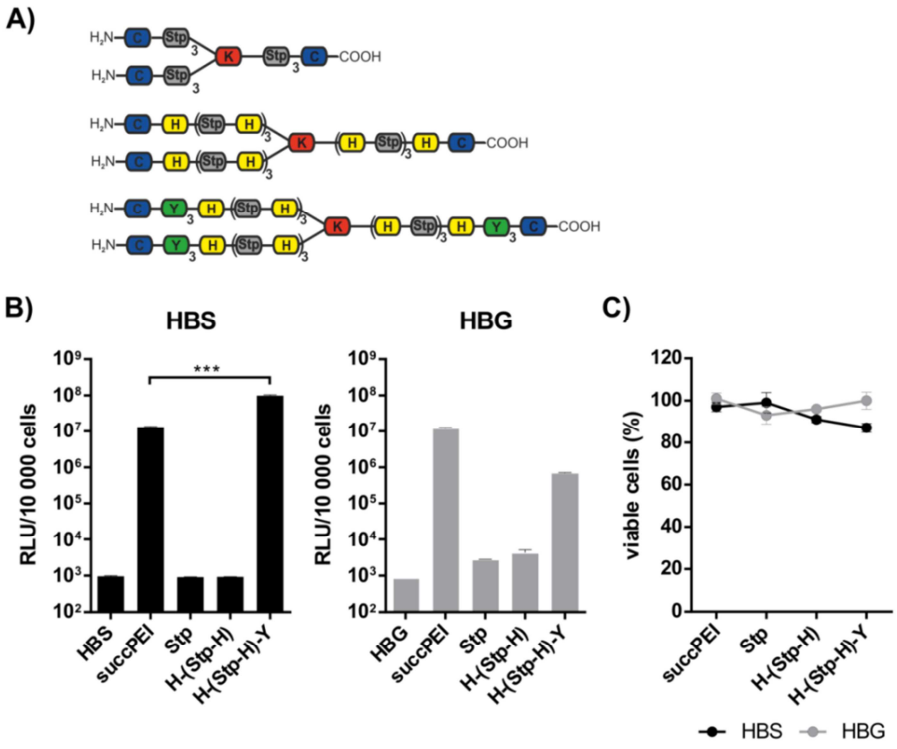

Figure 15 (A) Schematic structures of sequence-defined 3-arm oligomers (Stp: succinoyl-tetraethylene-pentamine, C: cysteine, K: lysine, H: histidine, Y: tyrosine). **(B)** Luciferase reporter gene expression of DU145 cells treated with mRNA polyplexes formed with 3-arm oligomers at 24 h after transfection. Polyplexes were formed in HBS (left) or HBG (right) buffer. **(C)** Corresponding cell viability was assessed by Cell Titer Glo® Assay (Promega) and calculated as percentage to cells treated with HBS or HBG.

Nevertheless, in the evaluation of other sequence topologies, it was found that tyrosine Y_3 incorporation in the structure was not sufficient; additional incorporation of fatty acids plays an important role for optimal mRNA delivery (**Figure 16**). First of all, MyrA and OleA in T-shape structures showed advantageous luciferase expression over structures with SteA in HBS lipopolyplex formation in both cell lines (DU145 and N2a). Secondly, a beneficial effect of the tyrosine introduction in the same structures was also noted, especially in the case of CholA and OleA in DU145 cell line. Previous study demonstrated that additional tyrosine increase polyplex stability [112, 116]. Considering a higher stability of SteA polyplexes, the additional tyrosines did not shown any improvement in transfection. Besides, integration of additional cysteine and arginine (CRC motif) for supplemental stabilization also did not show any further advantageous for mRNA delivery. Regarding toxicity of above mentioned fatty acids, significant reduction of cell viability was observed only in MyrA formulations (**Figure 16C**) which is consistent with previous work [104].

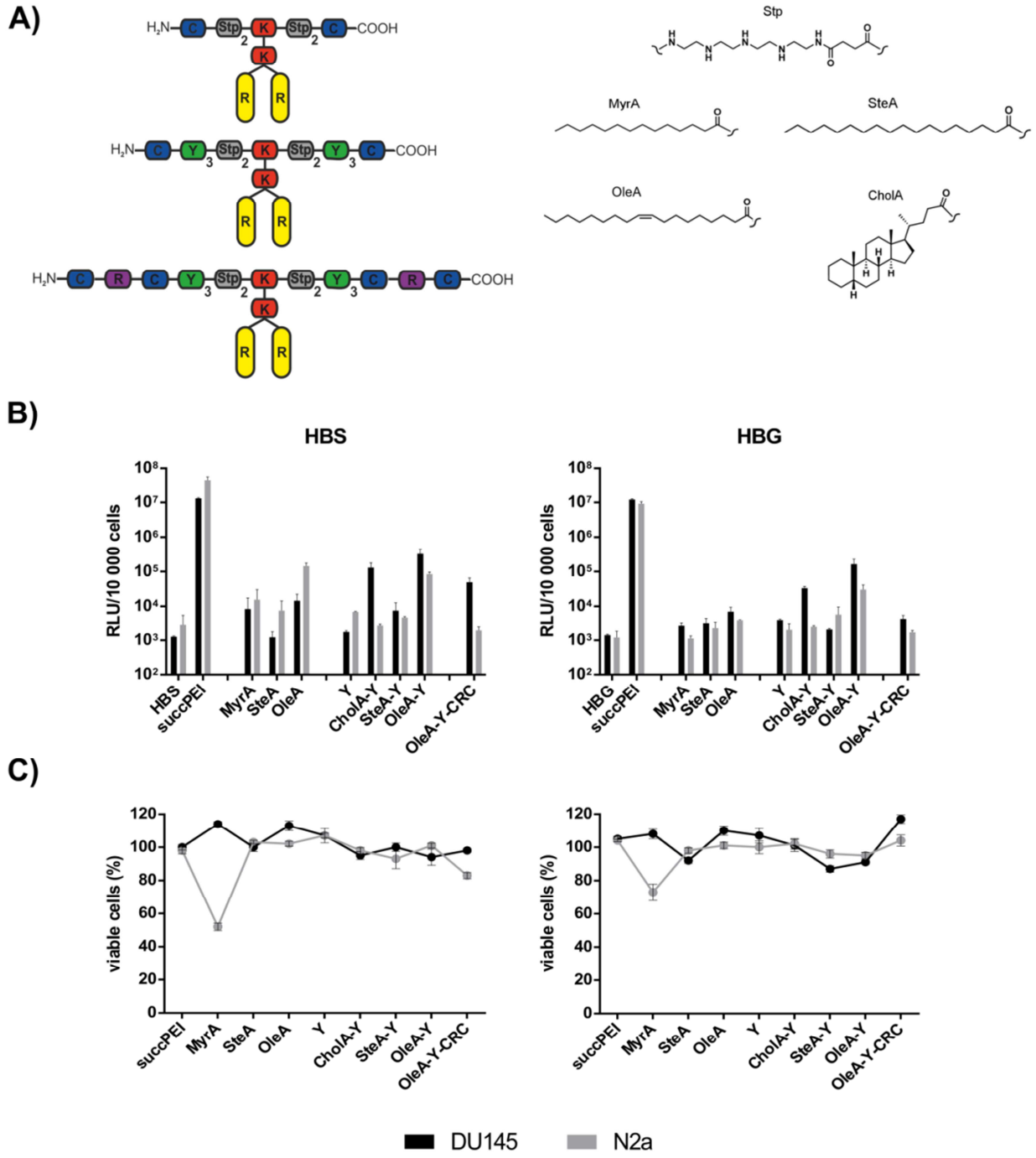

Figure 16 (A) Schematic structures of sequence-defined lipo-oligomers with T-shape topology and different modifications (Stp: succinoyl-tetraethylene-pentamine, C: cysteine, K: lysine, Y: tyrosine, R: arginine, MyrA: myristic acid, SteA: stearic acid, OleA: oleic acid, CholA: 5β-cholanic acid). **(B)** Luciferase reporter expression of mRNA lipopolyplexes formed with T-shape oligomers and lipo-oligomers (N/P ratio 12) at 24 h after transfection in DU145 and N2a cell lines. Lipopolyplexes were formed in HBS (left) or HBG (right) buffer. **(C)** Corresponding cell viability was assessed by Cell Titer Glo® Assay (Promega) and calculated as percentage to cells treated with HBS or HBG.

The findings of the importance of T-shape topology and also the influence of tyrosine and fatty acids in the structure for mRNA delivery led us to the next two similar and already published (for siRNA delivery) groups of T-shape lipo-oligomers. Lipo-oligomers with cationic backbone and hydrophobic domain such as unsaturated oleic acid are known as potent siRNA carriers because of strong electrostatic and hydrophobic lipopolyplex formation and endosomal membrane destabilization [105, 106, 116]. TFA (trifluoroacetic acid), used for removal of protecting groups and cleavage from the resin during lipo-oligomer synthesis through solid-phase-assisted synthesis, in case of the unsaturated fatty acid oleic acid can induce side products such as 10-30% hydroxystearic acid (OH-SteA) derivatives. This occurs via TFA addition, which after hydrolysis generates the hydroxylated product. Reinhard et al [289] optimized the cleavage protocol in terms of temperature and time to minimize unintended side products. As a results, highly pure T-shape lipo-oligomers, containing either only the unsaturated oleic acid (OleA) or linoleic acid (LinA), the saturated stearic acid (SteA), or T-shapes with the monohydroxylated hydrocarbon chain OH-SteA, LinA-OH, or alternatively 8-nonanamidooctanoic acid moieties (NonOcA) were synthesized [289]. To find out which fatty acid could be valuable for further improvement of mRNA delivery, aforementioned sequences with T-shapes topology, tyrosine tripeptides and the different fatty acids were tested (**Figure 17**). Transfections were performed with lipopolyplexes formed in HBS (**Figure 17B** left) or HBG (**Figure 17B** right) in DU145 and N2a cell lines. In general, lipopolyplexes formed in HBS showed enhanced transfection efficiency than those formed in HBG in case of all lipo-oligomers except OH-SteA. Nevertheless, the same efficiency of OH-SteA lipopolyplexes formed in HBS and HBG was observed only in the case of DU145 transfection. Again, saturated SteA lipopolyplexes showed significantly lower efficiency compared to structures with unsaturated or modified hydrocarbon chains, probably due to lower polyplex stability and enhanced lytic potential of OleA, OH-SteA and NonOcA. Besides, both OH-SteA and NonOcA showed increased efficiency relative to OleA lipopolyplex formation in HBS in both cell lines, closely related with their high lytic activity which is consistent with previous results [289]. Higher lytic activity may increase cellular internalization, but it can also be a reason for unwanted cytotoxicity as it was found in HBS lipopolyplex formation of NonOcA (both cell lines) and LinA-OH (N2a cell line) (**Figure 17C**).

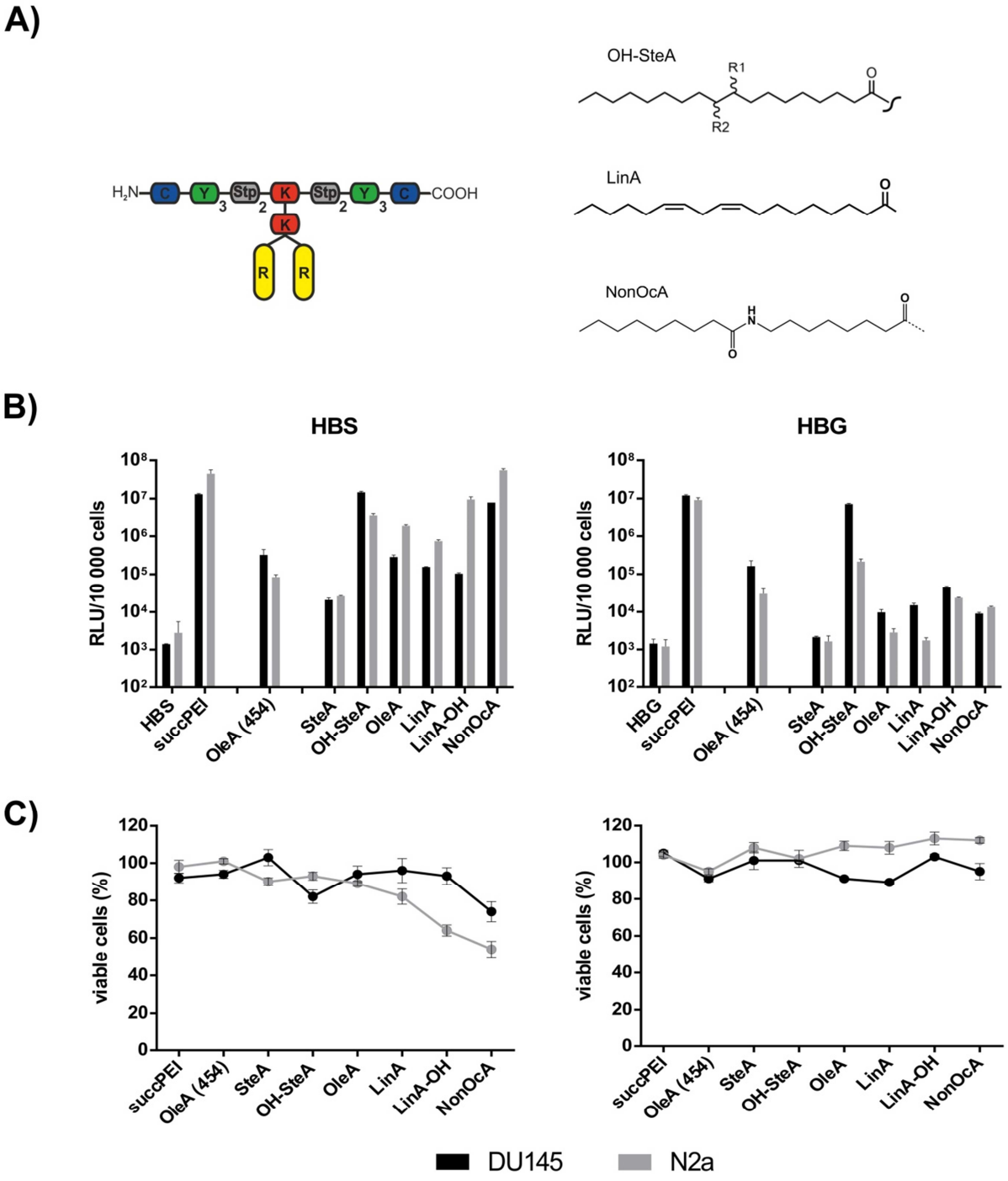

Figure 17 (A) Schematic structure of sequence-defined lipo-oligomers with T-shape topology and different modifications; Stp: succinoyl-tetraethylene-pentamine, C: cysteine, K: lysine, Y: tyrosine, OleA (***454***): oleic acid with OH-SteA impurity, SteA: stearic acid, OH-SteA: hydroxystearic acid, OleA: oleic acid, LinA: linoleic acid, LinA-OH: hydroxylinoleic acid, NonOcA: 8-nonanamidooctanoic-acid. **(B)** Luciferase reporter expression of mRNA lipopolyplexes (N/P ratio 12) at 24 h after transfection in DU145 and N2a cell lines. Lipopolyplexes were formed in HBS (left) or HBG (right) buffer. **(C)** Corresponding cell viability was assessed by Cell Titer Glo® Assay (Promega) and calculated as percentage to cells treated with HBS or HBG.

While in the extracellular condition high stability of polyplexes is important, intracellular disassembly is required for the cytosolic release of mRNA. The incorporation of a bioreducible disulfide bond (SSBB) between the cationic backbone and the hydrophobic domain [104] should enhance release of mRNA in the intracellular reductive space where higher concentration of glutathione (GSH) is present. Therefore, the second group of T-shape oligomers with tyrosine trimers and different fatty acids included bioreducible sequence-defined lipo-oligomers as well as their non-reducible analogs (**Figure 18**) [104]. Moreover, in contrast to the previous structures, these lipo-oligomers did not contain terminal cysteines.

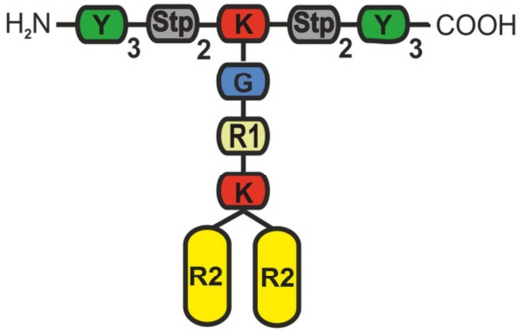

Abbreviation	R1	R2
CholA	-	CholA
CholA SSBB	SSBB	CholA
MyrA	-	MyrA
MyrA SSBB	SSBB	MyrA
SteA	-	SteA
SteA SSBB	SSBB	SteA
OleA	-	OleA
OleA SSBB	SSBB	OleA
NonOcA	-	NonOcA
NonOcA SSBB	SSBB	NonOcA

Figure 18 Schematic overview of the T-shape structures with different modifications (Y: tyrosine, Stp: succinoyl-tetraethylene-pentamine, K: lysine, G: glycine, SSBB: succinoyl-cystamine, CholA: 5β-cholanic acid, MyrA: myristic acid, SteA: stearic acid, OleA: oleic acid, NonOcA: 8-nonanamidooctanoic acid).

As well as in the aforementioned experiments, lipopolyplexes were formed in HBS or HBG and all transfection experiments were performed in DU145 and N2a cell lines (**Figure 19**). Results revealed again enhanced transfection efficiency of lipopolyplexes formed in HBS than those formed in HBG in the case of all lipo-oligomers except SteA SSBB (only N2a cell line) (**Figure 19A** and **B**). Statistical significant enhanced transfection efficiency has been observed also in the almost all cases of HBS formed bioreducible lipopolyplexes comparing to their non-reducible analogs, except in the case of SteA (**Figure 19A** and **B**, top). In general, saturated SteA lipopolyplexes once more showed significantly lower efficiency compare to other fatty acids, which was particularly pronounced in the case of HBS

lipopolyplexes formation. Whereas in the case of HBG lipopolyplex formation, the similar low transfection efficiency was also observed for CholA and NonOcA in both cell lines and MyrA in N2a cell line (**Figure 19A** and **B**, bottom). Although HBG lipopolyplex formation showed lower transfection efficiency, enhanced efficiency of bioreducible lipopolyplexes over their non-reducible analogs, was achieved as well. Besides OleA SSBB, which showed significant better transfection over OleA in both cell lines, MyrA SSBB and NonOcA SSBB lipopolyplexes also showed superior efficiency compare to their non-reducible analogs, but only in the case of DU145 cell line. Notably, high cytotoxicity of MyrA lipopolyplexes was observed in HBS lipopolyplexes formation in both cell lines. Interestingly, OleA lipopolyplexes formed in HBS also showed high toxicity (especially in the case of DU145 cell line), whereas bioreducible OleA (OleA SSBB) lipopolyplexes were found to be non-toxic (**Figure 19C**).

Luciferase expression was tested in DU145 and N2a cell lines. Some differences in transfection efficiency were noticed, but the transfection profile was similar for all oligomers used in the study. Therefore DU145 cell line was chosen for further experiments.

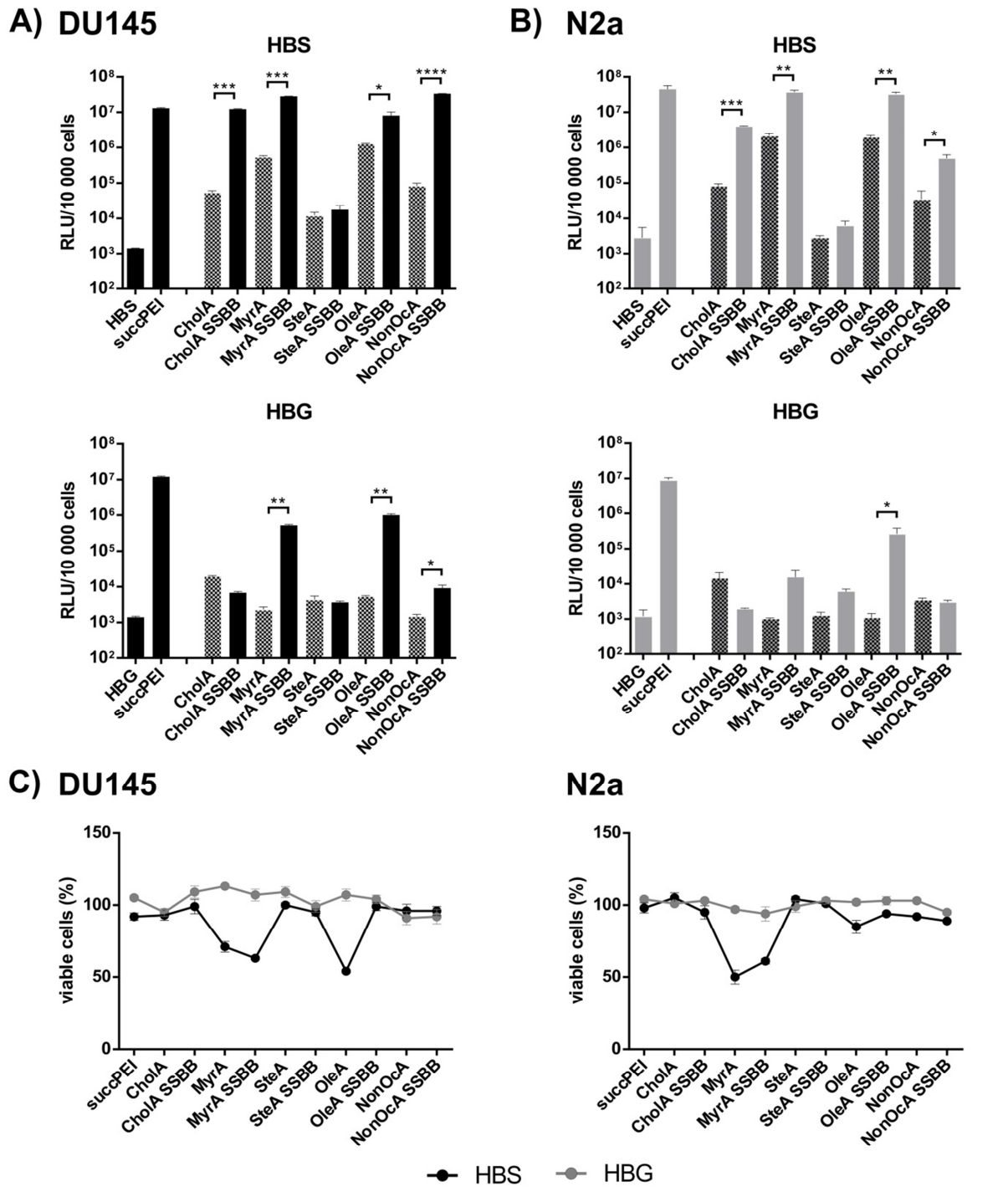

Figure 19 Luciferase reporter expression at 24 h after transfection with mRNA lipopolyplexes formed with T-shape structures presented in Figure 5. **(A)** DU145 cell line. **(B)** N2a cell line. Lipopolyplexes were formed in HBS (top) or HBG (bottom) buffer. Statistical analysis (Student's t-test): *$p < 0.05$; **$p < 0.01$; ***$p < 0.001$; ****$p < 0.0001$. **(C)** Corresponding cell viability was assessed by Cell Titer Glo® Assay (Promega) and calculated as percentage to cells treated with HBS or HBG.

3.2.2 Biophysical characterization of mRNA polyplexes and lipopolyplexes

Nucleic acid compaction with gene carriers into nanosized particles is an important requirement for successful mRNA delivery, therefore different characterization methods were used to compare various polyplex and lipopolyplex formations.

3.2.2.1 Size and zeta potential of carriers

Particle sizes and zeta potential of polyplexes and lipopolyplexes formed at N/P ratio 12 were determined by dynamic light scattering (**Table 3**). Polyplexes and lipopolyplexes were formed in both HBS and HBG. In general, bigger particles were observed when prepared in HBS than in HBG. Only in the cases of succPEI polyplexes and LinA-OH lipopolyplexes the sizes were consistent regardless of whether they were formed in HBS or HBG. Most of the carrier formulations prepared in HBS exhibited particle sizes of more than 1000 nm, while the size of nanoparticles formed in HBG were almost in all cases within the size limit for cellular uptake (<200 nm) [14]. Nevertheless, succPEI, OleA (***454***), LinA and LinA-OH carriers prepared in HBS also exhibiting particle sizes of <200 nm, while only OH-SteA prepared in HBG formed nanoparticles >1000 nm. Interestingly, all bioreducible carriers, prepared in HBG, showed larger size as their corresponding non-reducible analogs. Zeta potential measurements display the expected positive surface charges between +~20 mV and +~40 mV for all the polyplexes and lipopolypexes formed in HBG, and lower surface charges between +~3 mV and +~15 mV for polyplexes and lipopolyplexes formed in HBS.

Table 3 Particle size (Z-average) and zeta potential of polyplexes and lipopolyplexes formed in HBG or HBS buffer determined with DLS.

		HBS			HBG		
Polyplex/lipopolyplex	**N/P**	**Z-average (nm)**	**Mean PDI**	**Mean zeta potential (mV)**	**Z-average (nm)**	**Mean PDI**	**Mean zeta potential (mV)**
succPEI	4	61,6 ± 3,4	0,23 ± 0,01	5,6 ± 0,5	59,8 ± 0,9	0,29 ± 0,05	27,8 ± 3,9
Stp	12	1633,3 ± 47,4	0,35 ± 0,02	4,8 ± 0,1	157,5 ± 1,4	0,09 ± 0,01	24,5 ± 0,8
H-(Stp-H)	12	1390,0 ± 56,6	0,29 ± 0,08	4,9 ± 0,3	75,4 ± 0,3	0,15 ± 0,00	30,4 ± 1,2
H-(Stp-H)-Y	12	999,0 ± 60,6	0,28 ± 0,04	5,8 ± 0,1	79,1 ± 1,2	0,21 ± 0,01	33,3 ± 2,3
OleA (***454***)	12	79,8 ± 0,3	0,14 ± 0,01	6,9 ± 0,7	46,0 ± 0,3	0,19 ± 0,01	27,9 ± 0,7
SteA	12	2211,3 ± 45,6	0,38 ± 0,15	11,6 ± 1,2	69,8 ± 1,	0,31 ± 0,02	37,2 ± 2,1
OH-SteA	12	1752,3 ± 14,0	0,22 ± 0,04	3,0 ± 0,2	1360,3 ± 84,1	0,27 ± 0,02	16,6 ± 0,3
OleA	12	2171,0 ± 136,5	0,35 ± 0,06	8,6 ± 0,7	62,0 ± 0,9	0,16 ± 0,02	28,4 ± 1,5
LinA	12	113,8 ± 0,9	0,10 ± 0,01	13,2 ± 1,0	71,7 ± 0,5	0,25 ± 0,01	35,7 ± 0,8
LinA-OH	12	70,5 ± 1,0	0,15 ± 0,01	14,2 ± 1,2	68,4 ± 0,7	0,24 ± 0,01	24,7 ± 0,0
NonOcA	12	246,5 ± 6,3	0,46 ± 0,02	12,0 ± 0,7	86,4 ± 0,1	0,25 ± 0,01	37,6 ± 2,6
CholA	12	3125,3 ± 183,3	0,23 ± 0,09	6,5 ± 0,8	79,4 ± 1,3	0,27 ± 0,01	28,4 ± 0,6
CholA SSBB	12	2448,3 ± 145,1	0,31 ± 0,03	6,9 ± 0,6	165,2 ± 5,3	0,11 ± 0,01	25,8 ± 1,0
MyrA	12	2353,6 ± 89,3	0,21 ± 0,08	14,8 ± 1,3	79,0 ± 0,1	0,27 ± 0,01	39,3 ± 2,0
MyrA SSBB	12	3752,0 ± 136,4	0,37 ± 0,07	3,8 ± 0,6	102,0 ± 0,7	0,21 ± 0,01	33,6 ± 1,5
SteA	12	3781,3 ± 327,2	0,26 ± 0,08	7,4 ± 1,5	55,2 ± 0,4	0,17 ± 0,01	27,3 ± 0,7
SteA SSBB	12	3361,3 ± 80,4	0,25 ± 0,05	5,0 ± 2,0	102,2 ± 0,8	0,21 ± 0,01	31,7 ± 0,7
OleA	12	3368,6 ± 92,2	0,42 ± 0,14	7,3 ± 1,3	73,2 ± 0,9	0,20 ± 0,01	32,5 ± 0,2
OleA SSBB	12	2087,6 ± 136,3	0,37 ± 0,05	8,4 ± 1,1	77,1 ± 1,4	0,21 ± 0,01	41,1 ± 0,4
NonOcA	12	2115,6 ± 56,7	0,26 ± 0,06	15,2 ± 1,9	66,6 ± 0,5	0,22 ± 0,01	39,7 ± 2,6
NonOcA SSBB	12	2631,0 ± 27,8	0,36 ± 0,29	7,2 ± 0,5	116,1 ± 0,6	0,11 ± 0,02	30,0 ± 1,6

3.2.2.2 Stability of mRNA polyplexes and lipopolyplexes determined in agarose gel shift assays

Polyplexes and lipopolyplexes were formed only in HBG, because of agglomeration in HBS. Complete binding of 250 ng of mRNA by lipo-oligomers at N/P 12 was determined by measuring the electrophoretic mobility of mRNA in a 1% agarose gel. In general, all tested formulations showed complete binding under above mentioned conditions (**Figure 20**).

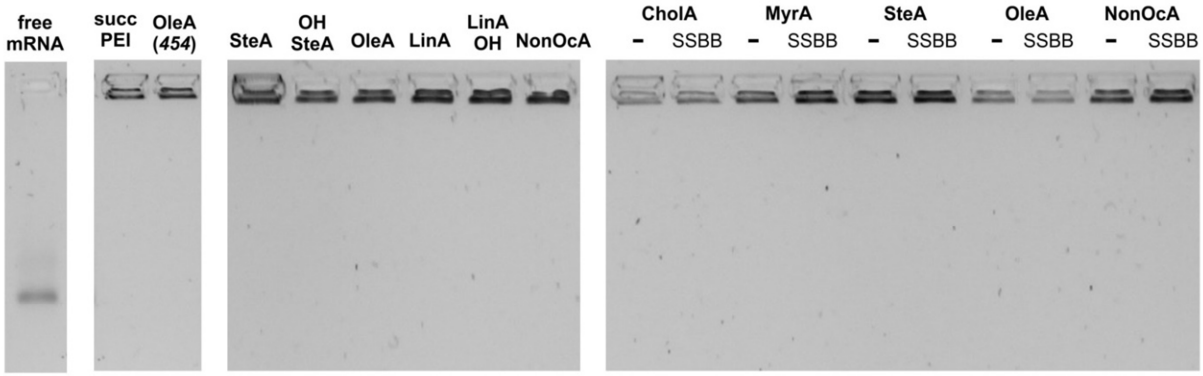

Figure 20 Agarose gel shift assays of mRNA binding at N/P ratio 12. Polyplexes and lipopolyplexes were formed in HBG.

3.2.2.3 Ethidium bromide compaction assay, polyanionic and GSH stress test

To further investigate the ability of different carriers in compacting mRNA, mRNA compaction ability was determined with an ethidium bromide (EtBr) exclusion assay. Polyplexes and lipopolyplexes were formed in HBG. In **Figure 21** (black bars), it is displayed the intensity of EtBr fluorescence normalized to uncomplexed mRNA. SuccPEI polyplexes (<5% EtBr fluorescence) showed the best compaction. Interestingly, all lipopolyplexes displayed good compaction in the range between 20 and 30% EtBr fluorescence, but for OH-SteA lipopolyplexes (~50% EtBr fluorescence), mRNA compaction decreased, which is consistent with the other presented work. The addition of 250IU of heparin sulfate causes anionic dissociative stress and results in partial release of mRNA from polyplexes and lipopolyplexes. Dotted bars in **Figure 21** presents the EtBr fluorescence after the addition of 250IU of heparin sulfate. Under these conditions, mRNA polyplexes of succPEI are less dissociated (~75% EtBr fluorescence) compare to standard OleA (***454***) lipopolyplexes, which completely release mRNA and cause full EtBr fluorescence,

indicating succPEI polyplexes are more stable. Besides, lipopolyplexes formed with OH-SteA displayed the least release of mRNA (~65% EtBr fluorescence), within the first group of T-shapes lipo-oligomers with tyrosine trimers and different fatty acids, whereas other carriers cause higher EtBr fluorescence between 85% and 95% (**Figure 21B**). On the other side, polyplexes formed with bioreducible lipo-oligomers as well as their non-reducible analogs display full dissociation (**Figure 21C**).

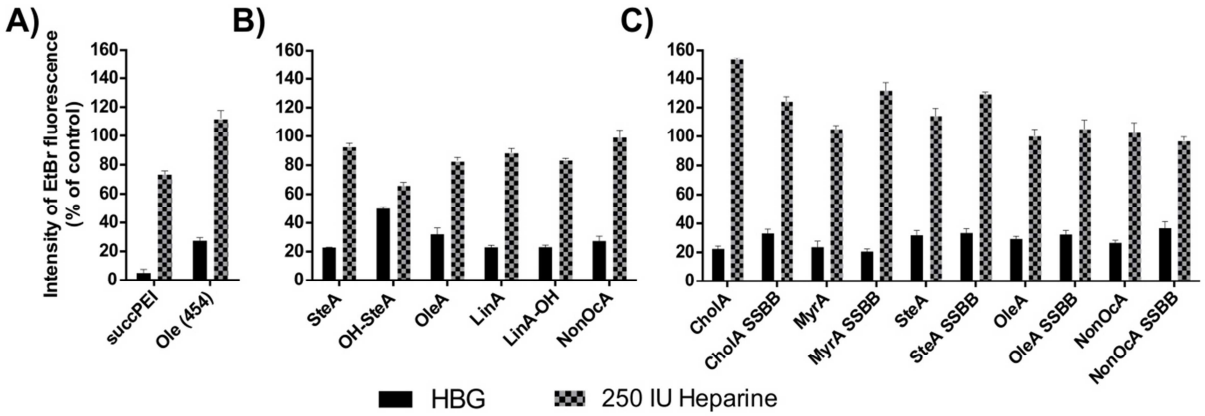

Figure 21 Ethidium bromide exclusion assay to determine the ability of mRNA compaction of the lipo-oligomers, inversely correlating with the remaining fluorescence of mRNA intercalating ethidium bromide (EtBr). Results are presented in % against free mRNA. Polyplexes and lipopolyplexes were formed in HBG at N/P 12 without (black bars) or with (with pattern) treatment by 250 IU of heparin. **(A)** succPEI and OleA (***454***). **(B)** T-shape lipo-oligomers with different fatty acids. **(C)** T-shape lipo-oligomers without and with succinoyl-cystamine building block.

Afterwards, stability of lipopolyplexes from the group of bioreducible lipo-oligomers as well as their non-reducible analogs at intracellular GSH concentrations (~10 mM) was investigated. Lipopolyplexes were formed in HBG at N/P 12 and subsequent 90 min incubated at 37°C with 10 mM of physiological reducing agent GSH in HEPES buffer pH 7.4. Consequently, mRNA binding efficacy of carriers significantly decreased for the reducible but not the stable lipo-oligomers (**Figure 22**). The most significant difference between reducible and stable lipo-oligomers was observed in the case of OleA. Whereas, mRNA binding efficacy of reducible NonOcA remained the same compare to its stabile analog, consistently mRNA compaction remained the same without and with GSH agent as well as transfection efficacy. Position of the SSBB within the carrier, allows the release of the lipid i.e. the most important

stabilization motif, however a weak binding ability of the remaining cationic backbone still exists [116]. Therefore, destabilization of lipopolyplexes, with reductive cleavage, ensure better availability of mRNA in intracellular space.

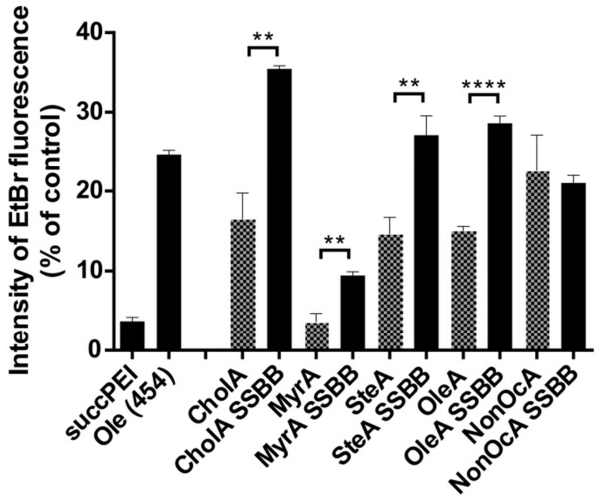

Figure 22 Ethidium bromide exclusion assay. Lipopolyplexes were formed in HBG at N/P 12 and subsequent incubated for 90 min at 37 °C with 10 mM of GSH in HEPES buffer pH 7.4. Results are presented in % against free mRNA. Statistical analysis (Student's t-test): *$p < 0.05$; **$p < 0.01$; ***$p < 0.001$; ****$p < 0.0001$.

3.2.3 Evaluation of mRNA-EGFP transfection efficiency using polyethylenimine or different sequence-defined oligoaminoamides

For a more detailed investigation and direct comparison of the luciferase and GFP reporter systems, expression vector coding for GFP instead of luciferase containing the same backbone was transfected into the DU145 cells. On one side, a flow cytometric quantitative analysis of the transfected cells was performed; on the other side, qualitative GFP expression of cells was detected via fluorescence microscopy using a fluorescence microscope. Again, polyplexes and lipopolyplexes were formed in HBS or HBG and N/P ratio 12 was used. Expression of mRNA-EGFP was detected 24 h after transfection. In **Figure 23**, GFP expression of our control carriers succPEI and OleA (***454***) is presented. Surprisingly, much more GFP positive cells were measured in cells transfected with the OleA (***454***) lipopolyplexes than succPEI (**Figure 23A**). This finally brings up the dilemma of very high succPEI control transfections. Although succPEI polyplexes showed very high luciferase reporter expression (1.5 log scale unit higher than OleA (***454***)), the fraction of GFP positive cells in succPEI treated cultures was ~55% lower both in HBS and HBG polyplex formation. It is known that flow cytometry provides quantification of reporter gene expression in every cell of the transfected population, thus higher luciferase activity of succPEI polyplexes was probably due to very high expression of mRNA-luc in a smaller population of cells. This assumption can be further confirmed with mean fluorescence intensity (MFI) values to GFP expression determined by flow cytometry (**Figure 23C**). MFI value of succPEI polyplexes group is around 90% higher than in the case of OleA (***454***) lipopolyplexes group, which is consistent with the higher luciferase reporter expression of succPEI polyplexes. Besides, MFI value of OleA (***454***) lipopolyplexes treated cells is rather very low, which proves lower intensity of transfected cells. Therefore, flow cytometry analysis shows not only the total amount of protein expression, but also the percentage of mRNA transfected positive cells and is particularly useful when transfection efficiency of luciferase system is low, so that detection of cells that are transfected with a low intensity is also enabled. Thus, GFP expression showed us a quantitative impression of successful transfection at cellular level. The same results were confirmed when GFP expression cells was observed via fluorescence microscopy (Figure **23B**). There were no fluorescence signals imaged on the controls (non-treated cells, cells treated with HBS or HBG). Besides, there was increased fluorescence for cells transfected with either succPEI polyplexes or

OleA (***454***) lipopolyplexes as compared to controls. Again, we could notice a lower amount of GFP positive cells, with different intensity (few with very high intensity), when they were transfected with succPEI polyplexes. While, in the case of OleA (***454***) transfection, higher amount of GFP positive cells with more uniform low intensity was examined. In both experiments, flow cytometry and also fluorescence microscopy, very small differences in cells transfected between polyplexes or lipopolyplexes formed in HBS or HBG were observed.

Results of GFP expression studies of 3-arm oligomers (**Figure 24**) were consistent with their previous luciferase expression studies (**Figure 15**), showing almost nonexistent GFP expression when Stp or H-(Stp-H) carriers were used. While in the case of H-(Stp-H)-Y carrier significantly higher GFP expression was found, indicating the advantage of tyrosine trimers in structure. Besides, the difference between HBS and HBG polyplex formation is more emphasized in this experiment (as was the case with luciferase expression of the same vectors). HBS polyplex formation obviously lead to higher GFP expression in more cells and with different intensity, while HBG polyplex formation resulted in three time lower amount of transfected cell with lower intensity. It's also confirmed with corresponding MFI values to GFP expression (**Figure 24C**), high MFI value for HBS and low MFI for HBG polyplex formation.

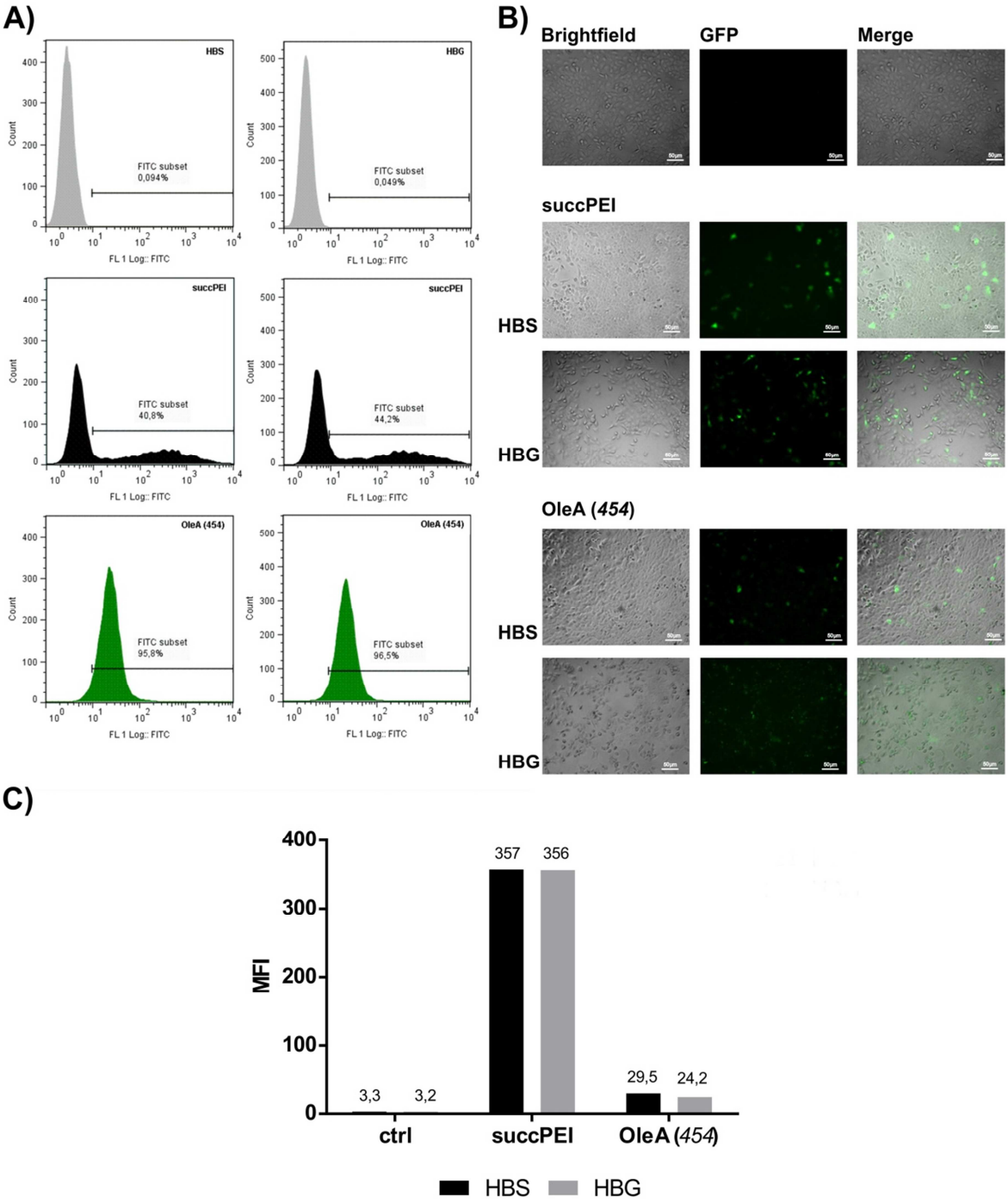

Figure 23 (A) GFP expression after 24h incubation of succPEI polyplexes or OleA (*454*) lipopolyplexes with DU145 cells as determined by flow cytometry. Polyplexes and lipopolyplexes were formed in HBS (left column) or HBG (right column) buffer. **(B)** Fluorescence microscopy of fixed untreated DU145 cells, cells treated with succPEI polyplexes or OleA (*454*) lipopolyplexes formed in HBS or HBG buffer for 24h. Left column: brightfield images of the treated cells. Middle column: GFP fluorescence of the treated cells. Right column: Merge. Scale bar is 50 µm. In **(C)** corresponding mean fluorescence intensity (MFI) values to GFP expression determined by flow cytometry are displayed.

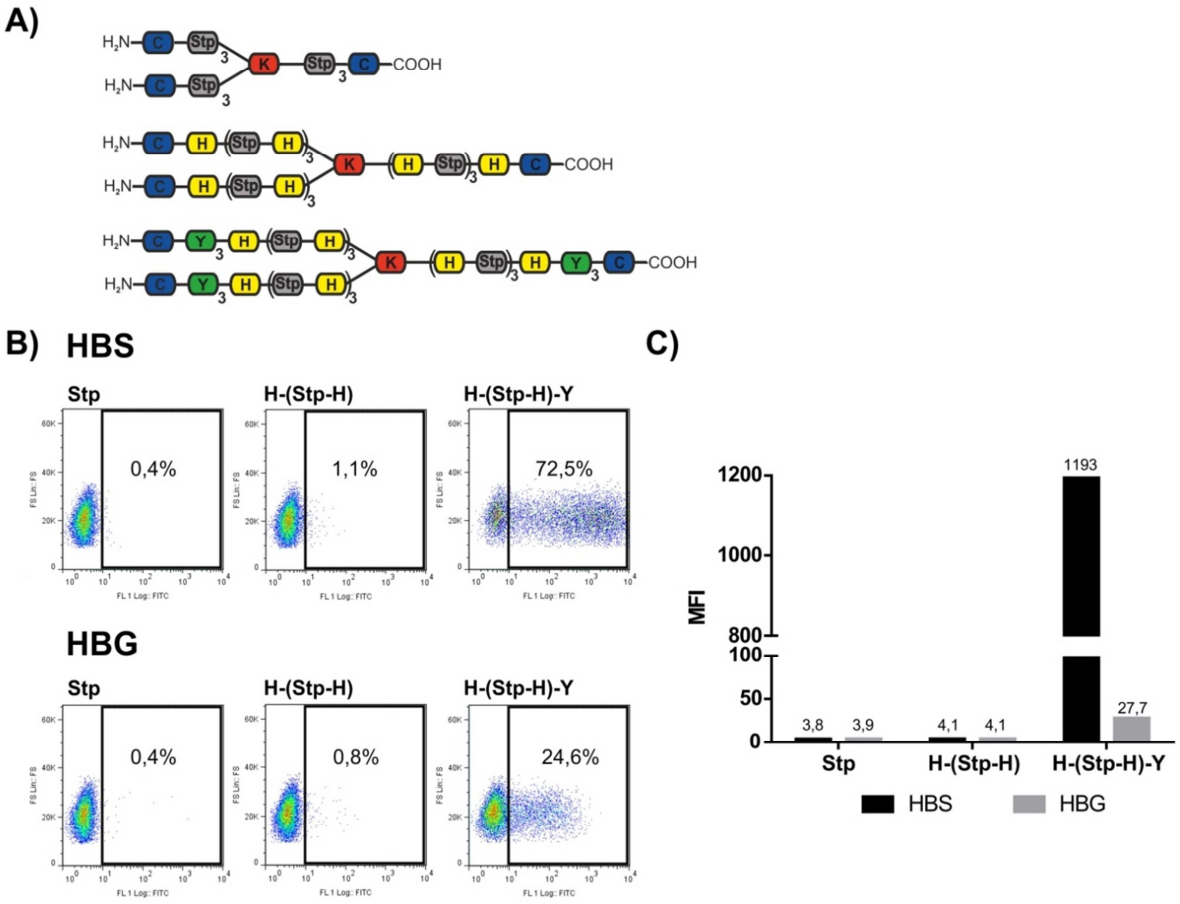

Figure 24 (A) Schematic structures of sequence-defined 3-arm oligomers (Stp: succinoyl-tetraethylene-pentamine, C: cysteine, K: lysine, H: histidine, Y: tyrosine). **(B)** GFP expression after 24h incubation of Stp, H-(Stp-H) and H-(Stp-H)-Y polyplexes with DU145 cells as determined by flow cytometry. Polyplexes were formed in HBS (top) or HBG (bottom) buffer at N/P ratio 12. **(C)** Corresponding mean fluorescence intensity (MFI) values to GFP expression determined by flow cytometry.

Next, flow cytometry analyses and fluorescence microscopy were also performed for the last two groups of sequences with T-shape topology, tyrosine tripeptides and different fatty acids. The results of the first group of lipo-oligomers (**Figure 25**) emphasize superiority of the HBG over HBS lipopolyplex formation and at the same time demonstrate the difference to the luciferase expression system where HBS lipopolyplex formation resulted in higher transfection efficiency. In almost all cases (except LinA), GFP positive cells of lipopolyplexes group formed in HBG were more than the corresponding lipopolyplexes group formed in HBS (**Figure 25A**). Consistent with previous measured luciferase expression data, hight MFI value was measured for HBS lipopolyplex formation of OH-SteA and NonOcA, but also for OH-SteA

lipopolyplexes formed in HBG (**Figure 25B**). Besides, the high intensity of GFP expression of the same lipopolyplexes in some cells is demonstrated on **Figure 25A**. Again, this data correlate well with previous measured luciferase expression data. Nevertheless, very interesting results were observed also with others lipo-oligomers, which did not show especially notable luciferase expression previously. In HBS lipopolyplex formation group, 79% of cells expressed GFP when we used LinA-OH carrier and even more (92% of GFP expression) when we used LinA carrier. Even better results were obtained in HBG lipopolyplex formation, GFP expression of 78% for SteA, 96% for OleA, 89% for LinA, 83% for LinA-OH and 89% for NonOcA lipo-oligomers. Additionally, fluorescence microscopy confirmed GFP expression with more cells with different intensity in the case of OH-SteA (**Figure 25C**).

In the second group of lipo-oligomers, we compared GFP expression of bioreducible lipo-oligomers and their non-reducible analogs in HBS and HBG lipopolyplex formation (**Figure 26**). First imposed finding regarding difference in GFP expression determined by flow cytometry is correlated with bioreducibility (**Figure 26A** and **B**). Bioreducible carriers showed higher GFP expression in all carriers over their non-reducible analogs and in both options, HBS or HBG lipopolyplex formation. The only exception was OleA containing lipo-oligomers, where bioreducible OleA showed the same GFP expression as its non-reducible analog. Further, GFP positive cells of HBG formed lipopolyplexes was again higher compare to the same lipopolyplexes formed in HBS (except MyrA) (**Figure 26B**), which is opposite to previous luciferase expression results (**Figure 19A**). More than 80% of cells were observed in all lipopolyplexes formed in HBG, except MyrA (**Figure 26B**, grey bars). However, the highest (more than 95% transfected cells) GFP expression were achieved with bioreducible CholA and bioreducible NonOcA lipopolyplexes formed in HBG, while the lowest difference between bioreducible oligomer and its non-reducible analog was observed in the case of OleA. Next, the lowest GFP expression was detected when lipopolyplexes of NonOcA, MyrA and their bioreducible analogs were formed in HBS, probably due to their cytotoxicity. For the same bioreducible carriers the highest MFI value was measured (**Figure 26C**). Surprisingly, high GFP expression was observed also in the case of lipo-oligomers, which did not show especially interesting luciferase expression previously (presented on **Figure 19A**). Presence of reducible SteA in HBS lipopolyplex formation resulted in almost 80% of cells expressing GFP.

When we formed lipopolyplex in HBG, the obtained results were even better. Reducible lipo-oligomers and their non-reducible analogs containing CholA, SteA or NonOcA as well as non-reducible OleA showed very poor or no transfection efficiency in the case of luciferase expression system, whereas with flow cytometry analyses, GFP expression of more than 80% in all cases, were determined. Fluorescence microscopy results confirmed above mentioned flow cytometry data (**Figure 26D**). Again, higher GFP expression of bioreducible lipo-oligomers compare to their non-reducible analogs was observed. As flow cytometry data of bioreducible MyrA showed ~15% lower GFP positive cells and high MFI value when lipopolyplexes were formed in HBS compare to HBG lipopolyplex formation (low MFI value), fluorescence microscopy pictures clearly present differences in GFP expression intensity within the cell population (**Figure 26D**, left). Therefore, on one side, transfection with bioreducible MyrA (HBS) resulted also in quite high intensity of GFP expression, but on the other side also caused higher cytotoxicity as shown in the **Figure 26D**, but also with Cell Titer Glo® Assay (**Figure 19C**). In the case of OleA containing lipo-oligomers, similar percentage of GFP expression is in both, HBS and HBG lipopolyplex formation, and flow cytometry analyses can be also certificated by fluorescence microscopy. Non-reducible OleA polyplexes transfected the same amount of cells with poor GFP expression level, while reducible OleA transfected some cells with higher level of GFP (**Figure 26D**, right).

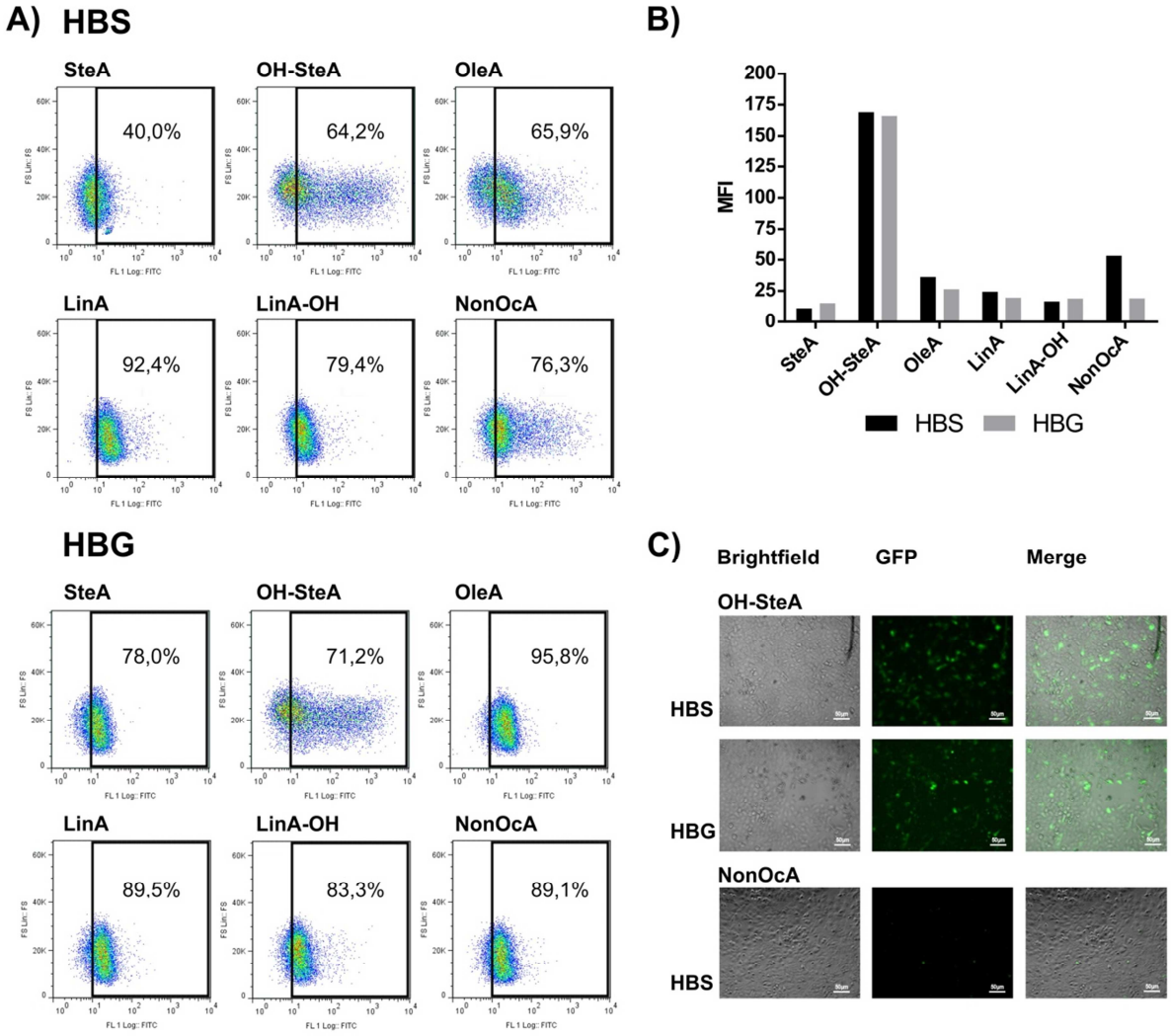

Figure 25 (A) GFP expression after 24h incubation of lipopolyplexes with DU145 cells as determined by flow cytometry. Lipopolyplexes were formed from T-shape oligomers modified with different fatty acids in HBS (top) or HBG (bottom) buffer. **(B)** Corresponding mean fluorescence intensity (MFI) values. **(C)** Fluorescence microscopy of fixed DU145 cells treated with OH-SteA or NonOcA lipopolyplexes for 24 h. Lipopolyplexes were formed in HBS or HBG buffer. Left column: brightfield images of the treated cells. Middle column: GFP fluorescence of the treated cells. Right column: Merge. Scale bar is 50 µm.

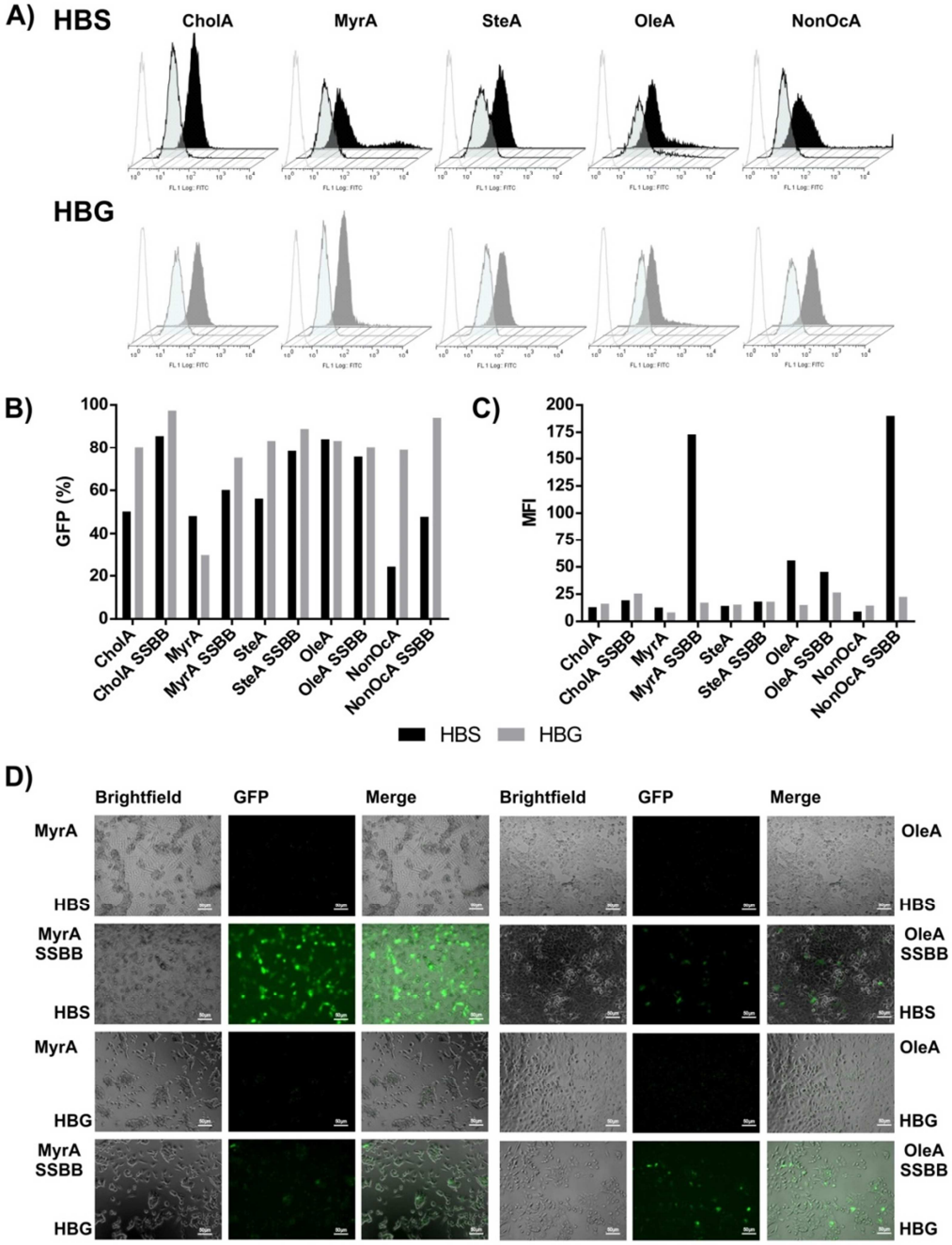

Figure 26 (A) GFP expression after 24h incubation of lipopolyplexes with DU145 cells as determined by flow cytometry. Lipopolyplexes were formed in HBS (top) or HBG (bottom) buffer. Empty peak present cells treated with HBS or HBG. Tinted peak present cells treated with lipopolyplexes formed by oligomers without SSBB, while filled peak present cells treated with lipopolyplexes formed by oligomers with SSBB. **(B)** GFP expression of the same samples as described in (A) presented as a percentage. **(C)** Corresponding mean fluorescence intensity (MFI) values. **(D)** Fluorescence microscopy of fixed DU145 cells treated with MyrA, MyrA SSBB, OleA or OleA SSBB lipopolyplexes for 24 h. Lipopolyplexes were formed in HBS or HBG buffer. Left column: brightfield images of the treated cells. Middle column: GFP fluorescence of the treated cells. Right column: Merge. Scale bar is 50 µm.

4 Discussion

4.1 Minicircle versus plasmid DNA delivery by receptor-targeted polyplexes

This chapter has been adapted from:
A. Krhac Levacic, S. Morys, S. Kempter, U. Lächelt and E. Wagner. Minicircle versus plasmid DNA delivery by receptor-targeted polyplexes. Human Gene Therapy 2017 28(10), 862-874

Due to its minimal size and lack of bacterial backbone sequences, minicircle (MC) DNA presents a promising alternative to plasmid DNA (pDNA) for non-viral gene delivery in terms of biosafety and improved gene transfer. Different nucleic acid cargos, due to their different size or nature, are known to differ in their formulation requirements [78, 79]. Therefore, the present study compared physicochemical and transfection characteristics of polyplexes formed with pDNA (pCMV-luc) or MC DNA (MC07.CMV-luc) and linPEI, as well as untargeted and targeted oligoaminoamides.

Four sequence-defined cationic oligoaminoamides were generated (**Table 1**) by solid-phase assisted synthesis; previously described [107] three-arm (***689***) and cmb-PEG (***442***) and Y_3-containing analogous carriers, three-arm-Y (***849***) and cmb-PEG-Y (***852***). The additional incorporation of tyrosine trimers (Y_3) had been found advantageous for aromatic and hydrophobic polyplex stabilization [112, 116]. Efficient DNA compaction is an important requirement for gene transfer. Recent work revealed suboptimal pDNA packaging by cmb-PEG; apparently, the PEG shielding domain interfered with DNA condensation [107, 108]. The PEG-free three arm oligomer and also the cmb-PEG/three-arm carrier combination effectively compacted DNA, resulting in effective pDNA gene transfer *in vitro* and *in vivo* [107]. For this reason, combination polyplexes were also analyzed in the current comparison of pDNA and MC DNA polyplexes.

Nucleic acid compaction with synthetic gene carriers into nanosized particles is an important requirement for successful gene delivery. This study compared pCMV-luc

and MC07.CMV-luc polyplex formation using a series of different characterizations methods: particle size and zeta potential (DLS), transmission electron microscopy (TEM) and EtBr exclusion assay. As expected, well-compacting cationic polymers such as linPEI or Y_3 oligomers formed polyplexes with similar diameters, irrespective of the different size of the cargos, whereas the tyrosine-free oligoaminoamides form polyplexes where sizes significantly differ for pDNA and MC. For plain polycations, the different cargo DNA size is compensated by aggregating different cargo copy numbers into one polyplex. The situation is different for carriers that avoid nano-aggregation and form monomolecular DNA polyplexes [133, 281]. However, addition of a three-arm structure to the cmb-targeted structure led to a smaller and more compact particle in the case of polyplex formation with both plasmids. These observations were confirmed by DLS as well as TEM. Investigating morphologies by TEM showed that nanoparticle shapes differing between the carriers but not the DNA used in polyplex formation. Nevertheless, TEM provided evidence for the presence of smaller ultrastructures for MC than for pDNA polyplexes. Notably, the majority of nanoparticles were within the <50nm nuclear envelope pore limit to enable transport of polyplexes into the nucleus [21]. In addition, EtBr exclusion assay confirmed best compaction for linPEI polyplexes, but also almost complete dissociation under stress conditions (addition of heparin sulfate), irrespective of the type of DNA. Interestingly, polyplexes formed with oligoaminoamides displayed better compaction and higher stability under stress conditions for MC compared to pDNA, while MC DNA combination polyplexes showed even better compaction and the highest stability. Oligoaminoamide polyplexes, stabilized by bioreversible disulfide crosslinks, are more resistant to stress conditions.

To compare transfection efficiency of polyplexes formed with either pCMV-luc or MC07.CMV-luc, luciferase gene transfer in the prostate carcinoma cell line DU145 which expresses the cell surface receptor HGFR/c-Met was performed. In general, polyplexes formed with MC07.CMV-luc mediated better transfection than polyplexes formed with pCMV-luc in all tested settings; short-term (0.75 h) and long-term (24h) incubations with polyplexes as well as equal mass quantities of used DNA and equimolar quantities of vectors. Besides, another three important findings were observed. First, when polyplexes were formed with pCMV-luc and linPEI, prolonged incubation helped to increase transgene expression to the same level as obtained

with MC07.CMV-luc polyplexes after short incubation. Second, an advantageous effect of the novel c-Met targeted oligomers with integrated tyrosine trimers analogously was noted, as previously observed for folate receptor targeted pDNA polyplexes [112, 116]. And third, higher copy number of MC07.CMV-luc than the corresponding pCMV-luc vector is not responsible for the enhanced transfection when equal mass quantities of DNA was used. Altogether, the beneficial effect of tyrosine trimer integration, formation of combination polyplexes, and use of MC added up to a ~200-fold enhanced gene expression.

The advantage of MC DNA in polyplex transfection, although confirmed in the current and other previous work, is not easy to understand. The clear-cut differences in physicochemical properties, such as smaller and more compacted nanostructures of MC DNA polyplexes, might favorably or unfavorably translate in the complex, multi-step process of non-viral gene delivery [130].

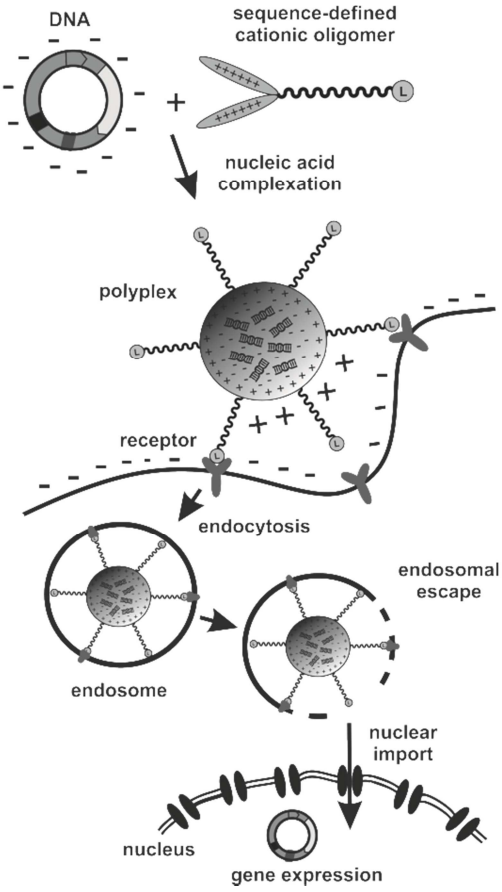

Figure 27 Schematic presentation of the gene delivery process of polyplexes formed from DNA and sequence-defined cationic oligomer.

For electroporation of free DNA, MC DNA presented a more effective vector uptake [255]. Maucksch et al. [290] also reported that a small pDNA size can be important for cell and nucleus entry upon electroporation; comparing 4.7 kb of pEGFP-monomer with 9.4 kb of pEGFP-dimer pDNA, a 17% versus 13% nuclear delivery was observed. For polyplexes, which usually package multiple vector molecules, nanoparticle size may have more impact for initial cellular uptake than vector size. On the one hand, larger PEI polyplexes were previously found to possess increased transfection efficiency due to their enhanced cellular contact by sedimentation in cell culture, subsequent uptake, and enhanced endosomal escape activity by the proton sponge effect [291]. On the other hand, smaller nanoparticle sizes may provide favorable characteristics in cellular uptake by mechanisms of receptor-mediated endocytosis, and favorable subsequent intracellular sorting pathways avoiding lysosomal destruction. Intuitively, by their smaller size, they might have advantages in sneaking across intracellular barriers. In particular, the intranuclear delivery of the vector presents a crucial size-dependent process, followed by unpackaging and successful gene expression in the nucleus [22]. Recent work suggests that DNA/PEI with a diameter <50 nm would pass through nuclear envelope pores [21]. Larger pDNA nanoparticles might enter the nucleus during the small window of mitosis, when the nuclear membrane breaks down. Smaller MC nanoparticles might have the advantage to enter the nucleus at any stage of cell cycle. Therefore, transfections using DU145 cells were performed in different stages of cell cycle. Irrespective of cell cycle stage, the MC formulations mediated up to a 10-fold higher gene expression. The transfections confirmed the lack of significant cell cycle dependence for linPEI/pDNA polyplexes, which correlates with previous studies [18], as well as for linPEI/MC polyplexes. An analogous lack of cell cycle dependence was found for both types (pDNA and MC) of well-compacted cmb-PEG-Y/three-arm-Y combination polyplexes. Thus, from these experiments, a hypothetically improved nuclear entry of smaller MC polyplexes over pDNA polyplexes can be neither verified nor excluded. It rather appears that nuclear import is a low barrier for both types of small compacted polyplexes. Interestingly, for the less compacting carrier cmb-PEG-Y, the pDNA- but not the MC-mediated transfection shows cell cycle dependence at 12 h (after mitosis), which is about 10-fold lower than for transfection before mitosis (0 or 6 h), and also about 10-fold lower than the better compacted pDNA polyplex. Importantly,

MC DNA polyplexes display lack of cell cycle dependence for all formulations, suggesting an advantage from their inherent smaller size.

MC DNA comprises several additional advantages beyond the aspects discussed above. In particular, for *in vivo* gene transfer, reduced innate immune responses and strongly improved maintenance of transgene expression are noteworthy [252, 255, 256]. This favorable sustained expression appears to be linked with incorporation of MC DNA into active chromatin [258]. Following *in vivo* gene transfer of standard pDNA into the liver of mice, the presence of the bacterial backbone resulted in a 10- to 1000-fold reduction of gene expression over a period of few weeks due to gene silencing at the nuclear transcription stage. Apparently, DNA elements in cis (directly linked with the transgene expression cassette) are responsible for transcriptional blockade; the *in vivo* excision of the transgene cassette from such elements strongly improved maintenance of gene expression [292]. Interestingly, the size (≥1 kb) of the extragenic DNA had more impact than the CpG content [293, 294], though the increase of A/T content in the backbone or antibiotic resistance genes reduced transcriptional silencing [295].

In conclusion, the work presented here demonstrates better physicochemical characteristics and transfection efficiencies of MC DNA polyplexes compared to standard pDNA with linPEI or sequence-defined oligoaminoamides. Within the latter class of carriers, novel c-Met targeted and tyrosine trimer-stabilized oligomers were designed, which by optimized formulation in combination with MC DNA yielded more than 100-fold enhanced gene transfer efficiency in receptor positive target cells. These results provide an encouraging future perspective for targeted *in vivo* gene delivery.

4.2 Sequence defined oligomers as carriers for mRNA delivery

Messenger RNA (mRNA) is recognized as versatile, safe, and cost-effective technologies for the treatment of cancer and also other disease; mRNA-based drug technologies have attracted serious attention over the past years. Since, the major limitations of mRNA, strong immunogenicity and limited stability, have been recently greatly improved by various chemical modifications, the important restriction remains in cellular entry. Cationic sequence-defined oligoaminoamides for delivery via endocytic pathways represent a promising approach to improve gene transfection. Therefore, this part of the thesis focused on the exploration of the cationic carrier requirements which could be necessary for the delivery of mRNA.

To find a carrier which could be used as positive control in the project, first the transfection efficiency of different types of the gene delivery “gold standard” polyethylenimine (PEI) was compared. Lower transfection efficiency of PEI is often a consequence of the toxicity, therefore introduction of succinic acid groups to the PEI structure had been recognized as less toxic alternative when applied at higher concentrations for enhanced siRNA transfection [278]. Since succPEI (10% succinylation, w/w ratio 4) showed the highest transfection efficiency under nontoxic conditions, we decided to use it as control polymer in all future experiments. In the next step, transfection efficiency of more than 60 oligomers with various sequences and topologies was tested. The main finding of this initial mRNA-luc transfection experiment was that tyrosine or/and fatty acids containing oligomers mediated higher transfection efficiency. Tyrosine trimers and fatty acids are already recognized as stability domains for pDNA and siRNA polyplex formation through hydrophobic interactions, thus they had been previously integrated into oligomers [106, 116]. Incorporation of only tyrosine trimers into the 3-arm structure was enough for enhanced transfection efficiency for 5 or 2.5 log scale units in HBS and HBG polyplex formation, respectively. In T-shape oligomer topology, like for siRNA delivery, the combination of tyrosine trimers with fatty acids was favorable. On one side, low stability of nanoparticles is a critical issue for successful delivery (especially for the small siRNA double helix), but on the other side, too stable nanoparticles (for single stranded mRNA) could also cause low protein expression as a results of low mRNA release and translation in the cytosol. Therefore, additional stability motif CRC [115]

did not show any further advantageous on transfection efficiency probably due to high stability of nanoparticles. Further on, the influence of different fatty acids in T-shape structures was examined. For this purpose, we used two groups of T-shape lipo-oligomers previous designed and used for siRNA delivery in our group. Sören Reinhard (PhD student, Pharmaceutical Biotechnology, LMU Munich) synthesized a first group of T-shape lipo-oligomers containing tyrosine tripeptides, terminal cysteines, and different fatty acids [289], while the second group of similar, but cysteine-free, bioreducible sequence-defined lipo-oligomers as well as their non-reducible analogs was created by Dr. Philipp Klein (PhD thesis 2017, LMU Munich) [104]. In general, several important assumptions can be made based on luciferase expression results. First, saturated SteA lipopolyplexes are less effective compare to lipo-oligomers with unsaturated or modified hydrocarbon chains. Second, enhanced lytic potential of OleA, OH-SteA and NonOcA caused enhanced transfection efficiency on one side, and unwanted cytotoxicity (associated with other transfection conditions as HBS lipopolyplex formation) in some cases on other side. Third, incorporation of a bioreducible disulfide bond (SSBB) between the cationic and the lipid arm of oligomers enhanced release of mRNA in the intracellular reductive space, reduced cytotoxicity, and also enhanced transfection efficiency of those lipopolypexes. Fourth, MyrA is recognized as cytotoxic regardless with or without SSBB in structure when the polyplexes were formed with HBS. And fifth, formation of polyplexes in HBS is responsible for enhanced transfection efficiency compared to those formed in HBG in almost all tested cases, but it sometimes also correlated with higher cytotoxicity. All aforementioned findings correlate well with our previous published data [104, 289, 291]. Although we noticed differences in transfection efficiency in different cell lines, the relative transfection profile of all oligomers used in the study was similar over several cell lines.

Nucleic acid compaction into nanosized particles is another important requirement for mRNA delivery. The size of nanoparticles formed in HBG in almost all cases was within the size limit for cellular uptake (<200 nm) [14], while HBS is recognized as the cause of the formation of particles bigger than 1000nm. Tendency of HBS causing large aggregates is already reported in previous work [291]. Unlike all other measured nanoparticles, only the sizes of succPEI polyplexes and LinA-OH lipopolyplexes were consistent regardless of whether they were formed in HBS or

HBG. It is consistent with previous published results that branched PEI during polyplex formation is slightly less dependent on the salt concentration [203, 286]. Although bigger particles can also enter the cells, the smaller particles usually can easier circumvent most of the cellular barriers and tend to show no or low toxicity. Previous studies in our laboratory showed that smaller nanoparticles could be less effective in transfection because of reduced cell binding, inefficient intracellular release or subsequent steps of intracellular delivery. Besides, it is shown that larger nanoparticle, in our case lipopolyplexes formed in HBS, could increase transfection efficiency, because of their enhanced uptake and endosome destabilizing activity [291]. Regardless of the small size of succPEI polyplexes in both HBS and HBG polyplex formation, enhanced luciferase expression in both cases was observed, probably due to endosomal escape capability of PEI by acting as a 'proton sponge' [28]. Next, increased PDI of HBS nanoparticles indicated less homogenous particle formation. Additionally, the zeta potential of HBS formed particles decreased indicating aggregates. To further investigate compaction of oligomers, ethidium bromide compaction assay was used. SuccPEI polyplexes showed best compaction, while others lipopolyplexes displayed well compaction in the range of between 20 and 30% residual EtBr fluorescence. The worst compaction was observed for OH-SteA (~50% residual EtBr fluorescence) probably also correlating with particle sizes of >1000 nm. However, these characteristics of OH-SteA are presumably responsible for its high efficiency. The addition of 250IU of heparin sulfate causes anionic dissociative stress and results in partial release of mRNA from polyplexes and lipopolyplexes. Under these conditions, succPEI polyplexes were more stable compared to other carriers which caused EtBr fluorescence increase to more than 85% and displayed high dissociation. This finding indicated that endosomal escape of other lipopolyplexes formed in HBG should be better or at least the same comparing to succPEI. Additionally, destabilization of bioreducible lipopolyplexes with disulfide building block (SSBB) at intracellular GSH concentrations (~10 mM) was observed. The position of the SSBB linkage within the carrier allows the release of the lipid i.e. the most important nanoparticle stabilization motif, from a small cationic backbone [104]. Therefore, destabilization of lipopolyplexes with reductive cleavage may ensure better availability of mRNA in the intracellular space. As expected, mRNA binding efficacy of carriers significantly decreased for the reducible but not the analogous stable lipo-oligomers under reducing cytosolic conditions. These results

explained the transfection experiments that transfection efficiency of bioreducible lipopolypexes was enhanced over their non-reducible analogs.

Alternatively, a lower fraction of luciferase expressing cells or a prevalence of cells with lower expression levels could be the reason of decreased transfection efficiency of smaller nanoparticles. Therefore, for a more detailed investigation of cellular mRNA expression, transfer of GFP mRNA was applied to detect GFP expression of DU145 cells by flow cytometry and fluorescence microscopy of the transfected cells. Results obtained by flow cytometry point at the dilemma of a very high succPEI standard transfection activity. Although succPEI polyplexes showed very high luciferase reporter system expression (1.5 log scale unit higher than OleA (***454***)), the fraction of GFP positive cells in the succPEI group was ~55% lower compare to OleA (***454***). Flow cytometry as a sensitive method enables quantification of reporter gene expression in every cell of the transfected population, while higher luciferase activity of succPEI polyplexes was obviously resulting from high expression of mRNA-luc in a smaller population of cells. This assumption was confirmed with mean fluorescence intensity (MFI) values of GFP expression determined by flow cytometry. MFI value of succPEI polyplexes is around 90% higher than for OleA (***454***) lipopolyplexes, which is directly correlated to the higher luciferase reporter system expression of succPEI polyplexes. Besides, low MFI value of OleA (***454***) lipopolyplexes proves lower intensity of transfected cells. Therefore, flow cytometry analysis is particularly powerful in detection of cells that are transfected with a low intensity. Similar findings regarding correlation of low luciferase expression with more GFP positive cells and low MFI value or contrariwise were identified when we tested other lipo-oligomers. Therefore, very interesting results i.e. high GFP positive cells were observed also with others lipo-oligomers such as SteA, OleA, LinA, LinA-OH, NonOcA lipo-oligomers as well as reducible lipo-oligomers and their non-reducible analogs containing CholA, SteA or NonOcA. These observations suggest that also those aforementioned oligomers can transfect high percentage of cell population, but with a lower intensity of expressed protein. The lowest GFP expression value was detected when MyrA lipopolyplexes were used, most probably due to cytotoxicity of MyrA lipo-oligomers which was noticed already in luciferase expression system (especially when bigger HBS particles were used) and in GFP expression system become even more obvious. High luciferase transfection efficiency of reducible MyrA lipopolyplexes

is due to high expression level per cell as was confirmed with fluorescence microscopy. Importantly, bioreducible carriers showed higher GFP expression in all carriers over their non-reducible analogs. In general, GFP expression detected with flow cytometry is consistent with our previous findings, however some differences were observed. Firstly, both results demonstrate the transfection efficiency depending on lipopolyplex formation solution. Contrary to luciferase expression system where HBS lipopolyplex formation resulted in higher transfection efficiency, HBG lipopolyplexes showed enhanced GFP positive cells over the same HBS lipopolyplex. As is already explained before, expression level of smaller in HBG formed lipopolyplexes per cell was probably lower and therefore more hardly detectable in the case of luciferase expression system. And secondly, reducible OleA and its non-reducible analog showed similar percentage of GFP expression in both HBS and HBG lipopolyplex formation. Fluorescence microscopy results also showed us that non-reducible OleA transfected higher amount of cells which expressed very poor level of GFP, while in cells transfected by reducible OleA higher level of GFP were noticed. Altogether, fluorescence microscopy results correlated well with flow cytometry data and enabled us to visualize the quantity of transfected cells as well as differences in GFP expression intensity.

To sum up, an appropriate carrier mediating successful mRNA delivery depends on cell line type, type of carrier, its modification and also buffer used for complex formation. Two different topology of carriers, 3-arm and T-shape sequence-defined oligoaminoamides, were recognized as potentially successful mRNA delivery platform. Overall, this work is consistent with our previous work, pointing out the positive effect of different carrier modifications as tyrosine trimers or/and fatty acids which present stability enhancement domains through hydrophobic interactions. Ideally, formed mRNA complexes should be stable and homogenous, and they differ not only because of different carrier sequence but also depending on solutions (HBS, HBG) used for complexes formation. Complexes formed in HBS were larger and more efficient in luciferase mRNA transfer probably due to their enhanced uptake and endosome escape activity. GFP expression enabled us detection of a high fraction of cells with lower GFP expression level, which was particularly important in the case of smaller complexes formed in HBG. Both results are valuable, but for different applications. The superior effect of reducible lipo-oligomers over their non-reducible

analogs confirmed the importance of destabilization in the intracellular cytosolic place, leading to the release of the mRNA for protein translation by the ribosomal machinery. In conclusion, several carriers were identified which showed positive characteristics and could be used for mRNA delivery, depending on purpose.

Table 4 Summary of oligomer characteristics

		HBS complex formation				HBG complex formation					
ID	**Carrier abbreviation**	**Luciferase gene transfer**	**Toxicity**	**GFP expression (%)**	**Size**	**Luciferase gene transfer**	**Toxicity**	**GFP expression (%)**	**Size**	**Compaction**	**Heparin resistance**
	succPEI	++++		40,8	+	++++		44,2	+	+++	-
3-arm											
386	Stp	-		0,4	+++	-		0,4	+	/	/
689	H-(Stp-H)	-		1,1	+++	-		0,8	+	/	/
849	H-(Stp-H)-Y	+++++		72,5	++	+++		24,6	+	/	/
T shapes with terminal Y_3-Cys											
454	OleA (***454***)	++		95,8	+	++		96,5	+	++	-
	SteA	+		40,0	+++	-		78,0	+	++	-
1105	OH-SteA	++++		64,2	+++	+++		71,2	+++	+	+
	OleA	++		65,9	+++	-		95,8	+	++	-
1165	LinA	++		92,4	+	-		89,5	+	++	-
1166	LinA-OH	++		79,4	+	+		83,3	+	++	-
1104	NonOcA	++++		76,3	++	-		89,1	+	++	-
Cys-free T shapes with terminal Y_3											
991	CholA	+		50,2	+++	+		80,4	+	++	-
992	CholA SSBB	++++		85,5	+++	-		97,4	+	++	-
1081	MyrA	++		48,1	+++	-		29,6	+	++	-
1082	MyrA SSBB	++++		60,2	+++	++		75,2	+	++	-
989	SteA	-		56,2	+++	-		83,3	+	++	-
990	SteA SSBB	-		78,4	+++	-		88,9	+	++	-
1107	OleA	+++		84,1	+++	-		83,3	+	++	-
1108	OleA SSBB	++++		75,7	+++	+++		80,4	+	++	-
1083	NonOcA	+		24,3	+++	-		78,9	+	++	-
1084	NonOcA SSBB	++++		47,8	+++	+		94,0	+	++	-

Luciferase gene transfer of polyplexes (DU145 cell line): +++++ transfection efficacy ≥ 10^8 RLU/10000cells, ++++ between 10^7 and 10^8, +++ between 10^6 and 10^7, ++ between 10^5 and 10^6, + between 10^4 and 10^5, - no transfection signal compared to untreated cells (≤ 10^4).

Toxicity: ≥ 85% viable cells, between 70% and 85%, ≤ 70%.

Size: + smaller than 200nm, ++ between 200 nm and 1000 nm, +++ bigger than 1000 nm.

Particle compaction: +++ highest compaction, ++ mediate compaction, + compaction (evaluated by EtBr exclusion assay).

Heparin resistance against 250 IU: +/- indicates Yes/No.

/ indicates Not measured.

5 Summary

Over the past decades, significant progress has been made in the field of nucleic acid delivery vehicles. Sequence-defined macromolecular carriers synthesized by SPS play a significant role in this development. As several different extracellular and intracellular barriers must be overcome for successful transfer, the multifunctional nature of such carriers is of greatest importance. Carriers need to be dynamic [296, 297]. On the one hand, stability of complexes is important at the time of extracellular delivery steps, while on the other hand, the carrier must release therapeutic nucleic acid after delivery inside the cell. SPS offers excellent opportunities to develop structural precise carriers, which is crucial for establishing appropriate structure–activity relationships. Still further optimization of delivery carriers is required. A better understanding of structures characteristics in nucleic acid complexation, target cell recognition, endosomal escape, nuclear delivery, and transgene expression or toxicity is necessary.

The first part of the thesis focuses on the optimization of DNA nucleic acid cargo as well as the compacting carrier system. Bacterial sequences within the standard plasmids reduce their efficacy, biocompatibility and safety, therefore minicircle (MC) DNA with its minimal size and lack of bacterial backbone sequences presents a promising alternative to plasmid DNA (pDNA) for non-viral gene delivery. Herein, we compared physicochemical and transfection characteristics of polyplexes formed with pDNA (pCMV-luc) or MC DNA (MC07.CMV-luc) and linPEI as well as untargeted and targeted oligoaminoamides. For this purpose four sequence-defined cationic oligoaminoamides were generated by solid-phase assisted synthesis; previously described three-arm (***689***) and targeted cmb-PEG (***442***) and Y_3-containing analogous carriers, three-arm-Y (***849***) and targeted cmb-PEG-Y (***852***). The carriers were found to dominate the shape of polyplexes, whereas the DNA type was decisive for the nanoparticle size. c-Met-targeted, tyrosine trimer-containing polyplexes were optimized into compacted rod structures with a size of 65–100nm for pDNA and 35–40nm for MC. Notably, these MC polyplexes display a lack of cell cycle dependence of transfection and a ~200-fold enhanced gene transfer efficiency in c-Met-positive

DU145 prostate carcinoma cultures over their tyrosine-free pDNA analogues. These results provide an encouraging future perspective for targeted *in vivo* gene delivery.

In the second part the thesis focused on the development of appropriate carriers for mRNA delivery starting from examination of different sequence-defined oligoaminoamides which had been previously synthesized as library in purpose of pDNA or siRNA delivery. These initial mRNA transfections had to figure out structure-activity relationships, as a basis to find the optimal carrier for mRNA delivery. Two different topology of carriers (3-arm and T-shape) modified by tyrosine tripeptides or/and fatty acids were recognized as potentially successful mRNA delivery platforms. Different carrier sequences and also buffers (HBS, HBG) used for complex formation were evaluated side by side. The importance of high extracellular stability and destabilization in the intracellular environment, leading to the release of the mRNA in the cytosol, was confirmed.

In sum, sequence-defined delivery carriers containing natural and/or artificial building blocks represent a valuable part in the development of “smart” delivery systems for gene encoding minicircle DNAs or therapeutic mRNAs, which most likely will have great impact in the medicine of tomorrow.

6 Appendix

6.1 Abbreviations

Boc	*tert*-Butoxycarbonyl protecting group
BrPEI	Branched polyethylenimine
CholA	5β-Cholanic acid
DLS	Dynamic light scattering
DMEM	Dulbecco's modified Eagle's medium
DNA	Desoxyribonucleic acid
EDTA	Ethylendiaminetetraacetic acid
EGF/EGFR	Epidermal growth factor / (receptor)
EtBr	Ethidium bromide
FBS	Fetal bovine serum
Fmoc	Fluorenylmethoxycarbonyl protecting group
FolA	Folic acid
FR	Folate receptor
GSH	Glutathione
HBG	Hepes-buffered glucose
HEPES	*N*-(2-Hydroxethyl) piperazine-N'-(2-ethansulfonic acid)
HGF/HGFR	Hepatocyte growth factor (receptor)
Inf7	Endosomolytic influenza virus derived peptide
kDa	Kilodalton
LinA	Linoleic acid
LinA-OH	Hydroxylinoleic acid
linPEI	Linear polyethylenimine
MC07.CMV-luc	Minicircle plasmid encoding for firefly luciferase under the control of the cytomegaly virus (CMV) promoter
mM	Millimolar
mRNA	Messenger RNA
mRNA-luc	Messenger RNA encoding firefly luciferase
mRNA-EGFP	Messenger RNA encoding enhanced green fluorescent protein
MTT	3-(4,5-Dimethylthiazol-2-yl)-2,5-diphenyltetrazolium bromide

mV	Millivolt
MyrA	Myristic acid
N/P	Nitrogen to phosphates ratio
nm	Nanometer
NMR	Nuclear magnetic resonance
NonOcA	8-nonanamidooctanoic acid
OH-SteA	Hydroxystearic acid
OleA	Oleic acid
pCMVLuc	Plasmid encoding for firefly luciferase under the control of the cytomegaly virus (CMV) promoter
pHPMA	Poly-*N*-(2-hydroxypropyl)methacrylamide
PDI	Polydispersity index
pDNA	Plasmid DNA
PEG	Polyethylene glycol
pKa	$-\log_{10} K_a$ (acid dissociation constant)
RLU	Relative light units
RNA	Ribonucleic acid
siRNA	Small interfering RNA
SSBB	Succinoyl-cystamine
Spermine	N,N-(Butane-1,4-diyl)bis(propane-1,3-diamine)
SPS	Solid-phase synthesis
SteA	Stearic acid
Stp	Succinyl-tetraethylene pentamine
succPEI	Succinylated polyethylenimine
TBE	Tris-boric acid-EDTA buffer
TFA	Trifluoroacetic acid

6.2 Summary of SPS derived oligomers

Table 5 Overview of the used sequence defined oligomers, their abbreviations used in the chapter 3.2 and internal library compound IDs

Carrier abbreviation	ID	Sequence	Synthesized by
Stp	***386***	C-Stp_3-K(Stp_3-C)$_2$	Dr. Dongsheng He
H-(Stp-H)	***689***	C-H-(Stp-H)$_3$-K-[H-(Stp-H)$_3$-C]$_2$	Dr. Dongsheng He
H-(Stp-H)-Y	***849***	C-Y_3-H-(Stp-H)$_3$-K-[H-(Stp-H)$_3$-Y_3-C]$_2$	Dr. Stephan Morys
MyrA	***48***	C-Stp_2-K-(K-$MyrA_2$)-Stp_2-C	Dr. Christina Troiber
SteA	***462***	C-Stp_2-K-(K-$SteA_2$)-Stp_2-C	Dr. Christina Troiber
OleA	***49***	C-Stp_2-K-(K-$OleA_2$)-Stp_2-C	Dr. Christina Troiber
Y	***465***	C-Y_3-Stp_2-K-(K)-Stp_2-Y_3-C	Dr. Christina Troiber
CholA-Y	***1021***	C-Y_3-Stp_2-K-(K-$CholA_2$)-Stp_2-Y_3-C	Dr. Philipp Klein
SteA-Y	***1072***	C-Y_3-Stp_2-K-(K-$SteA_2$)-Stp_2-Y_3-C	Dr. Philipp Klein
OleA-Y	***454***	C-Y_3-Stp_2-K-(K-$OleA_2$)-Stp_2-Y_3-C	Dr. Philipp Klein
OleA-Y-CRC	***595***	C-R-C-Y_3-Stp_2-K-(K-$OleA_2$)-Stp_2-Y_3-C-R-C	Dr. Christina Troiber
OleA (***454***)	***454***	C-Y_3-Stp_2-K-(K-$OleA_2$)-Stp_2-Y_3-C	Dr. Philipp Klein
SteA		C-Y_3-Stp_2-K-(G-K-$SteA_2$)-Stp_2-Y_3-C	Sören Reinhard
OH-SteA	***1105***	C-Y_3-Stp_2-K-(K-$OHSteA_2$)-Stp_2-Y_3-C	Sören Reinhard
OleA		C-Y_3-Stp_2-K-(K-$OleA_2$)-Stp_2-Y_3-C	Sören Reinhard
LinA	***1165***	C-Y_3-Stp_2-K-(K-$LinA_2$)-Stp_2-Y_3-C	Sören Reinhard
LinA-OH	***1166***	C-Y_3-Stp_2-K-(K-$OHLinA_2$)-Stp_2-Y_3-C	Sören Reinhard
NonOcA	***1104***	C-Y_3-Stp_2-K-(K-[OcA-NonA]$_2$)-Stp_2-Y_3-C	Sören Reinhard
CholA	***991***	Y_3-Stp_2-K-(G-K-$CholA_2$)-Stp_2-Y_3	Dr. Philipp Klein
CholA SSBB	***992***	Y_3-Stp_2-K-(G-SSBB-K-$CholA_2$)-Stp_2-Y_3	Dr. Philipp Klein
MyrA	***1081***	Y_3-Stp_2-K-(G-K-$MyrA_2$)-Stp_2-Y_3	Sören Reinhard
MyrA SSBB	***1082***	Y_3-Stp_2-K-(G-SSBB-K-$MyrA_2$)-Stp_2-Y_3	Sören Reinhard
SteA	***989***	Y_3-Stp_2-K-(G-K-$SteA_2$)-Stp_2-Y_3	Sören Reinhard
SteA SSBB	***990***	Y_3-Stp_2-K-(G-SSBB-K-$SteA_2$)-Stp_2-Y_3	Sören Reinhard
OleA	***1107***	Y_3-Stp_2-K-(G-K-$OleA_2$)-Stp_2-Y_3	Dr. Philipp Klein
OleA SSBB	***1108***	Y_3-Stp_2-K-(G-SSBB-K-$OleA_2$)-Stp_2-Y_3	Dr. Philipp Klein
NonOcA	***1083***	Y_3-Stp_2-K-(G-K-[OcA-NonA]$_2$)-Stp_2-Y_3	Dr. Philipp Klein
NonOcA SSBB	***1084***	Y_3-Stp_2-K(G-SSBB-K-[OcA-NonA]$_2$)-Stp_2-Y_3	Dr. Philipp Klein

7 References

[1] T. Friedmann, R. Roblin. Gene therapy for human genetic disease? Science 175(4025) (**1972**) 949-955.

[2] T. Wirth, N. Parker, S. Yla-Herttuala. History of gene therapy. Gene 525(2) (**2013**) 162-169.

[3] N. Touchot, M. Flume. Early insights from commercialization of gene therapies in Europe. Genes 8(2) (**2017**) 78-81.

[4] R. Titze-de-Almeida, C. David, S.S. Titze-de-Almeida. The race of 10 synthetic RNAi-based drugs to the pharmaceutical market. Pharm. Res. 34(7) (**2017**) 1339-1363.

[5] C.A. Stein, D. Castanotto. FDA-approved oligonucleotide therapies in 2017. Mol. Ther. 25(5) (**2017**) 1069-1075.

[6] R. Parmar, J.L. Willoughby, J. Liu, D.J. Foster, B. Brigham, C.S. Theile, K. Charisse, A. Akinc, E. Guidry, Y. Pei, W. Strapps, M. Cancilla, M.G. Stanton, K.G. Rajeev, L. Sepp-Lorenzino, M. Manoharan, R. Meyers, M.A. Maier, V. Jadhav. 5'-(E)-Vinylphosphonate: A stable phosphate mimic can improve the RNAi activity of siRNA-GalNAc conjugates. ChemBioChem 17(11) (**2016**) 985-989.

[7] M.A. Behlke. Chemical modification of siRNAs for *in vivo* use. Oligonucleotides 18(4) (**2008**) 305-319.

[8] C.L. Hardee, L.M. Arevalo-Soliz, B.D. Hornstein, L. Zechiedrich. Advances in non-viral DNA vectors for gene therapy. Genes 8(2) (**2017**) 65-87.

[9] U. Lächelt, E. Wagner. Nucleic acid therapeutics using polyplexes: a journey of 50 years (and beyond). Chem. Rev. 115(19) (**2015**) 11043-11078.

[10] W. Walther, M. Schmeer, D. Kobelt, R. Baier, A. Harder, V. Walhorn, D. Anselmetti, J. Aumann, I. Fichtner, M. Schleef. A seven-year storage report of good manufacturing practice-grade naked plasmid DNA: stability, topology, and *in vitro*/*in vivo* functional analysis. Hum. Gene Ther.: Clin. Dev. 24(4) (**2013**) 147-153.

[11] P.L. Felgner, Y. Barenholz, J.P. Behr, S.H. Cheng, P. Cullis, L. Huang, J.A. Jessee, L. Seymour, F. Szoka, A.R. Thierry, E. Wagner, G. Wu. Nomenclature for synthetic gene delivery systems. Hum. Gene Ther. 8(5) (**1997**) 511-512.

[12] D.W. Pack, A.S. Hoffman, S. Pun, P.S. Stayton. Design and development of polymers for gene delivery. Nat. Rev. Drug Discov. 4(7) (**2005**) 581-593.

[13] P. Zhang, E. Wagner. History of polymeric gene delivery systems. Top. Curr. Chem. 375(2) (**2017**) 26-65.

[14] J. Rejman, V. Oberle, I.S. Zuhorn, D. Hoekstra. Size-dependent internalization of particles via the pathways of clathrin- and caveolae-mediated endocytosis. Biochem.J. 377(1) (**2004**) 159-169.

[15] D. Hoekstra, J. Rejman, L. Wasungu, F. Shi, I. Zuhorn. Gene delivery by cationic lipids: in and out of an endosome. Biochem. Soc. Trans. 35(1) (**2007**) 68-71.

[16] D. Lechardeur, A.S. Verkman, G.L. Lukacs. Intracellular routing of plasmid DNA during non-viral gene transfer. Adv. Drug Deliv.Rev. 57(5) (**2005**) 755-767.

[17] J. Vacik, B.S. Dean, W.E. Zimmer, D.A. Dean. Cell-specific nuclear import of plasmid DNA. Gene Ther. 6(6) (**1999**) 1006-1014.

[18] S. Brunner, E. Furtbauer, T. Sauer, M. Kursa, E. Wagner. Overcoming the nuclear barrier: cell cycle independent nonviral gene transfer with linear polyethylenimine or electroporation. Mol.Ther. 5(1) (**2002**) 80-86.

[19] S. Brunner, T. Sauer, S. Carotta, M. Cotten, M. Saltik, E. Wagner. Cell cycle dependence of gene transfer by lipoplex, polyplex and recombinant adenovirus. Gene Ther. 7(5) (**2000**) 401-407.

[20] G. Grandinetti, A.E. Smith, T.M. Reineke. Membrane and nuclear permeabilization by polymeric pDNA vehicles: efficient method for gene delivery or mechanism of cytotoxicity? Mol. Pharm. 9(3) (**2012**) 523-538.

[21] H. Andersen, L. Parhamifar, A.C. Hunter, V. Shahin, S.M. Moghimi. AFM visualization of sub-50nm polyplex disposition to the nuclear pore complex without compromising the integrity of the nuclear envelope. J. Control. Release 244 (**2016**) 24-29.

[22] H. Akita, D. Kurihara, M. Schmeer, M. Schleef, H. Harashima. Effect of the compaction and the size of DNA on the nuclear transfer efficiency after microinjection in synchronized cells. Pharmaceutics 7(2) (**2015**) 64-73.

[23] S.T. Crowley, J.A. Poliskey, N.J. Baumhover, K.G. Rice. Efficient expression of stabilized mRNA PEG-peptide polyplexes in liver. Gene Ther. 22(12) (**2015**) 993-999.

[24] H. Youn, J.K. Chung. Modified mRNA as an alternative to plasmid DNA (pDNA) for transcript replacement and vaccination therapy. Expert Opin. Biol. Ther. 15(9) (**2015**) 1337-1348.

[25] A. Yamamoto, M. Kormann, J. Rosenecker, C. Rudolph. Current prospects for mRNA gene delivery. Eur. J. Pharm. Biopharm. 71(3) (**2009**) 484-489.

[26] Z. Meng, J. O'Keeffe-Ahern, J. Lyu, L. Pierucci, D. Zhou, W. Wang. A new developing class of gene delivery: messenger RNA-based therapeutics. Biomater. Sci. 5(12) (**2017**) 2381-2392.

[27] J.C. Kaczmarek, P.S. Kowalski, D.G. Anderson. Advances in the delivery of RNA therapeutics: from concept to clinical reality. Genome Med. 9(1) (**2017**) 60-76.

[28] O. Boussif, F. Lezoualc'h, M.A. Zanta, M.D. Mergny, D. Scherman, B. Demeneix, J.P. Behr. A versatile vector for gene and oligonucleotide transfer into cells in culture and *in vivo*: polyethylenimine. Proc. Natl. Acad. Sci. U.S.A. 92(16) (**1995**) 7297-7301.

[29] J.L. Coll, P. Chollet, E. Brambilla, D. Desplanques, J.P. Behr, M. Favrot. *In vivo* delivery to tumors of DNA complexed with linear polyethylenimine. Hum. Gene Ther. 10(10) (**1999**) 1659-1666.

[30] Z. Kadlecova, Y. Rajendra, M. Matasci, L. Baldi, D.L. Hacker, F.M. Wurm, H.A. Klok. DNA delivery with hyperbranched polylysine: a comparative study with linear and dendritic polylysine. J. Control. Release 169(3) (**2013**) 276-288.

[31] S. Werth, B. Urban-Klein, L. Dai, S. Hobel, M. Grzelinski, U. Bakowsky, F. Czubayko, A. Aigner. A low molecular weight fraction of polyethylenimine (PEI) displays increased transfection efficiency of DNA and siRNA in fresh or lyophilized complexes. J.Control. Release 112(2) (**2006**) 257-270.

[32] G.-J. Jeong, H.-M. Byun, J.M. Kim, H. Yoon, H.-G. Choi, W.-K. Kim, S.-J. Kim, Y.-K. Oh. Biodistribution and tissue expression kinetics of plasmid DNA complexed with polyethylenimines of different molecular weight and structure. J. Control. Release 118(1) (**2007**) 118-125.

[33] C. Scholz, P. Kos, L. Leclercq, X. Jin, H. Cottet, E. Wagner. Correlation of length of linear oligo(ethanamino) amides with gene transfer and cytotoxicity. ChemMedChem 9(9) (**2014**) 2104-2110.

[34] C. Scholz, P. Kos, E. Wagner. Comb-like oligoaminoethane carriers: change in topology improves pDNA delivery. Bioconjug. Chem. 25(2) (**2014**) 251-261.

[35] R. Tang, R.N. Palumbo, L. Nagarajan, E. Krogstad, C. Wang. Well-defined block copolymers for gene delivery to dendritic cells: probing the effect of polycation chain-length. J. Control. Release 142(2) (**2010**) 229-237.

[36] R.N. Johnson, D.S. Chu, J. Shi, J.G. Schellinger, P.M. Carlson, S.H. Pun. HPMA-oligolysine copolymers for gene delivery: optimization of peptide length and polymer molecular weight. J Control. Release 155(2) (**2011**) 303-311.

[37] H. Wei, J.A. Pahang, S.H. Pun. Optimization of brush-like cationic copolymers for nonviral gene delivery. Biomacromolecules 14(1) (**2013**) 275-284.

[38] D. Sprouse, T.M. Reineke. Investigating the effects of block versus statistical glycopolycations containing primary and tertiary amines for plasmid DNA delivery. Biomacromolecules 15(7) (**2014**) 2616-2628.

[39] R.B. Merrifield. Solid phase peptide pynthesis. I. The synthesis of a tetrapeptide. J. Am. Chem. Soc. 85(14) (**1963**) 2149-2154.

[40] P. Wang, S. Dong, J.-H. Shieh, E. Peguero, R. Hendrickson, M.A.S. Moore, S.J. Danishefsky. Erythropoietin derived by chemical synthesis. Science 342 (**2013**) 1357-1360.

[41] M.H. Caruthers, S.L. Beaucage, C. Becker, J.W. Efcavitch, E.F. Fisher, G. Galluppi, R. Goldman, P. deHaseth, M. Matteucci, L. McBride, et al. Deoxyoligonucleotide synthesis via the phosphoramidite method. Gene Amplif. Anal. 3 (**1983**) 1-26.

[42] D.G. Gibson, J.I. Glass, C. Lartigue, V.N. Noskov, R.Y. Chuang, M.A. Algire, G.A. Benders, M.G. Montague, L. Ma, M.M. Moodie, C. Merryman, S. Vashee, R. Krishnakumar, N. Assad-Garcia, C. Andrews-Pfannkoch, E.A. Denisova, L. Young, Z.Q. Qi, T.H. Segall-Shapiro, C.H. Calvey, P.P. Parmar, C.A. Hutchison, 3rd, H.O. Smith, J.C. Venter. Creation of a bacterial cell controlled by a chemically synthesized genome. Science 329(5987) (**2010**) 52-56.

[43] E. Wagner. Biomaterials in RNAi therapeutics: quo vadis? Biomater. Sci. 1 (**2013**) **1**, 804-809.

[44] M.A. Islam, E.K. Reesor, Y. Xu, H.R. Zope, B.R. Zetter, J. Shi. Biomaterials for mRNA delivery. Biomater. Sci. 3(12) (**2015**) 1519-1533.

[45] H. Debus, P. Baumhof, J. Probst, T. Kissel. Delivery of messenger RNA using poly(ethylene imine)-poly(ethylene glycol)-copolymer blends for polyplex formation: biophysical characterization and *in vitro* transfection properties. J. Control. Release 148(3) (**2010**) 334-343.

[46] N. J. Oldenhuis, A. O. Burts, K. Ah Ryu, J. Chung, M. E. Johnson and Z. Guan. Biodegradable dendronized polymers for efficient mRNA delivery. ChemistrySelect 1 (**2016**) 4413-4417.

[47] J. Li, Y. He, W. Wang, C. Wu, C. Hong, P.T. Hammond. Polyamine-mediated stoichiometric assembly of ribonucleoproteins for enhanced mRNA delivery. Angew. Chem. Int. Ed. Engl. 56(44) (**2017**) 13709-13712.

[48] J. Li, W. Wang, Y. He, Y. Li, E.Z. Yan, K. Zhang, D.J. Irvine, P.T. Hammond. Structurally programmed assembly of translation initiation nanoplex for superior mRNA delivery. ACS Nano 11(3) (**2017**) 2531-2544.

[49] Y. Liu, M.N. Krishnan, K.K.L. Phua. Suppression of mRNA nanoparticle transfection in human fibroblasts by selected interferon inhibiting small molecule compounds. Biomolecules 7(3) (**2017**) 56-66.

[50] M.K. Abraham, K. Peter, T. Michel, H.P. Wendel, S. Krajewski, X. Wang. Nanoliposomes for safe and efficient therapeutic mRNA delivery: a step toward nanotheranostics in

inflammatory and cardiovascular diseases as well as cancer. Nanotheranostics 1(2) (**2017**) 154-165.

[51] D.M. Anderson, L.L. Hall, A.R. Ayyalapu, V.R. Irion, M.H. Nantz, J.G. Hecker. Stability of mRNA/cationic lipid lipoplexes in human and rat cerebrospinal fluid: methods and evidence for nonviral mRNA gene delivery to the central nervous system. Hum. Gene Ther. 14(3) (**2003**) 191-202.

[52] K.J. Kauffman, J.R. Dorkin, J.H. Yang, M.W. Heartlein, F. DeRosa, F.F. Mir, O.S. Fenton, D.G. Anderson. Optimization of lipid nanoparticle formulations for mRNA delivery *in vivo* with fractional factorial and definitive screening designs. Nano Lett. 15(11) (**2015**) 7300-7306.

[53] J.C. Kaczmarek, A.K. Patel, K.J. Kauffman, O.S. Fenton, M.J. Webber, M.W. Heartlein, F. DeRosa, D.G. Anderson. Polymer-lipid nanoparticles for systemic delivery of mRNA to the lungs. Angew. Chem. Int. Ed. Engl. 55(44) (**2016**) 13808-13812.

[54] X. Su, J. Fricke, D.G. Kavanagh, D.J. Irvine. *In vitro* and *in vivo* mRNA delivery using lipid-enveloped pH-responsive polymer nanoparticles. Mol. Pharm. 8(3) (**2011**) 774-787.

[55] M.A. Oberli, A.M. Reichmuth, J.R. Dorkin, M.J. Mitchell, O.S. Fenton, A. Jaklenec, D.G. Anderson, R. Langer, D. Blankschtein. Lipid nanoparticle assisted mRNA delivery for potent cancer immunotherapy. Nano Lett. 17(3) (**2017**) 1326-1335.

[56] Z.S. Badieyan, T. Berezhanskyy, M. Utzinger, M.K. Aneja, D. Emrich, R. Erben, C. Schuler, P. Altpeter, M. Ferizi, G. Hasenpusch, C. Rudolph, C. Plank. Transcript-activated collagen matrix as sustained mRNA delivery system for bone regeneration. J. Control. Release 239 (**2016**) 137-148.

[57] M. Utzinger, A. Jarzebinska, N. Haag, M. Schweizer, G. Winter, C. Dohmen, C. Rudolph, C. Plank. cmRNA/lipoplex encapsulation in PLGA microspheres enables transfection via calcium phosphate cement (CPC)/PLGA composites. J. Control. Release 249 (**2017**) 143-149.

[58] J. Rejman, G. Tavernier, N. Bavarsad, J. Demeester, S.C. De Smedt. mRNA transfection of cervical carcinoma and mesenchymal stem cells mediated by cationic carriers. J. Control. Release 147(3) (**2010**) 385-391.

[59] S. Guan, J. Rosenecker. Nanotechnologies in delivery of mRNA therapeutics using nonviral vector-based delivery systems. Gene Ther. 24(3) (**2017**) 133-143.

[60] K.G. Wagner, R. Arav. On the interaction of nucleotides with poly-L-lysine and poly-L-arginine. I. The influence of the nucleotide base on the binding behavior. Biochemistry 7(5) (**1968**) 1771-1777.

[61] F.E. Farber, J.L. Melnick, J.S. Butel. Optimal conditions for uptake of exogenous DNA by Chinese hamster lung cells deficient in hypoxanthine-guanine phosphoribosyltransferase. Biochim. Biophys .Acta 390(3) (**1975**) 298-311.

[62] G.Y. Wu, C.H. Wu. Receptor-mediated gene delivery and expression *in vivo*. J. Biol. Chem. 263(29) (**1988**) 14621-14624.

[63] E. Wagner, M. Cotten, R. Foisner, M.L. Birnstiel. Transferrin-polycation-DNA complexes: the effect of polycations on the structure of the complex and DNA delivery to cells. Proc. Natl. Acad. Sci. U.S.A 88(10) (**1991**) 4255-4259.

[64] M.S. Wadhwa, W.T. Collard, R.C. Adami, D.L. McKenzie, K.G. Rice. Peptide-mediated gene delivery: influence of peptide structure on gene expression. Bioconjug. Chem. 8(1) (**1997**) 81-88.

[65] R.C. Adami, W.T. Collard, S.A. Gupta, K.Y. Kwok, J. Bonadio, K.G. Rice. Stability of peptide-condensed plasmid DNA formulations. J. Pharm. Sci. 87(6) (**1998**) 678-683.

[66] S.M. van Rossenberg, A.C. van Keulen, J.W. Drijfhout, S. Vasto, H.K. Koerten, F. Spies, J.M. van 't Noordende, T.J. van Berkel, E.A. Biessen. Stable polyplexes based on arginine-containing oligopeptides for *in vivo* gene delivery. Gene Ther. 11(5) (**2004**) 457-464.

[67] A.L. Parker, K.D. Fisher, D. Oupicky, M.L. Read, S.A. Nicklin, A.H. Baker, L.W. Seymour. Enhanced gene transfer activity of peptide-targeted gene-delivery vectors. J. Drug Target. 13(1) (**2005**) 39-51.

[68] C. Plank, M.X. Tang, A.R. Wolfe, F.C. Szoka Jr. Branched cationic peptides for gene delivery: role of type and number of cationic residues in formation and *in vitro* activity of DNA polyplexes. Hum. Gene Ther. 10(2) (**1999**) 319-332.

[69] A. Kwok, D. McCarthy, S.L. Hart, A.D. Tagalakis. Systematic comparisons of formulations of linear oligolysine peptides with siRNA and plasmid DNA. Chem. Biol. Drug Des. 87(5) (**2016**) 747-763.

[70] S.L. Hart, R.P. Harbottle, R. Cooper, A. Miller, R. Williamson, C. Coutelle. Gene delivery and expression mediated by an integrin-binding peptide. Gene Ther. 2(8) (**1995**) 552-554.

[71] R.P. Harbottle, R.G. Cooper, S.L. Hart, A. Ladhoff, T. McKay, A.M. Knight, E. Wagner, A.D. Miller, C. Coutelle. An RGD-oligolysine peptide: a prototype construct for integrin-mediated gene delivery. Hum. Gene Ther. 9(7) (**1998**) 1037-1047.

[72] A.D. Tagalakis, D.H. Lee, A.S. Bienemann, H. Zhou, M.M. Munye, L. Saraiva, D. McCarthy, Z. Du, C.A. Vink, R. Maeshima, E.A. White, K. Gustafsson, S.L. Hart. Multifunctional, self-assembling anionic peptide-lipid nanocomplexes for targeted siRNA delivery. Biomaterials 35(29) (**2014**) 8406-8415.

[73] Q.R. Chen, L. Zhang, S.A. Stass, A.J. Mixson. Branched co-polymers of histidine and lysine are efficient carriers of plasmids. Nucleic Acids Res. 29(6) (**2001**) 1334-1340.

[74] Q. Leng, A.J. Mixson. Small interfering RNA targeting Raf-1 inhibits tumor growth *in vitro* and *in vivo*. Cancer Gene Ther. 12(8) (**2005**) 682-690.

[75] Q. Leng, P. Scaria, J. Zhu, N. Ambulos, P. Campbell, A.J. Mixson. Highly branched HK peptides are effective carriers of siRNA. J. Gene Med. 7(7) (**2005**) 977-986.

[76] Q. Leng, A.J. Mixson. Modified branched peptides with a histidine-rich tail enhance *in vitro* gene transfection. Nucleic Acids Res. 33(4) (**2005**) e40.

[77] S.T. Chou, K. Hom, D. Zhang, Q. Leng, L.J. Tricoli, J.M. Hustedt, A. Lee, M.J. Shapiro, J. Seog, J.D. Kahn, A.J. Mixson. Enhanced silencing and stabilization of siRNA polyplexes by histidine-mediated hydrogen bonds. Biomaterials 35(2) (**2014**) 846-855.

[78] C. Scholz, E. Wagner. Therapeutic plasmid DNA versus siRNA delivery: Common and different tasks for synthetic carriers. J. Control. Release 161(2) (**2012**) 554-565.

[79] A. Kwok, S.L. Hart. Comparative structural and functional studies of nanoparticle formulations for DNA and siRNA delivery. Nanomedicine 7(2) (**2011**) 210-219.

[80] Q. Leng, L. Goldgeier, J. Zhu, P. Cambell, N. Ambulos, A.J. Mixson. Histidine-lysine peptides as carriers of nucleic acids. Drug News Perspect. 20(2) (**2007**) 77-86.

[81] M.L. Read, K.H. Bremner, D. Oupicky, N.K. Green, P.F. Searle, L.W. Seymour. Vectors based on reducible polycations facilitate intracellular release of nucleic acids. J. Gene Med. 5(3) (**2003**) 232-245.

[82] M.L. Read, S. Singh, Z. Ahmed, M. Stevenson, S.S. Briggs, D. Oupicky, L.B. Barrett, R. Spice, M. Kendall, M. Berry, J.A. Preece, A. Logan, L.W. Seymour. A versatile reducible polycation-based system for efficient delivery of a broad range of nucleic acids. Nucleic Acids Res. 33(9) (**2005**) 86-102.

[83] D.L. McKenzie, K.Y. Kwok, K.G. Rice. A potent new class of reductively activated peptide gene delivery agents. J. Biol. Chem. 275(14) (**2000**) 9970-9977.

[84] D.L. McKenzie, E. Smiley, K.Y. Kwok, K.G. Rice. Low molecular weight disulfide cross-linking peptides as nonviral gene delivery carriers. Bioconjug. Chem. 11(6) (**2000**) 901-909.

[85] M.D. Ericson, K.G. Rice. A convergent synthesis of homogeneous reducible polypeptides. Tetrahedron Lett. 54(35) (**2013**) 4746-4748.

[86] N.J. Baumhover, K. Anderson, C.A. Fernandez, K.G. Rice. Synthesis and *in vitro* testing of new potent polyacridine-melittin gene delivery peptides. Bioconjug. Chem. 21(1) (**2010**) 74-83.

[87] K. Kizzire, S. Khargharia, K.G. Rice. High-affinity PEGylated polyacridine peptide polyplexes mediate potent *in vivo* gene expression. Gene Ther. 20(4) (**2013**) 407-416.

[88] S. Khargharia, K. Kizzire, M.D. Ericson, N.J. Baumhover, K.G. Rice. PEG length and chemical linkage controls polyacridine peptide DNA polyplex pharmacokinetics, biodistribution, metabolic stability and *in vivo* gene expression. J. Control. Release 170(3) (**2013**) 325-333.

[89] C.A. Fernandez, N.J. Baumhover, J.T. Duskey, S. Khargharia, K. Kizzire, M.D. Ericson, K.G. Rice. Metabolically stabilized long-circulating PEGylated polyacridine peptide polyplexes mediate hydrodynamically stimulated gene expression in liver. Gene Ther. 18(1) (**2011**) 23-37.

[90] T. Bettinger, R.C. Carlisle, M.L. Read, M. Ogris, L.W. Seymour. Peptide-mediated RNA delivery: a novel approach for enhanced transfection of primary and post-mitotic cells. Nucleic Acids Res. 29(18) (**2001**) 3882-3891.

[91] S.E. Andaloussi, T. Lehto, I. Mager, K. Rosenthal-Aizman, Oprea, II, O.E. Simonson, H. Sork, K. Ezzat, D.M. Copolovici, K. Kurrikoff, J.R. Viola, E.M. Zaghloul, R. Sillard, H.J. Johansson, F. Said Hassane, P. Guterstam, J. Suhorutsenko, P.M. Moreno, N. Oskolkov, J. Halldin, U. Tedebark, A. Metspalu, B. Lebleu, J. Lehtio, C.I. Smith, U. Langel. Design of a peptide-based vector, PepFect6, for efficient delivery of siRNA in cell culture and systemically *in vivo*. Nucleic Acids Res. 39(9) (**2011**) 3972-3987.

[92] X.L. Wang, S. Ramusovic, T. Nguyen, Z.R. Lu. Novel polymerizable surfactants with pH-sensitive amphiphilicity and cell membrane disruption for efficient siRNA delivery. Bioconjug. Chem. 18(6) (**2007**) 2169-2177.

[93] X.L. Wang, R. Jensen, Z.R. Lu. A novel environment-sensitive biodegradable polydisulfide with protonatable pendants for nucleic acid delivery. J. Control. Release 120(3) (**2007**) 250-258.

[94] L. Hartmann, E. Krause, M. Antonietti, H.G. Borner. Solid-phase supported polymer synthesis of sequence-defined, multifunctional poly(amidoamines). Biomacromolecules 7(4) (**2006**) 1239-1244.

[95] L. Hartmann, S. Häfele, R. Peschka-Süss, M. Antonietti, H.G. Börner. Sequence positioning of disulfide linkages to program the degradation of monodisperse poly(amidoamines). Macromolecules 40(22) (**2007**) 7771-7776.

[96] L. Hartmann, S. Hafele, R. Peschka-Suss, M. Antonietti, H.G. Borner. Tailor-made poly(amidoamine)s for controlled complexation and condensation of DNA. Chemistry 14(7) (**2008**) 2025-2033.

[97] L. Hartmann, H.G. Borner. Precision polymers: monodisperse, monomer-sequence-defined segments to target future demands of polymers in medicine. Adv. Mater. 21(32-33) (**2009**) 3425-3431.

[98] S. Mosca, F. Wojcik, L. Hartmann. Precise positioning of chiral building blocks in monodisperse, sequence-defined polyamides. Macromol. Rapid Commun. 32(2) (**2011**) 197-202.

[99] F. Wojcik, S. Mosca, L. Hartmann. Solid-phase synthesis of asymmetrically branched sequence-defined poly/oligo(amidoamines). J. Org. Chem. 77(9) (**2012**) 4226-4234.

[100] D. Ponader, F. Wojcik, F. Beceren-Braun, J. Dernedde, L. Hartmann. Sequence-defined glycopolymer segments presenting mannose: synthesis and lectin binding affinity. Biomacromolecules 13(6) (**2012**) 1845-1852.

[101] D. Schaffert, N. Badgujar, E. Wagner. Novel Fmoc-polyamino acids for solid-phase synthesis of defined polyamidoamines. Org. Lett. 13(7) (**2011**) 1586-1589.

[102] E.E. Salcher, P. Kos, T. Fröhlich, N. Badgujar, M. Scheible, E. Wagner. Sequence-defined four-arm oligo(ethanamino)amides for pDNA and siRNA delivery: Impact of building blocks on efficacy. J. Control. Release 164(3) (**2012**) 380-386.

[103] J.P. Behr. The proton sponge: A trick to enter cells the viruses did not exploit. Chimia 51(1-2) (**1997**) 34-36.

[104] P.M. Klein, S. Reinhard, D.J. Lee, K. Müller, D. Ponader, L. Hartmann, E. Wagner. Precise redox-sensitive cleavage sites for improved bioactivity of siRNA lipopolyplexes. Nanoscale 8(42) (**2016**) 18098-18104.

[105] D. Schaffert, C. Troiber, E.E. Salcher, T. Fröhlich, I. Martin, N. Badgujar, C. Dohmen, D. Edinger, R. Kläger, G. Maiwald, K. Farkasova, S. Seeber, K. Jahn-Hofmann, P. Hadwiger, E. Wagner. Solid-phase synthesis of sequence-defined T-, i-, and U-shape polymers for pDNA and siRNA delivery. Angew. Chem. Int. Ed. Engl. 50(38) (**2011**) 8986-8989.

[106] T. Fröhlich, D. Edinger, R. Kläger, C. Troiber, E. Salcher, N. Badgujar, I. Martin, D. Schaffert, A. Cengizeroglu, P. Hadwiger, H.P. Vornlocher, E. Wagner. Structure-activity relationships of siRNA carriers based on sequence-defined oligo (ethane amino) amides. J. Control. Release 160(3) (**2012**) 532-541.

[107] P. Kos, U. Lächelt, A. Herrmann, F.M. Mickler, M. Döblinger, D. He, A. Krhac Levacic, S. Morys, C. Bräuchle, E. Wagner. Histidine-rich stabilized polyplexes for cMet-directed tumor-targeted gene transfer. Nanoscale 7(12) (**2015**) 5350-5362.

[108] S. Morys, A. Krhac Levacic, S. Urnauer, S. Kempter, S. Kern, J.O. Rädler, C. Spitzweg, U. Lächelt, E. Wagner. Influence of defined hydrophilic blocks within oligoaminoamide copolymers: compaction versus shielding of pDNA nanoparticles. Polymers 9(4) (**2017**) 142-162.

[109] U. Lächelt, P. Kos, F.M. Mickler, A. Herrmann, E.E. Salcher, W. Rödl, N. Badgujar, C. Bräuchle, E. Wagner. Fine-tuning of proton sponges by precise diaminoethanes and histidines in pDNA polyplexes. Nanomedicine 10(1) (**2014**) 35-44.

[110] C. Dohmen, D. Edinger, T. Fröhlich, L. Schreiner, U. Lächelt, C. Troiber, J. Rädler, P. Hadwiger, H.P. Vornlocher, E. Wagner. Nanosized multifunctional polyplexes for receptor-mediated siRNA delivery. ACS Nano 6(6) (**2012**) 5198-5208.

[111] I. Martin, C. Dohmen, C. Mas-Moruno, C. Troiber, P. Kos, D. Schaffert, U. Lächelt, M. Teixido, M. Gunther, H. Kessler, E. Giralt, E. Wagner. Solid-phase-assisted synthesis of targeting peptide-PEG-oligo(ethane amino)amides for receptor-mediated gene delivery. Org. Biomol. Chem. 10(16) (**2012**) 3258-3268.

[112] D. He, K. Müller, A. Krhac Levacic, P. Kos, U. Lächelt, E. Wagner. Combinatorial optimization of sequence-defined oligo(ethanamino)amides for folate receptor-targeted pDNA and siRNA delivery. Bioconjug Chem. 27(3) (**2016**) 647-659.

[113] S. Wang, S. Reinhard, C. Li, M. Qian, H. Jiang, Y. Du, U. Lächelt, W. Lu, E. Wagner, R. Huang. Antitumoral cascade-targeting ligand for IL-6 receptor-mediated gene delivery to glioma. Mol. Ther. 25(7) (**2017**) 1556-1566.

[114] P.M. Klein, E. Wagner. Bioreducible polycations as shuttles for therapeutic nucleic acid and protein transfection. Antioxid. Redox Signaling 21(5) (**2014**) 804-817.

[115] P.M. Klein, K. Müller, C. Gutmann, P. Kos, A. Krhac Levacic, D. Edinger, M. Hohn, J.C. Leroux, M.A. Gauthier, E. Wagner. Twin disulfides as opportunity for improving stability and transfection efficiency of oligoaminoethane polyplexes. J. Control. Release 205 (**2015**) 109-119.

[116] C. Troiber, D. Edinger, P. Kos, L. Schreiner, R. Kläger, A. Herrmann, E. Wagner. Stabilizing effect of tyrosine trimers on pDNA and siRNA polyplexes. Biomaterials 34(5) (**2013**) 1624-1633.

[117] D. Schaffert, C. Troiber, E. Wagner. New sequence-defined polyaminoamides with tailored endosomolytic properties for plasmid DNA delivery. Bioconjug. Chem. 23(6) (**2012**) 1157-1165.

[118] M. Nothisen, M. Kotera, E. Voirin, J.S. Remy, J.P. Behr. Cationic siRNAs provide carrier-free gene silencing in animal cells. J. Am. Chem. Soc. 131(49) (**2009**) 17730-17731.

[119] P. Perche, M. Kotera, J.S. Remy. MMT, Npeoc-protected spermine, a valuable synthon for the solid phase synthesis of oligonucleotide oligospermine conjugates via guanidine linkers. Bioorg. Med. Chem. 19(6) (**2011**) 1972-1977.

[120] M. Nothisen, J. Bagilet, J.P. Behr, J.S. Remy, M. Kotera. Structure tuning of cationic oligospermine-siRNA conjugates for carrier-free gene silencing. Mol. Pharm. 13(8) (**2016**) 2718-2728.

[121] P. Perche, M. Nothisen, J. Bagilet, J.P. Behr, M. Kotera, J.S. Remy. Cell-penetrating cationic siRNA and lipophilic derivatives efficient at nanomolar concentrations in the presence of serum and albumin. J. Control. Release 170(1) (**2013**) 92-98.

[122] K.A. Mislick, J.D. Baldeschwieler. Evidence for the role of proteoglycans in cation-mediated gene transfer. Proc. Natl. Acad. Sci. U.S.A 93(22) (**1996**) 12349-12354.

[123] I. Kopatz, J.S. Remy, J.P. Behr. A model for non-viral gene delivery: through syndecan adhesion molecules and powered by actin. J. Gene Med. 6(7) (**2004**) 769-776.

[124] E. Wagner. Polymers for siRNA delivery: Inspired by viruses to be targeted, dynamic, and precise. Acc. Chem. Res. 45(7) (**2012**) 1005-1013.

[125] A. Yousefi, G. Storm, R. Schiffelers, E. Mastrobattista. Trends in polymeric delivery of nucleic acids to tumors. J. Control. Release 170(2) (**2013**) 209-218.

[126] S. Uzgun, G. Nica, C. Pfeifer, M. Bosinco, K. Michaelis, J.F. Lutz, M. Schneider, J. Rosenecker, C. Rudolph. PEGylation improves nanoparticle formation and transfection efficiency of messenger RNA. Pharm. Res. 28(9) (**2011**) 2223-2232.

[127] C. Plank, K. Mechtler, F.C. Szoka, Jr., E. Wagner. Activation of the complement system by synthetic DNA complexes: a potential barrier for intravenous gene delivery. Hum. Gene Ther. 7(12) (**1996**) 1437-1446.

[128] O.M. Merkel, R. Urbanics, P. Bedocs, Z. Rozsnyay, L. Rosivall, M. Toth, T. Kissel, J. Szebeni. *In vitro* and *in vivo* complement activation and related anaphylactic effects associated with polyethylenimine and polyethylenimine-graft-poly(ethylene glycol) block copolymers. Biomaterials 32(21) (**2011**) 4936-4942.

[129] R.S. Burke, S.H. Pun. Extracellular barriers to *in vivo* PEI and PEGylated PEI polyplex-mediated gene delivery to the liver. Bioconjug. Chem. 19(3) (**2008**) 693-704.

[130] A. Hall, U. Lächelt, J. Bartek, E. Wagner, S.M. Moghimi. Polyplex evolution: Understanding biology, optimizing performance. Mol. Ther. 25(7) (**2017**) 1476-1490.

[131] K. Knop, R. Hoogenboom, D. Fischer, U.S. Schubert. Poly(ethylene glycol) in drug delivery: pros and cons as well as potential alternatives. Angew. Chem. Int. Ed. Engl. 49(36) (**2010**) 6288-308.

[132] M. Kursa, G.F. Walker, V. Roessler, M. Ogris, W. Roedl, R. Kircheis, E. Wagner. Novel shielded transferrin-polyethylene glycol-polyethylenimine/DNA complexes for systemic tumor-targeted gene transfer. Bioconjug. Chem. 14(1) (**2003**) 222-231.

[133] J. DeRouchey, G.F. Walker, E. Wagner, J.O. Rädler. Decorated rods: a "bottom-up" self-assembly of monomolecular DNA complexes. J. Phys. Chem. B 110(10) (**2006**) 4548-4554.

[134] C. Fella, G.F. Walker, M. Ogris, E. Wagner. Amine-reactive pyridylhydrazone-based PEG reagents for pH-reversible PEI polyplex shielding. Eur. J. Pharm. Sci 34(4-5) (**2008**) 309-320.

[135] O.M. Merkel, D. Librizzi, A. Pfestroff, T. Schurrat, K. Buyens, N.N. Sanders, S.C. De Smedt, M. Behe, T. Kissel. Stability of siRNA polyplexes from poly(ethylenimine) and poly(ethylenimine)-g-poly(ethylene glycol) under *in vivo* conditions: effects on pharmacokinetics and biodistribution measured by Fluorescence Fluctuation Spectroscopy and Single Photon Emission Computed Tomography (SPECT) imaging. J. Control. Release 138(2) (**2009**) 148-159.

[136] R.S. Burke, S.H. Pun. Synthesis and characterization of biodegradable HPMA-oligolysine copolymers for improved gene delivery. Bioconjug. Chem. 21(1) (**2010**) 140-150.

[137] L. Beckert, L. Kostka, E. Kessel, A. Krhac Levacic, H. Kostkova, T. Etrych, U. Lächelt, E. Wagner. Acid-labile pHPMA modification of four-arm oligoaminoamide pDNA polyplexes balances shielding and gene transfer activity *in vitro* and *in vivo*. Eur. J. Pharm. Biopharm. 105 (**2016**) 85-96.

[138] M. Noga, D. Edinger, R. Kläger, S.V. Wegner, J.P. Spatz, E. Wagner, G. Winter, A. Besheer. The effect of molar mass and degree of hydroxyethylation on the controlled shielding and deshielding of hydroxyethyl starch-coated polyplexes. Biomaterials 34(10) (**2013**) 2530-2538.

[139] P. Heller, A. Birke, D. Huesmann, B. Weber, K. Fischer, A. Reske-Kunz, M. Bros, M. Barz. Introducing PeptoPlexes: polylysine-block-polysarcosine based polyplexes for transfection of HEK 293T cells. Macromol. Biosci. 14(10) (**2014**) 1380-1395.

[140] D.J. Lee, E. Kessel, D. Edinger, D. He, P.M. Klein, L. Voith von Voithenberg, D.C. Lamb, U. Lächelt, T. Lehto, E. Wagner. Dual antitumoral potency of EG5 siRNA nanoplexes armed with cytotoxic bifunctional glutamyl-methotrexate targeting ligand. Biomaterials 77 (**2016**) 98-110.

[141] C. Dohmen, T. Fröhlich, U. Lächelt, I. Rohl, H.-P. Vornlocher, P. Hadwiger, E. Wagner. Defined folate-PEG-siRNA conjugates for receptor-specific gene silencing. Mol. Ther. Nucleic Acids 1(1) (**2012**) 7-13.

[142] H. Hatakeyama, H. Akita, H. Harashima. A multifunctional envelope type nano device (MEND) for gene delivery to tumours based on the EPR effect: a strategy for overcoming the PEG dilemma. Adv. Drug Deliv. Rev. 63(3) (**2011**) 152-160.

[143] T.A. Tockary, K. Osada, Y. Motoda, S. Hiki, Q. Chen, K.M. Takeda, A. Dirisala, S. Osawa, K. Kataoka. Rod-to-globule transition of pDNA/PEG-poly(l-Lysine) polyplex micelles induced by a collapsed balance between DNA rigidity and PEG crowdedness. Small 12(9) (**2016**) 1193-1200.

[144] S. Morys, S. Urnauer, C. Spitzweg, E. Wagner. EGFR targeting and shielding of pDNA lipopolyplexes via bivalent attachment of a sequence-defined PEG agent. Macromol. Biosci. 18(1) (**2018**) 1-13.

[145] K. Müller, P.M. Klein, P. Heissig, A. Roidl, E. Wagner. EGF receptor targeted lipo-oligocation polyplexes for antitumoral siRNA and miRNA delivery. Nanotechnology 27(46) (**2016**) 464001.

[146] W. Zhang, K. Müller, E. Kessel, S. Reinhard, D. He, P.M. Klein, M. Hohn, W. Rödl, S. Kempter, E. Wagner. Targeted siRNA delivery using a lipo-oligoaminoamide nanocore with an influenza peptide and transferrin shell. Adv. Healthcare Mater. 5(12) (**2016**) 1493-1504.

[147] K. Müller, E. Kessel, P.M. Klein, M. Hohn, E. Wagner. Post-PEGylation of siRNA lipo-oligoamino amide polyplexes using tetra-glutamylated folic acid as ligand for receptor-targeted delivery. Mol. Pharm. 13(7) (**2016**) 2332-2345.

[148] G.F. Walker, C. Fella, J. Pelisek, J. Fahrmeir, S. Boeckle, M. Ogris, E. Wagner. Toward synthetic viruses: endosomal pH-triggered deshielding of targeted polyplexes greatly enhances gene transfer *in vitro* and *in vivo*. Mol. Ther. 11(3) (**2005**) 418-425.

[149] V. Knorr, L. Allmendinger, G.F. Walker, F.F. Paintner, E. Wagner. An acetal-based PEGylation reagent for pH-sensitive shielding of DNA polyplexes. Bioconjug. Chem. 18(4) (**2007**) 1218-1225.

[150] D.B. Rozema, D.L. Lewis, D.H. Wakefield, S.C. Wong, J.J. Klein, P.L. Roesch, S.L. Bertin, T.W. Reppen, Q. Chu, A.V. Blokhin, J.E. Hagstrom, J.A. Wolff. Dynamic PolyConjugates for targeted *in vivo* delivery of siRNA to hepatocytes. Proc. Natl. Acad. Sci U.S.A 104(32) (**2007**) 12982-12987.

[151] M. Das, C. Mohanty, S.K. Sahoo. Ligand-based targeted therapy for cancer tissue. Expert Opin. Drug Deliv. 6(3) (**2009**) 285-304.

[152] M. Ogris, E. Wagner. To be targeted: is the magic bullet concept a viable option for synthetic nucleic acid therapeutics? Hum. Gene Ther. 22(7) (**2011**) 799-807.

[153] J.T. Duskey, K.G. Rice. Nanoparticle ligand presentation for targeting solid tumors. AAPS Pharm. Sci. Tech. 15(5) (**2014**) 1345-1354.

[154] M.S. Wadhwa, D.L. Knoell, A.P. Young, K.G. Rice. Targeted gene delivery with a low molecular weight glycopeptide carrier. Bioconjug. Chem. 6 (**1995**) 283-291.

[155] H. Ueyama, M. Takagi, M. Waki, S. Takenaka. DNA binding behavior of peptides carrying acridinyl units: First example of effective poly-intercalation. Nucleic Acids Res. Suppl. (1) (**2001**) 163-164.

[156] K. Anderson, C. Fernandez, K.G. Rice. N-glycan targeted gene delivery to the dendritic cell SIGN receptor. Bioconjug. Chem. 21(8) (**2010**) 1479-1485.

[157] M. Colin, S. Moritz, P. Fontanges, M. Kornprobst, C. Delouis, M. Keller, A.D. Miller, J. Capeau, C. Coutelle, M.C. Brahimi-Horn. The nuclear pore complex is involved in nuclear transfer of plasmid DNA condensed with an oligolysine-RGD peptide containing nuclear localisation properties. Gene Ther. 8(21) (**2001**) 1643-1653.

[158] X.L. Wang, R. Xu, X. Wu, D. Gillespie, R. Jensen, Z.R. Lu. Targeted systemic delivery of a therapeutic siRNA with a multifunctional carrier controls tumor proliferation in mice. Mol. Pharm. 6(3) (**2009**) 738-746.

[159] E. Broda, F.M. Mickler, U. Lächelt, S. Morys, E. Wagner, C. Bräuchle. Assessing potential peptide targeting ligands by quantification of cellular adhesion of model nanoparticles under flow conditions. J. Control. Release 213 (**2015**) 79-85.

[160] S. Urnauer, K. Klutz, G.K. Grünwald, S. Morys, N. Schwenk, C. Zach, F.J. Gildehaus, W. Roedl, M. Ogris, E. Wagner, C. Spitzweg. Systemic tumor-targeted sodium iodide symporter (NIS) gene therapy of hepatocellular carcinoma mediated by B6 peptide polyplexes. J. Gene Med. 19(5) (**2017**).

[161] S. Urnauer, S. Morys, A. Krhac Levacic, A.M. Müller, C. Schug, K.A. Schmohl, N. Schwenk, C. Zach, J. Carlsen, P. Bartenstein, E. Wagner, C. Spitzweg. Sequence-defined cMET/HGFR-targeted polymers as gene delivery vehicles for the theranostic sodium iodide symporter (NIS) gene. Mol. Ther. 24(8) (**2016**) 1395-1404.

[162] P. Kos, U. Lächelt, D. He, Y. Nie, Z. Gu, E. Wagner. Dual-targeted polyplexes based on sequence-defined peptide-PEG-oligoamino amides. J. Pharm. Sci.104(2) (**2015**) 464-475.

[163] E. Wagner, M. Zenke, M. Cotten, H. Beug, M.L. Birnstiel. Transferrin-polycation conjugates as carriers for DNA uptake into cells. Proc. Natl. Acad. Sci. U.S.A 87(9) (**1990**) 3410-3414.

[164] E. Wagner, M. Cotten, K. Mechtler, H. Kirlappos, M.L. Birnstiel. DNA-binding transferrin conjugates as functional gene-delivery agents: synthesis by linkage of polylysine or ethidium homodimer to the transferrin carbohydrate moiety. Bioconjug. Chem. 2(4) (**1991**) 226-231.

[165] S. Schreiber, E. Kampgen, E. Wagner, D. Pirkhammer, J. Trcka, H. Korschan, A. Lindemann, R. Dorffner, H. Kittler, F. Kasteliz, Z. Kupcu, A. Sinski, K. Zatloukal, M. Buschle, W. Schmidt, M. Birnstiel, R.E. Kempe, T. Voigt, H.A. Weber, H. Pehamberger, R. Mertelsmann, E.B. Brocker, K. Wolff, G. Stingl. Immunotherapy of metastatic malignant melanoma by a vaccine consisting of autologous interleukin 2-transfected cancer cells: outcome of a phase I study. Hum. Gene Ther. 10(6) (**1999**) 983-993.

[166] R. Kircheis, A. Kichler, G. Wallner, M. Kursa, M. Ogris, T. Felzmann, M. Buchberger, E. Wagner. Coupling of cell-binding ligands to polyethylenimine for targeted gene delivery. Gene Ther. 4(5) (**1997**) 409-418.

[167] R. Kircheis, S. Schuller, S. Brunner, M. Ogris, K.H. Heider, W. Zauner, E. Wagner. Polycation-based DNA complexes for tumor-targeted gene delivery *in vivo*. J. Gene Med. 1(2) (**1999**) 111-120.

[168] R. Kircheis, L. Wightman, A. Schreiber, B. Robitza, V. Rossler, M. Kursa, E. Wagner. Polyethylenimine/DNA complexes shielded by transferrin target gene expression to tumors after systemic application. Gene Ther. 8(1) (**2001**) 28-40.

[169] M.E. Davis, J.E. Zuckerman, C.H. Choi, D. Seligson, A. Tolcher, C.A. Alabi, Y. Yen, J.D. Heidel, A. Ribas. Evidence of RNAi in humans from systemically administered siRNA via targeted nanoparticles. Nature 464 (**2010**) 1067-1070.

[170] W. Zhang, W. Rödl, D. He, M. Döblinger, U. Lächelt, E. Wagner. Combination of sequence-defined oligoaminoamides with transferrin-polycation conjugates for receptor-targeted gene delivery. J. Gene Med. 17(8-9) (**2015**) 161-172.

[171] R. Prades, B. Oller-Salvia, S.M. Schwarzmaier, J. Selva, M. Moros, M. Balbi, V. Grazu, J.M. de La Fuente, G. Egea, N. Plesnila, M. Teixido, E. Giralt. Applying the retro-enantio approach to obtain a peptide capable of overcoming the blood-brain barrier. Angew. Chem. Int. Ed. Engl. 54(13) (**2015**) 3967-3972.

[172] A.R. Hilgenbrink, P.S. Low. Folate receptor-mediated drug targeting: from therapeutics to diagnostics. J. Pharm. Sci. 94(10) (**2005**) 2135-2146.

[173] C.Y. Zhang, P. Kos, K. Müller, W. Schrimpf, C. Troiber, U. Lächelt, C. Scholz, D.C. Lamb, E. Wagner. Native chemical ligation for conversion of sequence-defined oligomers into targeted pDNA and siRNA carriers. J. Control. Release 180 (**2014**) 42-50.

[174] D.J. Lee, D. He, E. Kessel, K. Padari, S. Kempter, U. Lächelt, J.O. Rädler, M. Pooga, E. Wagner. Tumoral gene silencing by receptor-targeted combinatorial siRNA polyplexes. J. Control. Release 244 (**2016**) 280-291.

[175] S. An, D. He, E. Wagner, C. Jiang. Peptide-like polymers exerting effective glioma-targeted siRNA delivery and release for therapeutic application. Small 11(38) (**2015**) 5142-50.

[176] H. Uchida, K. Miyata, M. Oba, T. Ishii, T. Suma, K. Itaka, N. Nishiyama, K. Kataoka. Odd-even effect of repeating aminoethylene units in the side chain of N-substituted polyaspartamides on gene transfection profiles. J. Am. Chem. Soc. 133(39) (**2011**) 15524-15532.

[177] K. Miyata, N. Nishiyama, K. Kataoka. Rational design of smart supramolecular assemblies for gene delivery: chemical challenges in the creation of artificial viruses. Chem. Soc. Rev. 41(7) (**2012**) 2562-2574.

[178] R.V. Benjaminsen, M.A. Mattebjerg, J.R. Henriksen, S.M. Moghimi, T.L. Andresen. The possible "proton sponge " effect of polyethylenimine (PEI) does not include change in lysosomal pH. Mol. Ther. 21(1) (**2013**) 149-157.

[179] A.M. Funhoff, C.F. van Nostrum, G.A. Koning, N.M. Schuurmans-Nieuwenbroek, D.J. Crommelin, W.E. Hennink. Endosomal escape of polymeric gene delivery complexes is not always enhanced by polymers buffering at low pH. Biomacromolecules. 5(1) (**2004**) 32-39.

[180] Z. ur Rehman, D. Hoekstra, I.S. Zuhorn. Mechanism of polyplex- and lipoplex-mediated delivery of nucleic acids: real-time visualization of transient membrane destabilization without endosomal lysis. ACS Nano 7(5) (**2013**) 3767-3777.

[181] S. Boeckle, K. von Gersdorff, S. van der Piepen, C. Culmsee, E. Wagner, M. Ogris. Purification of polyethylenimine polyplexes highlights the role of free polycations in gene transfer. J. Gene Med. 6(10) (**2004**) 1102-1111.

[182] Y. Yue, F. Jin, R. Deng, J. Cai, Y. Chen, M.C. Lin, H.F. Kung, C. Wu. Revisit complexation between DNA and polyethylenimine - Effect of uncomplexed chains free in the solution mixture on gene transfection. J. Control. Release 155(1) (**2011**) 67-76.

[183] Y. Yue, F. Jin, R. Deng, J. Cai, Z. Dai, M.C. Lin, H.F. Kung, M.A. Mattebjerg, T.L. Andresen, C. Wu. Revisit complexation between DNA and polyethylenimine - Effect of length of free polycationic chains on gene transfection. J. Control. Release 152(1) (**2011**) 143-151.

[184] J. Cai, Y. Yue, Y. Wang, Z. Jin, F. Jin, C. Wu. Quantitative study of effects of free cationic chains on gene transfection in different intracellular stages. J. Control. Release 238 (**2016**) 71-79.

[185] H. Uchida, K. Itaka, T. Nomoto, T. Ishii, T. Suma, M. Ikegami, K. Miyata, M. Oba, N. Nishiyama, K. Kataoka. Modulated protonation of side chain aminoethylene repeats in N-substituted polyaspartamides promotes mRNA transfection. J. Am. Chem. Soc. 136(35) (**2014**) 12396-12405.

[186] K. Itaka, T. Ishii, Y. Hasegawa, K. Kataoka. Biodegradable polyamino acid-based polycations as safe and effective gene carrier minimizing cumulative toxicity. Biomaterials 31(13) (**2010**) 3707-3714.

[187] S. Uchida, K. Itaka, H. Uchida, K. Hayakawa, T. Ogata, T. Ishii, S. Fukushima, K. Osada, K. Kataoka. *In vivo* messenger RNA introduction into the central nervous system using polyplex nanomicelle. PLoS One 8(2) (**2013**) e56220.

[188] A. Jarzebinska, T. Pasewald, J. Lambrecht, O. Mykhaylyk, L. Kummerling, P. Beck, G. Hasenpusch, C. Rudolph, C. Plank, C. Dohmen. A single methylene group in oligoalkylamine-based cationic polymers and lipids promotes enhanced mRNA delivery. Angew. Chem. Int. Ed. Engl. 55(33) (**2016**) 9591-9595.

[189] P. Midoux, M. Monsigny. Efficient gene transfer by histidylated polylysine/pDNA complexes. Bioconjug. Chem. 10(3) (**1999**) 406-411.

[190] C. Pichon, M.B. Roufai, M. Monsigny, P. Midoux. Histidylated oligolysines increase the transmembrane passage and the biological activity of antisense oligonucleotides. Nucleic Acids Res. 28(2) (**2000**) 504-512.

[191] E. Bertrand, C. Goncalves, L. Billiet, J.P. Gomez, C. Pichon, H. Cheradame, P. Midoux, P. Guegan. Histidinylated linear PEI: a new efficient non-toxic polymer for gene transfer. Chem. Commun. 47(46) (**2011**) 12547-12549.

[192] J.P. Gomez, C. Pichon, P. Midoux. Ability of plasmid DNA complexed with histidinylated lPEI and lPEI to cross *in vitro* lung and muscle vascular endothelial barriers. Gene 525(2) (**2013**) 182-190.

[193] M. Stevenson, V. Ramos-Perez, S. Singh, M. Soliman, J.A. Preece, S.S. Briggs, M.L. Read, L.W. Seymour. Delivery of siRNA mediated by histidine-containing reducible polycations. J. Control. Release 130(1) (**2008**) 46-56.

[194] C. Goncalves, S. Akhter, C. Pichon, P. Midoux. Intracellular availability of pDNA and mRNA after transfection: A comparative study among polyplexes, lipoplexes, and lipopolyplexes. Mol. Pharm. 13(9) (**2016**) 3153-3163.

[195] C. Plank, B. Oberhauser, K. Mechtler, C. Koch, E. Wagner. The influence of endosome-disruptive peptides on gene transfer using synthetic virus-like gene transfer systems. J. Biol. Chem. 269(17) (**1994**) 12918-12924.

[196] S. Gottschalk, J.T. Sparrow, J. Hauer, M.P. Mims, F.E. Leland, S.L. Woo, L.C. Smith. A novel DNA-peptide complex for efficient gene transfer and expression in mammalian cells. Gene Ther. 3(5) (**1996**) 448-457.

[197] P. Midoux, A. Kichler, V. Boutin, J.C. Maurizot, M. Monsigny. Membrane permeabilization and efficient gene transfer by a peptide containing several histidines. Bioconjug. Chem. 9(2) (**1998**) 260-267.

[198] T.B. Wyman, F. Nicol, O. Zelphati, P.V. Scaria, C. Plank, F.C. Szoka, Jr. Design, synthesis, and characterization of a cationic peptide that binds to nucleic acids and permeabilizes bilayers. Biochemistry 36(10) (**1997**) 3008-3017.

[199] A. Kichler, C. Leborgne, J. Marz, O. Danos, B. Bechinger. Histidine-rich amphipathic peptide antibiotics promote efficient delivery of DNA into mammalian cells. Proc. Natl. Acad. Sci. U.S.A. 100(4) (**2003**) 1564-1568.

[200] S. Boeckle, J. Fahrmeir, W. Roedl, M. Ogris, E. Wagner. Melittin analogs with high lytic activity at endosomal pH enhance transfection with purified targeted PEI polyplexes. J. Control. Release 112(2) (**2006**) 240-248.

[201] K. Ezzat, S.E. Andaloussi, E.M. Zaghloul, T. Lehto, S. Lindberg, P.M. Moreno, J.R. Viola, T. Magdy, R. Abdo, P. Guterstam, R. Sillard, S.M. Hammond, M.J. Wood, A.A. Arzumanov, M.J. Gait, C.I. Smith, M. Hallbrink, U. Langel. PepFect 14, a novel cell-penetrating peptide for oligonucleotide delivery in solution and as solid formulation. Nucleic Acids Res. 39(12) (**2011**) 5284-5298.

[202] Y. Xu, F.C. Szoka, Jr. Mechanism of DNA release from cationic liposome/DNA complexes used in cell transfection. Biochemistry 35(18) (**1996**) 5616-5623.

[203] K. von Gersdorff, N.N. Sanders, R. Vandenbroucke, S.C. De Smedt, E. Wagner, M. Ogris. The internalization route resulting in successful gene expression depends on both cell line and polyethylenimine polyplex type. Mol. Ther. 14(5) (**2006**) 745-753.

[204] J. Rejman, A. Bragonzi, M. Conese. Role of clathrin- and caveolae-mediated endocytosis in gene transfer mediated by lipo- and polyplexes. Mol. Ther. 12(3) (**2005**) 468-474.

[205] K. Remaut, B. Lucas, K. Raemdonck, K. Braeckmans, J. Demeester, S.C. De Smedt. Can we better understand the intracellular behavior of DNA nanoparticles by fluorescence correlation spectroscopy? J. Control. Release 121(1–2) (**2007**) 49-63.

[206] B. Lucas, K. Remaut, N.N. Sanders, K. Braeckmans, S.C. De Smedt, J. Demeester. Towards a better understanding of the dissociation behavior of liposome-oligonucleotide complexes in the cytosol of cells. J. Control. Release 103(2) (**2005**) 435-450.

[207] J. Gilleron, W. Querbes, A. Zeigerer, A. Borodovsky, G. Marsico, U. Schubert, K. Manygoats, S. Seifert, C. Andree, M. Stoter, H. Epstein-Barash, L. Zhang, V. Koteliansky, K.

Fitzgerald, E. Fava, M. Bickle, Y. Kalaidzidis, A. Akinc, M. Maier, M. Zerial. Image-based analysis of lipid nanoparticle-mediated siRNA delivery, intracellular trafficking and endosomal escape. Nat. Biotechnol. 31(7) (**2013**) 638-646.

[208] A. Wittrup, A. Ai, X. Liu, P. Hamar, R. Trifonova, K. Charisse, M. Manoharan, T. Kirchhausen, J. Lieberman. Visualizing lipid-formulated siRNA release from endosomes and target gene knockdown. Nat. Biotechnol. 33(8) (**2015**) 870-876.

[209] G. Sahay, W. Querbes, C. Alabi, A. Eltoukhy, S. Sarkar, C. Zurenko, E. Karagiannis, K. Love, D. Chen, R. Zoncu, Y. Buganim, A. Schroeder, R. Langer, D.G. Anderson. Efficiency of siRNA delivery by lipid nanoparticles is limited by endocytic recycling. Nat. Biotechnol. 31(7) (**2013**) 653-658.

[210] D.J. Lee, E. Kessel, T. Lehto, X. Liu, N. Yoshinaga, K. Padari, Y.C. Chen, S. Kempter, S. Uchida, J.O. Rädler, M. Pooga, M.T. Sheu, K. Kataoka, E. Wagner. Systemic delivery of folate-PEG siRNA lipopolyplexes with enhanced intracellular stability for *in vivo* gene silencing in leukemia. Bioconjug. Chem. 28(9) (**2017**) 2393-2409.

[211] L. Wasungu, D. Hoekstra. Cationic lipids, lipoplexes and intracellular delivery of genes. J. Control. Release 116(2) (**2006**) 255-264.

[212] M. Conese, A. Biffi, G. Dina, N. Marziliano, A. Villa. Comparison between cationic polymer and lipid in plasmidic DNA delivery to the cell nucleus. Open Gene Ther. J. 2 (**2009**) 21-28.

[213] O. Zelphati, F.C. Szoka. Mechanism of oligonucleotide release from cationic liposomes. Proc. Natl. Acad. Sci. U.S.A. 93 (**1996**) 11493-11498.

[214] S. Hama, H. Akita, R. Ito, H. Mizuguchi, T. Hayakawa, H. Harashima. Quantitative comparison of intracellular trafficking and nuclear transcription between adenoviral and lipoplex systems. Mol. Ther. 13(4) (**2006**) 786-794.

[215] S. Sixou, F.C. Szoka, Jr., G.A. Green, B. Giusti, G. Zon, D.J. Chin. Intracellular oligonucleotide hybridization detected by fluorescence resonance energy transfer (FRET). Nucleic Acids Res. 22(4) (**1994**) 662-668.

[216] P. Heissig, W. Schrimpf, P. Hadwiger, E. Wagner, D.C. Lamb. Monitoring integrity and localization of modified single-stranded RNA oligonucleotides using ultrasensitive fluorescence methods. PLoS One 12(3) (**2017**) e0173401.

[217] A. Subramanian, P. Ranganathan, S.L. Diamond. Nuclear targeting peptide scaffolds for lipofection of nondividing mammalian cells. Nat. Biotechnol. 17(9) (**1999**) 873-877.

[218] M.A. Zanta, V.P. Belguise, J.P. Behr. Gene delivery: A single nuclear localization signal peptide is sufficient to carry DNA to the cell nucleus. Proc. Natl. Acad. Sci. U.S.A 96(1) (**1999**) 91-96.

[219] R. Tachibana, H. Harashima, Y. Shinohara, H. Kiwada. Quantitative studies on the nuclear transport of plasmid DNA and gene expression employing nonviral vectors. Adv. Drug Deliv. Rev. 52(3) (**2001**) 219-226.

[220] R. Cartier, R. Reszka. Utilization of synthetic peptides containing nuclear localization signals for nonviral gene transfer systems. Gene Ther. 9(3) (**2002**) 157-167.

[221] C.K. Chan, T. Senden, D.A. Jans. Supramolecular structure and nuclear targeting efficiency determine the enhancement of transfection by modified polylysines. Gene Ther. 7(19) (**2000**) 1690-1697.

[222] L.J. Branden, A.J. Mohamed, C.I. Smith. A peptide nucleic acid-nuclear localization signal fusion that mediates nuclear transport of DNA. Nat. Biotechnol. 17(8) (**1999**) 784-787.

[223] C. Ciolina, G. Byk, F. Blanche, V. Thuillier, D. Scherman, P. Wils. Coupling of nuclear localization signals to plasmid DNA and specific interaction of the conjugates with importin alpha. Bioconjug. Chem. 10(1) (**1999**) 49-55.

[224] K.H. Bremner, L.W. Seymour, A. Logan, M.L. Read. Factors influencing the ability of nuclear localization sequence peptides to enhance nonviral gene delivery. Bioconjug. Chem. 15(1) (**2004**) 152-161.

[225] Q. Leng, A.J. Mixson. The neuropilin-1 receptor mediates enhanced tumor delivery of H2K polyplexes. J. Gene Med. 18(7) (**2016**) 134-144.

[226] X.L. Wang, R. Xu, Z.R. Lu. A peptide-targeted delivery system with pH-sensitive amphiphilic cell membrane disruption for efficient receptor-mediated siRNA delivery. J. Control. Release 134(3) (**2009**) 207-213.

[227] R.M. Schiffelers, A. Ansari, J. Xu, Q. Zhou, Q. Tang, G. Storm, G. Molema, P.Y. Lu, P.V. Scaria, M.C. Woodle. Cancer siRNA therapy by tumor selective delivery with ligand-targeted sterically stabilized nanoparticle. Nucleic Acids Res. 32(19) (**2004**) e149.

[228] S.D. Li, L. Huang. Targeted delivery of antisense oligodeoxynucleotide and small interference RNA into lung cancer cells. Mol. pharmaceutics 3(5) (**2006**) 579-588.

[229] P.S. Low, W.A. Henne, D.D. Doorneweerd. Discovery and development of folic-acid-based receptor targeting for imaging and therapy of cancer and inflammatory diseases. Acc. Chem. Res. 41(1) (**2008**) 120-129.

[230] A. Schäfer, A. Pahnke, D. Schaffert, W.M. Van Weerden, C.M. de Ridder, W. Rödl, A. Vetter, C. Spitzweg, R. Kraaij, E. Wagner, M. Ogris. Disconnecting the yin and yang relation of epidermal growth factor receptor (EGFR) mediated delivery: a fully synthetic, EGFR-targeted gene transfer system avoiding receptor activation. Hum. Gene Ther. 22 (**2011**) 1463-1473.

[231] K. Klutz, D. Schaffert, M.J. Willhauck, G.K. Grünwald, R. Haase, N. Wunderlich, C. Zach, F.J. Gildehaus, R. Senekowitsch-Schmidtke, B. Goke, E. Wagner, M. Ogris, C. Spitzweg. Epidermal growth factor receptor-targeted (131)I-therapy of liver cancer following systemic delivery of the sodium iodide symporter gene. Mol. Ther. 19(4) (**2011**) 676-685.

[232] G. Abourbeh, A. Shir, E. Mishani, M. Ogris, W. Rödl, E. Wagner, A. Levitzki. PolyIC GE11 polyplex inhibits EGFR-overexpressing tumors. IUBMB Life 64(4) (**2012**) 324-330.

[233] H.S. Choi, W. Liu, F. Liu, K. Nasr, P. Misra, M.G. Bawendi, J.V. Frangioni. Design considerations for tumour-targeted nanoparticles. Nat. Nanotechnol. 5(1) (**2010**) 42-47.

[234] H. Maeda. The enhanced permeability and retention (EPR) effect in tumor vasculature: the key role of tumor-selective macromolecular drug targeting. Adv. Enzyme. Regul. 41 (**2001**) 189-207.

[235] H. Maeda, G.Y. Bharate, J. Daruwalla. Polymeric drugs for efficient tumor-targeted drug delivery based on EPR-effect. Eur. J. Pharm. Biopharm. 71(3) (**2009**) 409-419.

[236] B. Smrekar, L. Wightman, M.F. Wolschek, C. Lichtenberger, R. Ruzicka, M. Ogris, W. Rödl, M. Kursa, E. Wagner, R. Kircheis. Tissue-dependent factors affect gene delivery to tumors *in vivo*. Gene Ther. 10(13) (**2003**) 1079-1088.

[237] H. Cabral, Y. Matsumoto, K. Mizuno, Q. Chen, M. Murakami, M. Kimura, Y. Terada, M.R. Kano, K. Miyazono, M. Uesaka, N. Nishiyama, K. Kataoka. Accumulation of sub-100 nm polymeric micelles in poorly permeable tumours depends on size. Nat. Nanotechnol. 6(12) (**2011**) 815-823.

[238] S. Wilhelm, A.J. Tavares, Q. Dai, S. Ohta, J. Audet, H.F. Dvorak. Analysis of nanoparticle delivery to tumours. Nat. Rev. Mater. 1 (**2016**) 16014.

[239] H. Wei, L.R. Volpatti, D.L. Sellers, D.O. Maris, I.W. Andrews, A.S. Hemphill, L.W. Chan, D.S. Chu, P.J. Horner, S.H. Pun. Dual responsive, stabilized nanoparticles for efficient *in vivo* plasmid delivery. Angew. Chem. Int. Ed. Engl. 52(20) (**2013**) 5377-5381.

[240] Y. Cheng, R.C. Yumul, S.H. Pun. Virus-inspired polymer for efficient *in vitro* and *in vivo* gene delivery. Angew. Chem. Int. Ed. Engl. 55(39) (**2016**) 12013-12017.

[241] T. Merdan, K. Kunath, H. Petersen, U. Bakowsky, K.H. Voigt, J. Kopecek, T. Kissel. PEGylation of poly(ethylene imine) affects stability of complexes with plasmid DNA under *in vivo* conditions in a dose-dependent manner after intravenous injection into mice. Bioconjug. Chem. 16(4) (**2005**) 785-792.

[242] M. Neu, O. Germershaus, M. Behe, T. Kissel. Bioreversibly crosslinked polyplexes of PEI and high molecular weight PEG show extended circulation times *in vivo*. J. Control. Release 124(1-2) (**2007**) 69-80.

[243] P. Neuberg, A. Kichler. Recent developments in nucleic acid delivery with polyethylenimines. Adv. Genet. 88 (**2014**) 263-288.

[244] M. Breunig, U. Lungwitz, R. Liebl, A. Goepferich. Breaking up the correlation between efficacy and toxicity for nonviral gene delivery. Proc. Natl. Acad. Sci. U.S.A. 104(36) (**2007**) 14454-14459.

[245] R. Haase, T. Magnusson, B. Su, F. Kopp, E. Wagner, H. Lipps, A. Baiker, M. Ogris. Generation of a tumor- and tissue-specific episomal non-viral vector system. BMC Biotechnol. 13 (**2013**) 49-60.

[246] S.P. Wong, O. Argyros, R.P. Harbottle. Sustained expression from DNA vectors. Adv. Genet. 89 (**2015**) 113-152.

[247] S.P. Wong, R.P. Harbottle. Genetic modification of dividing cells using episomally maintained S/MAR DNA vectors. Mol. Ther. Nucleic Acids 2(8) (**2013**) e115.

[248] S.P. Wong, O. Argyros, S.J. Howe, R.P. Harbottle. Systemic gene transfer of polyethylenimine (PEI)-plasmid DNA complexes to neonatal mice. J. Control. Release 150(3) (**2011**) 298-306.

[249] U.S. Department of Health and Human Services, Center for Biologics Evaluation and Research. Guidance for human somatic cell therapy and gene therapy. Hum. Gene Ther. 12 (**2001**) 303–314

[250] A.M. Darquet, B. Cameron, P. Wils, D. Scherman, J. Crouzet. A new DNA vehicle for nonviral gene delivery: supercoiled minicircle. Gene Ther. 4(12) (**1997**) 1341-1349.

[251] S. Stenler, P. Blomberg, C.I. Smith. Safety and efficacy of DNA vaccines: plasmids vs. minicircles. Hum. Vaccin. Immunother. 10(5) (**2014**) 1306-1308.

[252] Z.Y. Chen, C.Y. He, A. Ehrhardt, M.A. Kay. Minicircle DNA vectors devoid of bacterial DNA result in persistent and high-level transgene expression *in vivo*. Mol. Ther. 8(3) (**2003**) 495-500.

[253] Z.Y. Chen, C.Y. He, M.A. Kay. Improved production and purification of minicircle DNA vector free of plasmid bacterial sequences and capable of persistent transgene expression *in vivo*. Hum. Gene Ther. 16(1) (**2005**) 126-131.

[254] M.A. Kay, C.Y. He, Z.Y. Chen. A robust system for production of minicircle DNA vectors. Nat. Biotechnol. 28(12) (**2010**) 1287-1289.

[255] S. Chabot, J. Orio, M. Schmeer, M. Schleef, M. Golzio, J. Teissie. Minicircle DNA electrotransfer for efficient tissue-targeted gene delivery. Gene Ther. 20(1) (**2013**) 62-68.

[256] A.M. Darquet, R. Rangara, P. Kreiss, B. Schwartz, S. Naimi, P. Delaere, J. Crouzet, D. Scherman. Minicircle: an improved DNA molecule for *in vitro* and *in vivo* gene transfer. Gene Ther. 6(2) (**1999**) 209-218.

[257] J. Zhao, L. Yang, P. Huang, Z. Wang, Y. Tan, H. Liu, J. Pan, C.Y. He, Z.Y. Chen. Synthesis and characterization of low molecular weight polyethyleneimine-terminated Poly(beta-amino ester) for highly efficient gene delivery of minicircle DNA. J. Colloid Interf. Sci. 463 (**2016**) 93-98.

[258] M.J. Gracey Maniar LE, Chen ZY, et al. Minicircle DNA vectors achieve sustained expression reflected by active chromatin and transcriptional level. Mol Ther. 21 (**2013**) 131–138.

[259] B.W. Bigger, O. Tolmachov, J.M. Collombet, M. Fragkos, I. Palaszewski, C. Coutelle. An araC-controlled bacterial cre expression system to produce DNA minicircle vectors for nuclear and mitochondrial gene therapy. J. Biol. Chem. 276(25) (**2001**) 23018-23027.

[260] C. Zhang, S. Gao, W. Jiang, S. Lin, F. Du, Z. Li, W. Huang. Targeted minicircle DNA delivery using folate-poly(ethylene glycol)-polyethylenimine as non-viral carrier. Biomaterials 31(23) (**2010**) 6075-6086.

[261] D. Kobelt, M. Schleef, M. Schmeer, J. Aumann, P.M. Schlag, W. Walther. Performance of high quality minicircle DNA for *in vitro* and *in vivo* gene transfer. Mol. Biotechnol. 53(1) (**2013**) 80-89.

[262] Q. Wan, L. Xie, L. Gao, Z. Wang, X. Nan, H. Lei, X. Long, Z.Y. Chen, C.Y. He, G. Liu, X. Liu, B. Qiu. Self-assembled magnetic theranostic nanoparticles for highly sensitive MRI of minicircle DNA delivery. Nanoscale 5(2) (**2013**) 744-752.

[263] M. Keeney, S.G. Ong, A. Padilla, Z. Yao, S. Goodman, J.C. Wu, F. Yang. Development of poly(beta-amino ester)-based biodegradable nanoparticles for nonviral delivery of minicircle DNA. ACS Nano 7(8) (**2013**) 7241-7250.

[264] T.Y. Chang, C.Y. Chung, W.M. Chuang, L.Y. Li, L.B. Jeng, W.L. Ma. Durable expression of minicircle DNA-liposome-delivered androgen receptor cDNA in mice with hepatocellular carcinoma. Biomed. Res. Int. 2014 (**2014**) 156356.

[265] V.M. Gaspar, C. Goncalves, D. de Melo-Diogo, E.C. Costa, J.A. Queiroz, C. Pichon, F. Sousa, I.J. Correia. Poly(2-ethyl-2-oxazoline)-PLA-g-PEI amphiphilic triblock micelles for co-delivery of minicircle DNA and chemotherapeutics. J. Control. Release 189 (**2014**) 90-104.

[266] Q. Wang, W. Jiang, Y. Chen, P. Liu, C. Sheng, S. Chen, H. Zhang, C. Pan, S. Gao, W. Huang. *In vivo* electroporation of minicircle DNA as a novel method of vaccine delivery to enhance HIV-1-specific immune responses. J. Virol. 88(4) (**2014**) 1924-1934.

[267] V.M. Gaspar, P. Baril, E.C. Costa, D. de Melo-Diogo, F. Foucher, J.A. Queiroz, F. Sousa, C. Pichon, I.J. Correia. Bioreducible poly(2-ethyl-2-oxazoline)-PLA-PEI-SS triblock copolymer micelles for co-delivery of DNA minicircles and Doxorubicin. J. Control. Release 213 (**2015**) 175-191.

[268] V. Gaspar, D. de Melo-Diogo, E. Costa, A. Moreira, J. Queiroz, C. Pichon, I. Correia, F. Sousa. Minicircle DNA vectors for gene therapy: advances and applications. Expert Opin. Biol. Ther. 15(3) (**2015**) 353-379.

[269] J. Zhao, P. Huang, Z. Wang, Y. Tan, X. Hou, L. Zhang, C.Y. He, Z.Y. Chen. Synthesis of amphiphilic poly(beta-amino ester) for efficiently minicircle DNA delivery *in vivo*. ACS Appl. Mater. Interfaces 8(30) (**2016**) 19284-19290.

[270] M.M. Munye, A.D. Tagalakis, J.L. Barnes, R.E. Brown, R.J. McAnulty, S.J. Howe, S.L. Hart. Minicircle DNA provides enhanced and prolonged transgene expression following airway gene transfer. Sci. Rep. 6 (**2016**) 23125.

[271] C.L. Trimble, M.P. Morrow, K.A. Kraynyak, X. Shen, M. Dallas, J. Yan, L. Edwards, R.L. Parker, L. Denny, M. Giffear, A.S. Brown, K. Marcozzi-Pierce, D. Shah, A.M. Slager, A.J. Sylvester, A. Khan, K.E. Broderick, R.J. Juba, T.A. Herring, J. Boyer, J. Lee, N.Y. Sardesai, D.B. Weiner, M.L. Bagarazzi. Safety, efficacy, and immunogenicity of VGX-3100, a therapeutic synthetic DNA vaccine targeting human papillomavirus 16 and 18 E6 and E7 proteins for cervical intraepithelial neoplasia 2/3: a randomised, double-blind, placebo-controlled phase 2b trial. Lancet 386(10008) (**2015**) 2078-2088.

[272] R. Heller, L.C. Heller. Gene electrotransfer clinical trials. Adv. Genet. 89 (**2015**) 235-262.

[273] L.M. Kranz, M. Diken, H. Haas, S. Kreiter, C. Loquai, K.C. Reuter, M. Meng, D. Fritz, F. Vascotto, H. Hefesha, C. Grunwitz, M. Vormehr, Y. Husemann, A. Selmi, A.N. Kuhn, J. Buck, E. Derhovanessian, R. Rae, S. Attig, J. Diekmann, R.A. Jabulowsky, S. Heesch, J. Hassel, P. Langguth, S. Grabbe, C. Huber, O. Tureci, U. Sahin. Systemic RNA delivery to dendritic cells exploits antiviral defence for cancer immunotherapy. Nature 534(7607) (**2016**) 396-401.

[274] M.A. Kay. State-of-the-art gene-based therapies: the road ahead. Nat. Rev. Genet. 12(5) (**2011**) 316-328.

[275] H. Yin, R.L. Kanasty, A.A. Eltoukhy, A.J. Vegas, J.R. Dorkin, D.G. Anderson. Non-viral vectors for gene-based therapy. Nat. Rev. Genet. 15(8) (**2014**) 541-555.

[276] S.M. Zou, P. Erbacher, J.S. Remy, J.P. Behr. Systemic linear polyethylenimine (L-PEI)-mediated gene delivery in the mouse. J. Gene Med. 2(2) (**2000**) 128-134.

[277] D. Schaffert, M. Kiss, W. Rödl, A. Shir, A. Levitzki, M. Ogris, E. Wagner. Poly(I:C)-mediated tumor growth suppression in EGF-receptor overexpressing tumors using EGF-polyethylene glycol-linear polyethylenimine as carrier. Pharm. Res. 28(4) (**2011**) 731-741.

[278] A. Zintchenko, A. Philipp, A. Dehshahri, E. Wagner. Simple modifications of branched PEI lead to highly efficient siRNA carriers with low toxicity. Bioconjug. Chem. 19(7) (**2008**) 1448-1455.

[279] E.M. Kim, E.H. Park, S.J. Cheong, C.M. Lee, H.J. Jeong, D.W. Kim, S.T. Lim, M.H. Sohn. *In vivo* imaging of mesenchymal-epithelial transition factor (c-Met) expression using an optical imaging system. Bioconjug. Chem. 20(7) (**2009**) 1299-1306.

[280] E.M. Kim, E.H. Park, S.J. Cheong, C.M. Lee, D.W. Kim, H.J. Jeong, S.T. Lim, M.H. Sohn, K. Kim, J. Chung. Characterization, biodistribution and small-animal SPECT of I-125-labeled c-Met binding peptide in mice bearing c-Met receptor tyrosine kinase-positive tumor xenografts. Nucl. Med. Biol. 36(4) (**2009**) 371-378.

[281] T. Blessing, J.S. Remy, J.P. Behr. Template oligomerization of DNA-bound cations produces calibrated nanometric particles. J. Am. Chem. Soc. 120 (**1998**) 8519-8520.

[282] N. Li, Y. Zhai, T.D. Oberley. Two distinct mechanisms for inhibition of cell growth in human prostate carcinoma cells with antioxidant enzyme imbalance. Free Radical Biol. Med. 26(11-12) (**1999**) 1554-1568.

[283] M. Platica, A. Ionescu, E. Ivan, J.F. Holland, J. Mandeli, O. Platica. PAR, a protein involved in the cell cycle, is functionally related to chromosomal passenger proteins. Int. J. Oncol. 38(3) (**2011**) 777-785.

[284] M.S. Kormann, G. Hasenpusch, M.K. Aneja, G. Nica, A.W. Flemmer, S. Herber-Jonat, M. Huppmann, L.E. Mays, M. Illenyi, A. Schams, M. Griese, I. Bittmann, R. Handgretinger, D. Hartl, J. Rosenecker, C. Rudolph. Expression of therapeutic proteins after delivery of chemically modified mRNA in mice. Nat. Biotechnol. 29(2) (**2011**) 154-157.

[285] K. Itaka, A. Harada, Y. Yamasaki, K. Nakamura, H. Kawaguchi, K. Kataoka. In situ single cell observation by fluorescence resonance energy transfer reveals fast intra-cytoplasmic delivery and easy release of plasmid DNA complexed with linear polyethylenimine. J. Gene Med. 6(1) (**2004**) 76-84.

[286] L. Wightman, R. Kircheis, V. Rossler, S. Carotta, R. Ruzicka, M. Kursa, E. Wagner. Different behavior of branched and linear polyethylenimine for gene delivery *in vitro* and *in vivo*. J. Gene Med. 3(4) (**2001**) 362-372.

[287] W.T. Godbey, K.K. Wu, G.J. Hirasaki, A.G. Mikos. Improved packing of poly(ethylenimine)/DNA complexes increases transfection efficiency. Gene Ther. 6(8) (**1999**) 1380-1388.

[288] W.T. Godbey, K.K. Wu, A.G. Mikos. Size matters: molecular weight affects the efficiency of poly(ethylenimine) as a gene delivery vehicle. J. Biomed. Mater. Res. 45(3) (**1999**) 268-275.

[289] S. Reinhard, W. Zhang, E. Wagner. Optimized solid-phase-assisted synthesis of oleic acid containing siRNA nanocarriers. ChemMedChem 12(17) (**2017**) 1464-1470.

[290] C. Maucksch, A. Bohla, F. Hoffmann, M. Schleef, M.K. Aneja, M. Elfinger, D. Hartl, C. Rudolph. Transgene expression of transfected supercoiled plasmid DNA concatemers in mammalian cells. J. Gene Med. 11(5) (**2009**) 444-453.

[291] M. Ogris, P. Steinlein, M. Kursa, K. Mechtler, R. Kircheis, E. Wagner. The size of DNA/transferrin-PEI complexes is an important factor for gene expression in cultured cells. Gene Ther. 5(10) (**1998**) 1425-1433.

[292] E. Riu, D. Grimm, Z. Huang, M.A. Kay. Increased maintenance and persistence of transgenes by excision of expression cassettes from plasmid sequences *in vivo*. Hum. Gene Ther. 16(5) (**2005**) 558-570.

[293] Z.Y. Chen, E. Riu, C.Y. He, H. Xu, M.A. Kay. Silencing of episomal transgene expression in liver by plasmid bacterial backbone DNA is independent of CpG methylation. Mol Ther. 16(3) (**2008**) 548-556.

[294] J. Lu, F. Zhang, S. Xu, A.Z. Fire, M.A. Kay. The extragenic spacer length between the 5' and 3' ends of the transgene expression cassette affects transgene silencing from plasmid-based vectors. Mol. Ther. 20(11) (**2012**) 2111-2119.

[295] J. Lu, F. Zhang, A.Z. Fire, M.A. Kay. Sequence-modified antibiotic resistance genes provide sustained plasmid-mediated transgene expression in mammals. Mol. Ther. 25(5) (**2017**) 1187-1198.

[296] E. Wagner. Programmed drug delivery: nanosystems for tumor targeting. Expert. Opin. Biol. Ther. 7(5) (**2007**) 587-593.

[297] J.A. Wolff, D.B. Rozema. Breaking the bonds: Non-viral vectors become chemically dynamic. Mol. Ther. 16(1) (**2008**) 8-15.

8 Publications

Original articles

A. Krhac Levacic, S. Morys, S. Kempter, U. Lächelt and E. Wagner. Minicircle versus plasmid DNA delivery by receptor-targeted polyplexes. Human Gene Therapy 28(10) (**2017**) 862-874.

S. Morys, **A. Krhac Levacic**, S. Urnauer, S. Kempter, S. Kern, J. O. Rädler, C. Spitzweg, U. Lächelt and E. Wagner. Influence of defined hydrophilic blocks within oligoaminoamide copolymers: compaction versus shielding of pDNA nanoparticles. Polymers 9(4) (**2017**) 142.

S. Urnauer, S. Morys, **A. Krhac Levacic**, A. M Müller, C. Schug, K. A Schmohl, N. Schwenk, C. Zach, J. Carlsen, P. Bartenstein, E. Wagner and C. Spitzweg. Sequence defined cMET/HGFR-targeted polymers as gene delivery vehicles for the theranostic sodium iodide symporter (NIS) gene. Molecular Therapy 24(8) (**2016**) 1395-1404.

L. Beckert, L. Kostka, E. Kessel, **A. Krhac Levacic**, H. Kostkova, T. Etrych, U. Lächelt, E. Wagner. Acid-labile pHPMA modification of four-arm oligoaminoamide pDNA polyplexes balances shielding and gene transfer activity *in vitro* and *in vivo*. European Journal of Pharmaceutics and Biopharmaceutics 105 (**2016**) 85-96.

M. Čemažar, J. Ambrožič Avguštin, D. Pavlin, G. Serša, A. Poli, **A. Krhač Levačić**, N. Tešić, U. Lampreht Tratar, M. Rak, N. Tozon. Efficacy and safety of electrochemotherapy combined with peritumoral IL-12 gene electrotransfer of canine mast cell tumours. Veterinary and Comparative Oncology (**2016**) 1-14.

D. He, K. Müller, **A. Krhac Levacic**, P. Kos, U. Lächelt, E. Wagner. Combinatorial optimization of sequence-defined oligo(ethanamino)amides for folate receptortargeted pDNA and siRNA delivery. Bioconjugate Chemistry 27(3) (**2016**) 647-659.

P. Kos, U. Lächelt, A. Herrmann, F. Martina Mickler, M. Döblinger, D. He, **A. Krhač Levačić**, S. Morys, C. Bräuchle, E. Wagner. Histidine-rich stabilized polyplexes for cMet-directed tumor-targeted gene transfer. Nanoscale 7(12) (**2015**) 5350-62.

P. M. Klein, K. Müller, C. Gutmann, P. Kos, **A. Krhac Levacic**, D. Edinger, M. Höhn, J.-C. Leroux, M. A. Gauthier, E. Wagner. Twin disulfides as opportunity for improving stability and transfection efficiency of oligoaminoethane polyplexes. Journal of Controlled Release 205 (**2015**) 109-19.

Review

A. Krhac Levacic, S. Morys, E. Wagner. Solid-phase supported design of carriers for therapeutic nucleic acid delivery. Bioscience Reports 37 (5) (**2017**)
doi 10.1042/BSR20160617

Meeting abstracts and poster presentations

U. Lächelt, **A. Krhac Levacic**, D. Wendel and E. Wagner. Nonviral gene transfer by sequence-defined proton-sponges with combined nucleic acid binding and endosomal buffering: balancing basicities. ASGCT Meeting, Washington DC, USA, **2016**

S. Urnauer, S. Morys, **A. Krhac Levacic**, A. M. Müller, C. Schug, K. A Schmohl, N. Schwenk, C. Zach, J. Carlsen, P. Bartenstein, E. Wagner, Christine Spitzweg. Sequence defined cMET/HGFR-targeted polymers as gene delivery vehicles for the theranostic sodium iodide symporter (NIS) gene. 59th Annual Meeting of the German Society of Endocrinology, Munich, Germany, **2016**

S. Urnauer, S. Morys, **A. Krhac Levacic**, A. M. Müller, C. Schug, K. A Schmohl, N. Schwenk, C. Zach, J. Carlsen, P. Bartenstein, E. Wagner, C. Spitzweg. Sequence defined cMET/HGFR-targeted polymers as gene delivery vehicles for the theranostic sodium iodide symporter (NIS) gene. 18th European Congress of Endocrinology Munich, Germany, **2016**

S. Hacker, S. Morys, **A. Krhac Levacic**, C. Schug, N. Schwenk, J. Carlsen, C. Zach, E. Wagner, C. Spitzweg. Systemic non-viral cMET/HGFR-targeted gene delivery using the theranostic function of the sodium iodide symporter (NIS). 15th

International Thyroid Congress and 85th Annual Meeting of the ATA (Hosted by the American Thyroid Association), Florida, USA, **2015**

M. Cemazar, J. Ambrozic, G. Sersa, D. Pavlin, **A. Krhac Levacic**, N. Tesic, M. Rak, U. Lampreht, N. Tozon. Interleukin-12 gene therapy combined with local ablative technique electrochemotherapy for treatment of canine mastocytoma. Bringing cancer discoveries to patients: Annual Meeting 2015, American Association for Cancer Research, Philadelphia, Pennsylvania, **2015**

D. He, **A. Krhac Levacic**, K. Müller, P. Kos, D.J. Lee, E. Wagner. Sequence defined oligo(ethanamino)amides for folate receptor targeted pDNA or siRNA delivery: optimization and preliminary structure-activity relationship study. CeNS/SFB1032 Workshop 2014 - Walk and Talk at the Nanoscale, Venice International University (VIU), San Servolo, Italy, **2014**

L. Kostka, L. Beckert, **A. Krhac Levacic**, T. Etrych, E. Wagner. Traceless pH sensitive coating of polyplexes prepared from well-defined polycations. Third Symposium on Innovative Polymers for Controlled Delivery, Suzhou, China, **2014**

M. Čemažar, J. Ambrožič Avguštin, D. Pavlin, G. Serša, **A. Krhač Levačić**, N. Tešić, M. Rak, U. Lampreht, N. Tozon. Interleukin-12 gene therapy in combination with electrochemotherapy for treatment of canine mastocytoma. The 14th International Conference on Progress in Vaccination against Cancer, Rome, Italy, **2014**

J. Ambrožič Avguštin, G. Serša, **A. Krhač Levačić**, D. Pavlin, N. Tozon, M. Čemažar. Cancer electrogene therapy with interleukin-12 in dogs: Risk assessment of ampicillin resistance gene transfer. 7th Conference on Experimental and Translational Oncology, Portorož, Slovenia, **2013**

9 Acknowledgements

At the end of my PhD, I would like to thank all the people that supported and helped me during the last 4 years and made this work possible.

My deepest gratitude goes first and foremost to my supervisor, Prof. Dr. Ernst Wagner for giving me the opportunity to perform my PhD thesis in his research group, for trusting in me and for motivating me throughout the work. I greatly appreciated his highly professional guidance, scientific as well as personal support and valuable advices over these four years.

I would also like to thank PD Dr. Carsten Rudolph for being my second Gutachter as well as the other members of my PhD defense committee for the interest shown in the present work by accepting to be referees.

I am also grateful to all my colleagues for the nice working atmosphere in the lab and many collaborations without whom this thesis would not have been possible. First of all, I would like to thank Petra for introducing me to the world of cell culture, sharing of knowledge and experiences and showing me all the techniques at the beginning of my PhD. Furthermore, I would like to thank to Stephan, Uli, Philipp, Sören and Dongsheng for the synthesis and continuous supply of so many oligomers for my projects. In this regard, special thanks go to Uli for helpful discussions and for sharing the enthusiasm for my projects. Special thanks also go to Stephan, not just for his synthetic work and collaboration in several projects, but also for support in many administrative issues and making my everyday life easier. Additionally, special thanks to Susanne Kempter (AK Rädler) for TEM measurements as well as ethris GmbH (especially to Dr. Christian Dohmen, Dr. Rebekka Kubisch-Dohmen and Dr. Olga Mykhailyk) for the collaboration on the mRNA project.

I would also like to thank Ruth, Katharina and Wei for being the perfect lab colleagues through all the years, for all theirs scientific input, equipping me with useful knowledge about methods, kind support, spending so much time together and the fun we had in and outside the lab. Special thanks go to Wei for proofreading of

my thesis, all the tips that contributed to its improvement and – you know – so many other things. In addition, many thanks also to Peng, Adam, Jonathan and Sarah for always having something to laugh about as well as Ann-Katrin and Melinda for always having an “open ear”. Thanks to all the other former and newer AK Wagner members for the great time we shared together.

Many thanks to Wolfgang for his inexhaustible patience and immediate help in any kinds of technical and computer problems. Also, I want to thank Miriam, Anna, Ursula, Melinda and Markus for keeping the everyday life in the lab running and Olga for administrative support. My gratitude goes also to Martina for her commitment in group events and practical courses. Thanks also to Uli and Andy which continued Martina's work.

Furthermore, I want to thank my whole family and ‘family-in-law’, as well as all my friends for the support. I owe my deepest gratitude to my parents Mira and Vladimir, who gave me the maximum that parents can give to their child, despite the great denials - love and the possibility of education; to my sister Eva and to my grandparents for their guidance, life-long support and for loving me unconditionally. Many thanks to my ‘sister-in-law’ Josipa for her boundless help to rapidly continue my PhD after maternal leave. Thanks also to my “old” friends Adela, Nina, Urška, Andreja, Tjaša, Eva and Ivana for always taking care and encouraging e-mails. I could not have done it without you!

Last but not least, my deepest thanks to my husband Tihomir for his immense patience, for listening to my worries, for encouraging me, always believing in me and for just being there for me at the end of the day. You are the best support one could wish for! Thank you Rebeka Elin - because of you, life actually got a new meaning. You are my source of joy, optimism and energy. You are the strength that keeps me going!

Hvala vam!